

Doctor of Engineering Thesis

Operation and Control of VSC based Grid Connected Wind Farm

**By
Linda Sartika**

**Department of Electrical and Electronic Engineering
Kitami Institute of Technology, Japan
2018**

Abstract

This thesis deals with the operation and control of VSC based grid connected wind farms. The fast growth of wind generation has led to concern about the effect of wind power on the stability of the electric grid. Therefore, it is essential to analyze the effect of wind farm penetration into power system on its frequency and other characteristics, especially frequency drop when unexpected generation loss due to a fault in the grid system or load increase occurs. During severe network disturbance such as a short circuit fault, the terminal voltage of wind farm decreases significantly and active power from wind farm cannot be supplied to the grid system. New studies must be performed in order to evaluate the behavior of the wind farms after severe faults and improve the design of the wind farms in an efficient and economical way. Therefore, the interaction between wind farm and grid system from points of view of transient and steady state characteristics has become a very important issue to be analyzed.

The Fixed Speed Wind Turbines with Squire Cage Induction Generators (FSWT-SCIGs) are widely used in wind farm due to their advantages of mechanical simplicity, robust construction, and lower cost. However, the FSWT-SCIG directly connected to the grid does not have any LVRT (Low Voltage Ride Through) capability when a short circuit occurs in the system. Moreover, under steady state condition its reactive power consumption cannot be controlled and hence terminal voltage of the wind generator leads to large fluctuation. Combined installation of PMSG (Permanent Magnet Synchronous Generator) and SCIG in a wind farm can be considered a good solution, because the PMSG can provide the required reactive power of SCIG during fault condition. Therefore, in this thesis new control system for cooperated stabilizing control of PMSG based grid connected wind farm is proposed and it is shown that the proposed control system can stabilize the wind farms effectively.

Currently, most of studies about PMSG system consider normal operation, for example, realization of maximum power point tracking. Studying on the PMSG system protection is not so much, meanwhile, enhancement of FRT (fault ride-through) capability is required for operating of wind farm. The wind farm should stay online during and after a network disturbance. When a fault occurs in the grid, a voltage dip appears at the terminal of wind generator and then the active power delivered to the grid is also reduced. As the generator side converter is decoupled with the grid, generator continues to generate the active power and thus the DC-link voltage increases due to the

energy unbalance between the generator side converter and the grid side converter. Usually, a simple DC chopper with a braking resistance is inserted into the DC-link circuit to dissipate the active power produced by PMSG in such a way that the active power balance in the DC-link circuit is maintained. However, it can have a problem if the active power coming from the PMSG is not balanced against the capacity of braking resistor. This is because the capacity of resistor in the protection system with a simple DC chopper is constant (uncontrolled). In order to solve the problem new topology of DC-link protection of PMSG by using buck converter is proposed in this thesis. From the simulation results, it is shown that the proposed method can control well the DC-link voltage as well as other dynamic responses of PMSG such as rotor speed and active power output. Therefore it is concluded that the dynamic performance of PMSG can be enhanced by the proposed DC-link protection system.

Offshore wind farm can be connected to onshore power system using HVAC transmission technology if the wind power plant is near the onshore. But HVDC technology may be more attractive for the transmission of bulk power over long distances. HVDC becomes a more economical solution than HVAC in the case of transmission over a certain distance called "break-even". The break-even distance is between 500-800 km for overhead lines and around 50 km for submarine cables.

In this thesis, Fixed Speed Wind Turbine-Squirrel Cage Induction Generator (SCIG) based wind farm which is connected to onshore power system through the VSC-HVDC transmission system is also considered. This is because, in comparison with DFIG and PMSG, SCIG has some superior characteristics such as a simple design with high reliability, brushless and rugged construction, low investment and maintenance cost, and operational simplicity. In addition, the SCIG needs no individual power converter in its operation. Although SCIGs have almost no Low Voltage Ride Through (LVRT) capability, the LVRT capability of the SCIG based wind farm can be enhanced if the wind farm is connected to onshore main grid through VSC-HVDC line and controlled by the proposed cluster VSC converter system. It is shown that the proposed system based on the SCIG wind turbines controlled by the new cluster converters with VSC-HVDC system can enhance the performance and stability of the SCIG based wind farm under both transient and steady state conditions.

Contents

Abstract

1. Introduction	1
1.1. Renewable Energy	1
1.2. Overview of Wind Power Capacity	2
1.3. Background of Thesis	3
1.4. Purpose and Contribution of Thesis	6
1.5. Outline of Thesis	7
2. Wind Turbine Model	9
2.1. Wind Turbine Model	9
2.2. Characteristics of Wind Power Generation	11
2.2.1. Wind Energy	11
2.2.2. Power Output from Practical Wind Turbine	12
2.3. Drive Train Model	12
2.4. Pitch Angel Controller	13
2.5. Fixed Speed Wind Generator	14
2.5.1. Basic of the Induction Machine	14
2.5.2. Equivalent Circuit of Induction Generator	15
2.5.3. SCIG Wind Turbine Topology	17
2.6. Variable Speed Wind Generator	18
2.6.1. PMSG Wind Turbine Topology	19
2.6.2. PMSG based Wind Turbine Model	20
2.7. VSC-HVDC System	20
2.8. Chapter Summary	21
3. Cooperated Stabilizing Control of PMSG based Grid Connected Wind Farm	22
3.1. Introduction	22
3.2. Power System Model	24
3.3. Governor and AVR Model	25

3.4. Wind Farm Model	26
3.5 Wind Turbine Model	30
3.6. Simulation Results	32
3.7. Chapter Summary	39
4. Enhancement of DC-Link Protection of PMSG based Wind Turbine under Network Disturbance by using New Buck Controller System	
4.1. Introduction	40
4.2. PMSG based Wind Turbine System	41
4.2.1. Aerodynamic model	42
4.2.2. Mechanical Model	44
4.2.3. Pitch Control Model	44
4.2.4. Permanent Magnet Synchronous Generator (PMSG) Model	45
4.2.5. Converter Controller System	45
4.3. DC-Link Protection System	46
4.4. Simulation Analysis	50
4.4.1. Power System Model	50
4.4.2. Simulation Results	51
4.5. Chapter Summary	55
5. Wind Turbines Cluster System Composed of Fixed Speed Wind Generators Controlled by Cluster Converter based VSC-HVDC System	
5.1. Introduction	56
5.2. Offshore Wind Farm Model	59
5.3. Fixed Speed Wind Turbine SCIG Model	60
5.3.1. Basic Configuration	60
5.3.2. Wind Turbine Model	61
5.3.3. Pitch Controller Model	62
5.3.4. Drive Train	63

5.3.5. SCIG Modeling	64
5.4. Multi-Terminal VSC-HVDC for Cluster SCIG based Wind Farm	65
5.4.1. Basic Configuration	65
5.4.2. Cluster Converter for SCIG based Wind Farm	66
5.4.3. Onshore Converter Model	69
5.4.4. Over Voltage Protection Circuit of HVDC System	71
5.5. Simulation Results	71
5.5.1 Transient Stability Analysis	72
5.5.2. Steady State Performance Analysis	80
5.6. Chapter Summary	83
6. Conclusions	84
Acknowledgment	88
References	89
List of Publication	97

Chapter 1








Introduction

1.1. Renewable Energy

Due to the depletion of fossil fuel and the need to decrease the pollution production, utilization of renewable energy resources for electrical energy generation has been interested and received much attention all over the world. Renewable energy uses energy sources that are continually provided by nature such as sunlight, wind, rain, tides, waves, and geothermal heat, etc. Renewable energy technologies drive these nature energy sources into usable forms of energy often in four important areas: electricity generation, air and water heating/cooling, transportation, and rural energy services [1].

Most of new renewable energy capacity has been installed in developing countries, and largely in China. In 2016, renewable energy spreads to a growing number of developing and emerging economies, some of which have become important markets. Renewable power generating capacity saw its largest annual increase ever in 2016, with an estimated 161 Giga Watts (GW) of capacity added. Total global capacity was up by nearly 9% compared to 2015, to almost 2,017 GW at year's end. The world has continued to add more renewable power capacity annually than that of the net capacity from all fossil fuels combined. In 2016, renewable energy accounted for an estimated nearly 62% of net additions to global power generating capacity [2]. Table 1.1 shows the record numbers reached for newly installed renewable power generating capacity.

Table 1.1. Record number for installed capacity of renewable energy in 2015-2016 (MW) [2]

POWER		2015	2016
Renewable power capacity (total, not including hydro)	GW	785	921
Renewable power capacity (total, including hydro)	GW	1,856	2,017
 Hydropower capacity ²	GW	1,071	1,096
 Bio-power capacity	GW	106	112
 Bio-power generation (annual)	TWh	464	504
 Geothermal power capacity	GW	13	13.5
 Solar PV capacity	GW	228	303
 Concentrating solar thermal power capacity	GW	4.7	4.8
 Wind power capacity	GW	433	487

1.2. Overview of Installed Wind Power Capacity

Since 2001 wind energy has become ongoing trend of renewable energy resource in market and industry highlights. Fig. 1.1 shows the annual and global total installed capacity of wind power in 2001-2016 reported by World Wind Energy Association (WWEA). By the end of 2016, the global wind power capacity reached 486,749 MW, in which 56,600 MW were added in the first six months of 2016 [3].

According to WWEA, the five leading countries, China, USA, Germany, Spain and India, represent together a total share of 72.5% of the global wind capacity as shown in Fig. 1.2. Again in 2016, PR China represents by far the largest wind markets. By the end of 2016, China has had an overall installed capacity of around 168,690 MW. In second place, the US had total installed capacity of around 82,148 MW at the end of 2016.

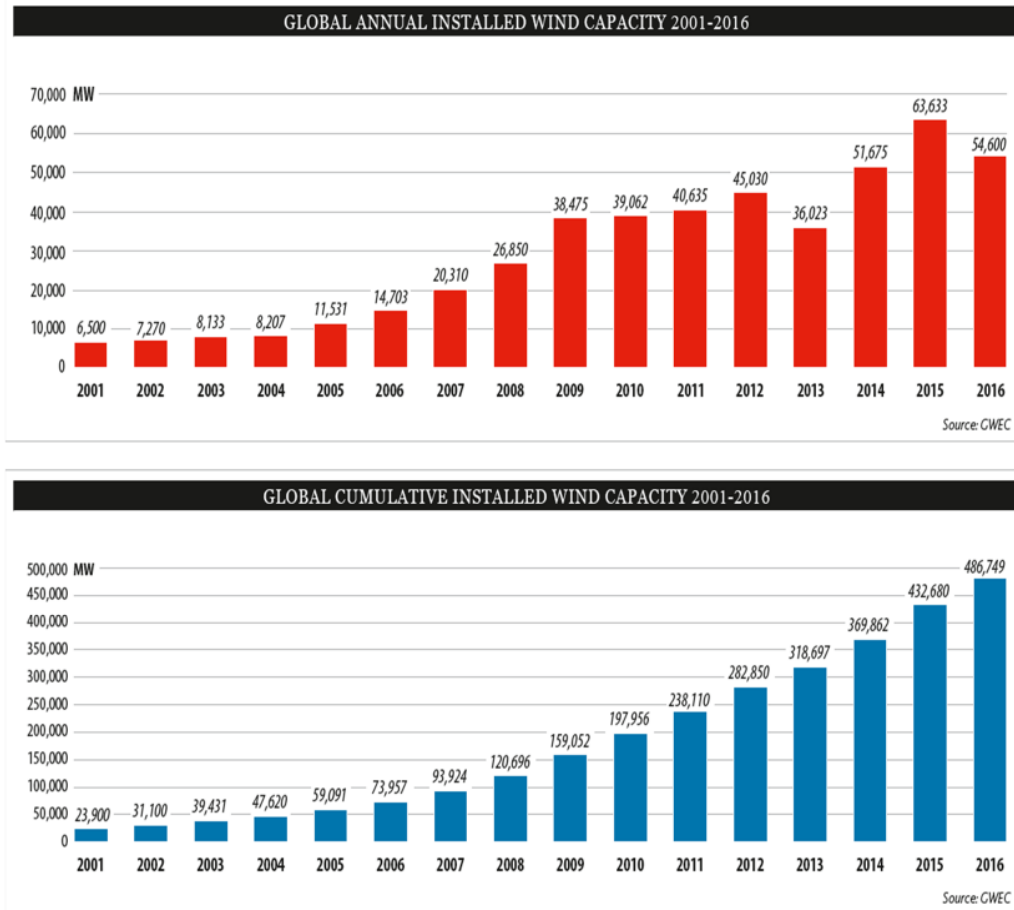


Fig. 1.1. Global annual and cumulative installed capacity of wind power in 200-2016 [3]

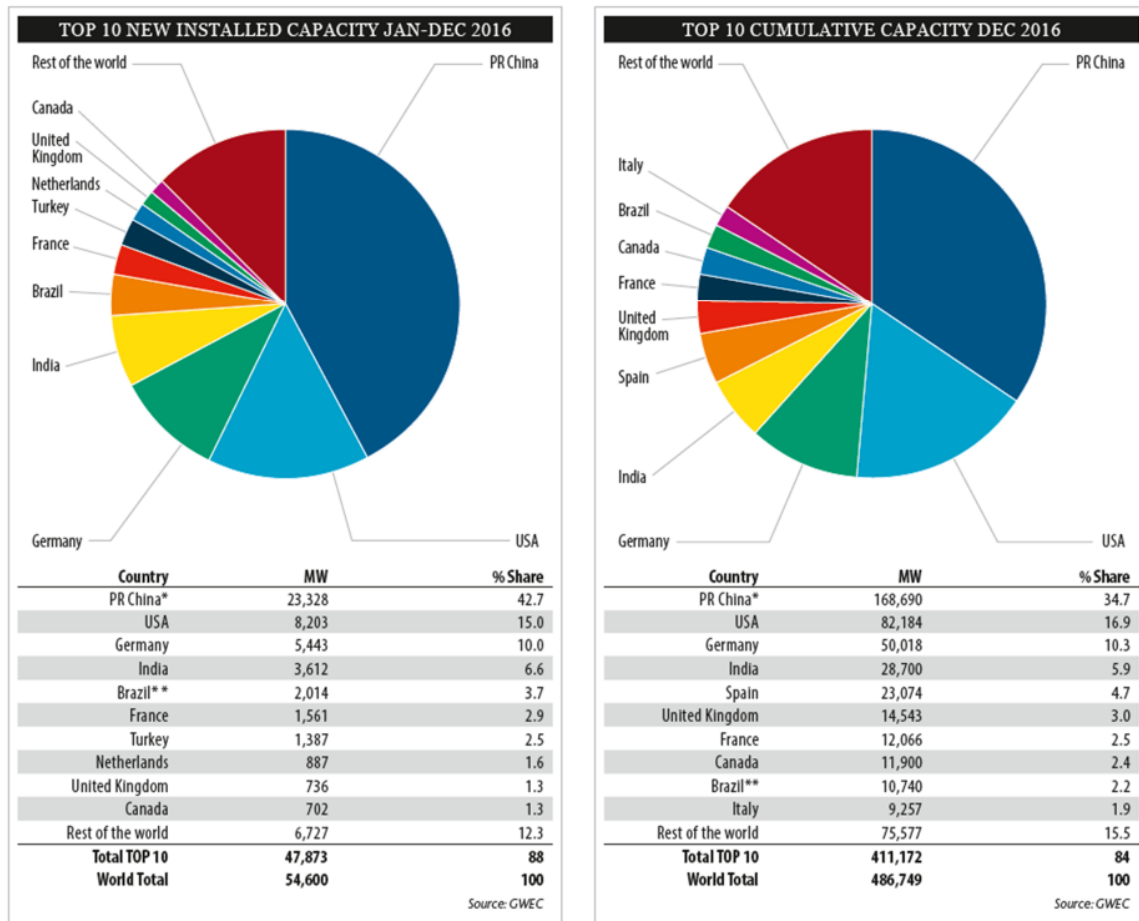


Fig. 1.2. New and cumulative installed capacity of wind power of Top 10 countries in 2016 [3]

1.3. Background of Thesis

The rapid increase in installation of large-scale wind farm into the grid system would have a serious impact on the system stability and power quality due to the variation of generated power from wind generators [4]-[7]. Increasing of the penetration level of the wind generator into grid system has led power system operators to revise the grid code connection requirements for their power system in many countries [8]. The grid code prosecutes that the wind generator should give a contribution to control the power in case of abnormal operating conditions such as network disturbance. The wind generators should be remained stay online during a network disturbance. The low voltage ride through grid code requirement should be taken into account when a short circuit occurs in grid system. Out of synchronism of a large number of wind generators becomes serious impact on power system stability. Therefore, the interaction between wind farm and power

system such as transient and steady state characteristics of wind farm has become important to be analyzed in the few last years.

The Fixed Speed Wind Turbines with Squirrel Cage Induction Generators (FSWT-SCIG) are most widely used in wind farms. This type of wind turbine is very popular and it has the advantages of mechanical simplicity, robust construction, low specific mass and smaller outer diameter, and lower cost [9]. However, some papers reported that the FSWT-SCIG directly connected to the grid does not have any low voltage ride-through (LVRT) capability when a short circuit occurs in the system [10]-[12]. The squirrel cage induction generators require large reactive power to recover the air gap flux when a short circuit fault occurs in the grid system. If the sufficient reactive power is not available enough, the electromagnetic torque of the SCIG decreases significantly, and then rotor speed of the generator increases rapidly and becomes unstable [13]. As a result, the induction generator becomes unstable and it requires to be disconnected from the grid system. Moreover, under steady state condition the reactive power consumption cannot be controlled and hence terminal voltage of the wind generator leads to large fluctuation which is a serious disadvantage of the SCIG wind turbine [14].

The variable speed wind turbine (VSWT) generator system has become the dominant type among installed wind turbine systems. VSWT system is designed to achieve maximum aerodynamic efficiency over the wide range of wind speed, increase energy capture, improve power quality, and reduce mechanical stress on the wind turbine [14]. In addition, VSWT system equipped with full or partial rating power electronic converters has strong fault ride through capability during a network disturbance [15]-[19]. Moreover, the VSWT system with fully scale converter not only recovers a network voltage drop preventing instability of FSWT -SCIG when fault occurs, but also generates electric power in steady state. Therefore, it is considered to be much effective for VSWT to be installed with SCIG in wind farm.

Variable Speed Wind Turbine with Permanent Magnet Synchronous Generator (VSWT-PMSG) has become a promising and attractive type of wind turbine concept [14]. Megawatt class of VSWT-PMSGs have been installed in large wind power stations and directly connected to electrical power transmission system. The advantages of VSWT-PMSG configuration are: 1) No Gearbox and no brushes, and thus higher reliability; 2) The full power converter totally decouples the generator from the grid, and hence grid disturbances have no direct effect on the generator; 3) No additional power supply for magnetic field excitation is needed; 4) The converter permits very

flexible control of active and reactive power in cases of normal and disturbed grid conditions; 5) The amplitude and frequency of the generator voltage can be fully controlled by the converter [20], [21]. The VSWT-PMSG system is equipped with back to back power electronic converters, and it has strong low voltage ride through capability during and after fault condition on grid system [22]-[26]. Compared with DFIG, PMSG is more efficient, and, it can support large reactive power [27]. However, this type of wind generator has more complex construction and more expensive compared with other types. Therefore, combined installation of VSWT-PMSG and FSWT- SCIG in a wind farm can be efficient to reduce system investment cost. VSWT-PMSG with power converters can be used to supply reactive power to recover network voltage in order to improve the LVRT of FSWT-SCIG when a fault occurs as well as to generate electric power in steady state operation.

Currently, most of PMSG system studies consider normal operation, for example, realization of maximum power point tracking. Studying on the PMSG system protection is not so much [28], meanwhile, enhancement of FRT (fault ride-through) capability is required for operating of wind farm. Therefore, enhancement of protection system of the wind generator is very important to be studied. When a fault occurs in the grid, a voltage dip appears at the terminal of wind generator and then the active power delivered to the grid is also reduced. As the generator side converter is decoupled with the grid, generator continues to generate the active power and thus the DC-link voltage increases due to the energy unbalance between the generator side converter and the grid side converter. Usually, a simple DC chopper with a braking resistance is inserted into the DC-link circuit to dissipate the active power produced by PMSG in such a way that the active power balance in the DC-link circuit is maintained [29-31]. However, it can have a problem if the active power coming from the PMSG is not balanced against the capacity of braking resistor. This is because the capacity of resistor in the protection system with a simple DC chopper is constant (uncontrolled).

Offshore wind farms have been introduced in many countries to harness the energy of strong, consistent winds over the oceans. Offshore wind farms have some advantages over onshore wind farms. They provide renewable energy, do not consume water, provide a domestic energy source, and do not emit any environmental pollutants. Compared to onshore winds the offshore winds blow stronger and more uniformly. Accordingly, offshore winds can generate much smoother electricity. Moreover, offshore wind power plants have more steady operation than onshore plants

[32]. Offshore wind farm can be connected to onshore power system using HVAC transmission technology if the wind power plant is near the onshore. But HVDC technology may be more attractive for the transmission of bulk power over long distances. HVDC becomes a more economical solution than HVAC in the case of transmission over a certain distance called "break-even". The break-even distance is between 500-800 km for overhead lines and around 50 km for submarine cables [33]. There are two kinds of technologies used in HVDC transmission system; thyristor based LCC (Line Commuted Converter) and transistor based VSC (Voltage Source Converter) [34]-[36]. VSC-HVDC provides some advantages compared with the LCC-HVDC such as black start capability, independent control of active and reactive powers, multi-terminal configuration, and high dynamic performance [27]. It can be also said that application of VSC-HVDC technology to offshore wind farm can enhance performance and stability of the wind farm.

1.4. Purpose and Contribution of Thesis

The main purpose of this thesis is stability enhancement of grid connected wind farm through VSC-HVDC. The results of this work are expected to provide valuable contributions in the following aspects:

1) A control system design for cooperated stabilizing control of PMSG based grid connected wind farm. In this study, a wind farm composed of PMSGs and SCIGs is considered to be connected to multi-machine power system. Though outputs of the SCIG based wind turbines are collected on AC network, PMSG based wind turbines are integrated in DC network with single grid side converter. In order to contribute to frequency and voltage stabilizing control, controller system of the inverter is modified in order for its active and reactive powers to be delivered to the grid easily and effectively. Simulation analysis is performed by using PSCAD/EMTDC, in which comparative analysis between proposed control strategy and conventional strategy is performed.

2) An improvement of DC-Link protection of PMSG based wind turbine under network disturbance by using new back controller system. Protection system for DC-link circuit of back-to-back converter of PMSG (Permanent Magnet Synchronous Generator) based wind turbine is essential part for the system to ride through a network fault in grid system. Voltage on the DC-link circuit can be increased significantly due to power unbalance between stator side converter and grid side converter. Increase of DC-link circuit voltage can lead to a damage of IGBT of the converter and control system failure. The buck converter is used to control supplied voltage of a

breaking resistor to dissipate energy from the wind generator during network disturbance. In order to investigate effectiveness of the proposed DC-link protection system, fault analysis is performed in the simulation study by using PSCAD/EMTDC software program. In addition, comparative analysis between the proposed protection system and the conventional protection system using DC chopper is also performed.

3) Enhancement of wind turbines cluster system composed of Squirrel Cage Induction Generators (SCIGs) controlled by cluster converter based VSC-HVDC System. The wind turbine cluster systems (multiple clusters) are installed in an offshore wind farm and connected to onshore system through a Voltage Source Converter based High Voltage Direct Current (VSC-HVDC) transmission line. A control scheme of cluster converter and VSC-HVDC converter systems are developed so that power production by SCIGs can be delivered to the onshore system effectively. In this study dynamic behavior of the wind turbines has been investigated by simulation study performed by using PSCAD/EMTDC for fluctuating wind speed and short circuit fault. Simulation results show that the proposed cluster system composed of SCIGs has high performance under transient and steady state conditions.

1.5. Outline of Thesis

Chapter 2 describes the detail of wind turbine generator modeling considered in this thesis. The general overview to basic principles of electrical power extraction from wind energy is presented. The drive train and pitch angel control models of wind turbine generator system are discussed. Finally, the topological overview and modeling are presented in detail for both FSWT-SCIG and VSWT-PMSG.

In Chapter 3, consideration on combined VSWT-PMSG and FSWT-SCIG from a view point of dynamic stability augmentation of wind farm is presented. A control strategy of power converter of VSWT-PMSG is developed to augment both transient and steady state stabilities of the wind farms. During fault condition the DC link voltage increases significantly due to unbalance in power produced by the generator and delivered to grid system. In order to avoid the converter damage, the protection scheme using DC chopper is embedded on DC link circuit. In order to evaluate the effectiveness and capability of the proposed control strategy, two wind farms composed of aggregated model of VSWT-PMSG and FSWT-SCIG, which are connected to an infinite bus and a multi-machine power system, are analysed.

In chapter 4, a new DC-link protection scheme using buck converter is proposed for permanent magnet wind generator and its performance under network disturbance condition is investigated. Comparative simulation analysis is performed for severe three-line to ground (3 LG) fault between the proposed DC-link protection system and the conventional protection system. From the simulation results, it will be shown that the proposed method can control well the DC-link voltage as well as other dynamic responses of PMSG such as rotor speed and active power output.

In Chapter 5, the new wind turbine cluster system composed of Squirrel Cage Induction Generators (SCIGs) controlled by cluster converters with VSC-HVDC system is proposed and investigated. The dynamic and steady state characteristics of the proposed system are analyzed through simulation studies by using PSCAD/EMTDC. The simulation study will demonstrate that the proposed system can enhance the performance and stability of the SCIG based offshore wind farm under both transient and steady state conditions.

Chapter 2

Wind Turbine Model

This chapter describes the overview of wind turbine generation system. First, a brief introduction to basic principles of energy extraction from wind is presented. Then, drive train and pitch angel control models of wind turbine generator system are presented. The topological overview and modeling are presented for both fixed speed and variable speed wind turbine generator systems and at the end of the chapter the VSC-HVDC (Voltage Source Converter based High Voltage Direct Current) system is discussed.

2.1. Wind Turbine Generator System (WTGS)

The modern wind turbine generator systems are mainly constructed as system with a wind turbine of horizontal axis rotation, generator with gear box and rotor brake located in nacelle, and tower as shown in Fig 2.1. The turbine captures power from wind and drives a generator. The tower supports the nacelle and usually contains the electrical conduits and yaw motor.

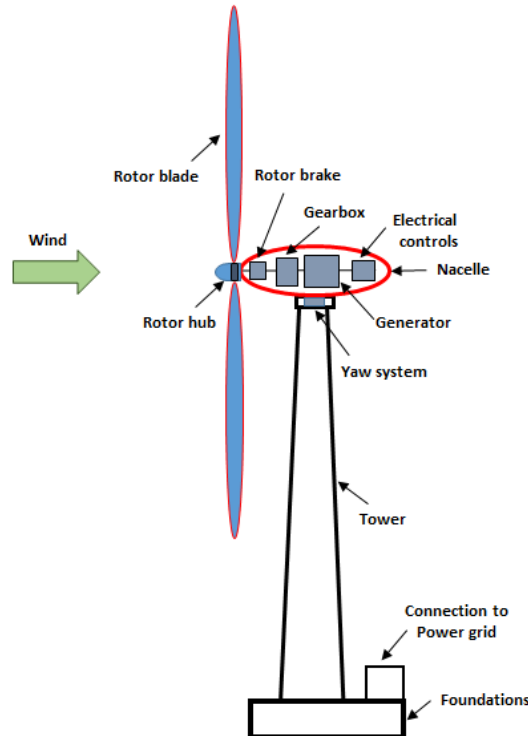


Fig. 2.1. Horizontal axis wind turbine [37].

The each part of wind generator system is shown in Fig 2.2. The modern wind turbine (sometimes called the rotor), mostly has three blades. Wind blowing over the blades causes the blades rotate. Wind speed is measured by using anemometer, and its data is transmitted to the controller. A disc brake can be applied mechanically, electrically, or hydraulically to stop the rotor in emergencies. Wind vane measures wind direction and communicates with the yaw drive to orient the turbine properly with respect to the wind. The yaw drive is used to keep the rotor facing into the wind as the wind direction changes.

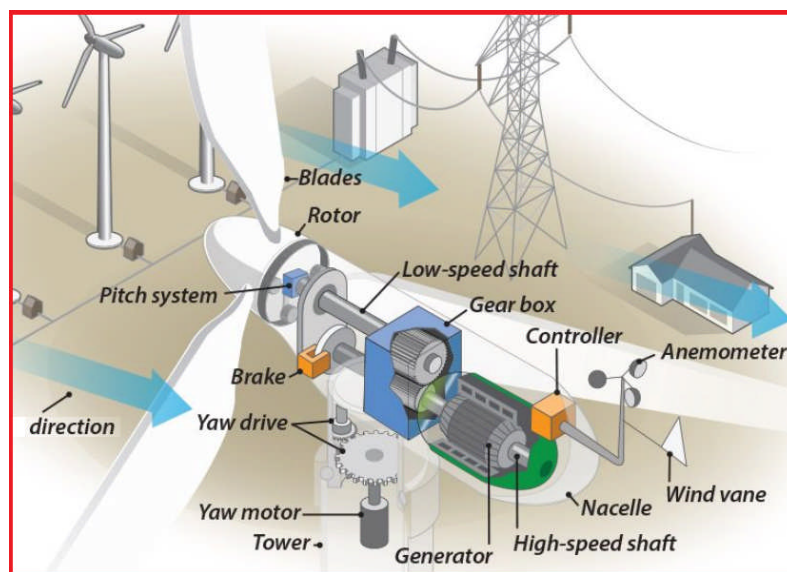


Fig. 2.2. Each part of the wind generator system [38].

The modern wind turbine generator system can operate as fixed speed or variable speed. The fixed speed wind turbines are equipped with an induction generator (squirrel cage rotor or wound rotor). This type of wind turbine is designed to achieve maximum efficiency at one particular wind speed. Fixed speed wind turbine has often two windings which are used at low and high wind speed respectively in order to increase power production. In variable speed wind turbines, it is possible to control continuously the rotational speed of the wind turbine according to the wind speed. By this way, the maximum aerodynamic efficiency can be achieved over a wide range of wind speed [39]. The variable speed wind turbine is typically equipped with an induction or synchronous generator. The Doubly Fed Induction Generator (DFIG) and Permanent Magnet Synchronous Generator (PMSG) are mostly used as variable speed wind generator.

2.2. Characteristic of Wind Power Generation

2.2.1. Wind Energy

Wind is one form of solar energy. Winds are caused by the uneven heating of the atmosphere by the sun, the irregularities of the earth's surface, and rotation of the earth. The wind moves from high-pressure air to low-pressure air. Wind flow patterns are modified by earth's terrain, bodies of water, and vegetative cover [40]. Wind energy can be converted into other energies such as, modern wind turbines to generate electricity, wind pumps for water pumping or drainage, windmills for mechanical power, or screens to push ships. Wind energy can be an alternative to fossil fuels, though there are many unlimited, renewable, widely distributed, clean energy, which does not produce greenhouse gas emissions in operation and can be used on small land [41]. Compared with other energy sources its negative effects are generally not so much.

To extract wind energy, the basic theory of wind power technology can be described by equations (2.1)-(2.4) below. The power of an air mass that flows at speed U_w through an area A can be calculated as follows [42]:

$$E_k = 0.5\rho V U_w^2 \quad (2.1)$$

where:

E_k = kinetic energy (Kg m²/sec² or Joules)

ρ = air density (kg/m³)

V = volume of air (m³)

U_w = wind speed (m/sec)

Power is expressed in kinetic energy per unit time, $K_e = d(E_k)/dt$. To obtain the expression of wind power, K_e can be expressed as:

$$K_e = 0.5\rho(A \cdot dx) U_w^2 \quad (2.2)$$

The volume of air V is expressed with an area A perpendicular to the wind flow multiplied by the horizontal displacement in the direction of wind flow dx . The power of the wind or change in kinetic energy per unit time is expressed by:

$$P = \frac{d(K_e)}{dt} = \frac{d}{dt} (0.5\rho(A \cdot dx) U_w^2) = 0.5\rho(A \cdot dx/dt) U_w^2 \quad (2.3)$$

Since dx/dt is in fact the wind speed V_w , the P can be expressed by:

$$P = 0.5\rho A \cdot U_w^3 \quad (2.4)$$

2.2.2. Power Output from Practical Wind Turbine

The fraction of power extracted from the wind power by a practical wind turbine is usually given by the symbol C_p , standing for coefficient of performance or power coefficient. Using this notation and dropping the subscripts of Eq. 2.6, the actual mechanical power output can be written as [43]:

$$P_{wt} = 0.5\rho\pi R^2 U_w^3 C_p(\lambda, \beta) \quad (2.7)$$

Where, R is the blade radius of the wind turbine [m], U_w is the wind speed [m/sec], ρ is the air density [kg/m³]. The co-efficient of performance is not constant, and varies with the wind speed, the rotational speed of the turbine, and turbine blade parameters like angle of attack and pitch angle. Generally, it is said that power co-efficient, C_p , is the function of the tip speed ratio, λ , and blade pitch angle, β [degree].

$$\lambda = \frac{\omega_r R}{U_w} \quad (2.8)$$

Where, ω_r is the mechanical angular velocity of the turbine rotor in rad/s, and U_w the wind speed in m/s. The angular velocity, ω_r , is determined from the rotational speed, n (r/min) by the equation

$$\omega_r = \frac{2\pi n}{60} \quad (2.9)$$

2.3. Drive Train Model

The drive train of a wind turbine generator system consists of the following elements: a blade-pitching mechanism with a spinner, a hub with blades, a rotor shaft and a gearbox with breaker and generator [44]. Depending on the complexity of the study, the complexity of the drive train modeling differs. For example, when the problems such as torsional fatigue are studied, dynamics of all parts have to be considered. For these reasons, two-lumped mass or more sophisticated models are required. However, when the study focuses on the interaction between wind farms and grid system, the drive train can be treated as one-lumped mass model with acceptable precision for the sake of time efficiency [45], [46]. In the present study, it is modelled by the following equation:

$$\frac{d\omega_r}{dt} = \frac{T_e - T_m}{J_{eq}} - \frac{B_m}{J_{eq}} \omega_r \quad (2.10)$$

where ω_r is the mechanical angular speed (rad/s) of the generator, B_m is the damping coefficient (Nm/s), T_e is the electromechanical torque (Nm), T_m is the mechanical torque of the wind turbine,

and J_{eq} is the equivalent rotational inertia of the generator (kg.m^2). The one mass model of wind turbine is shown in Fig. 2.4.

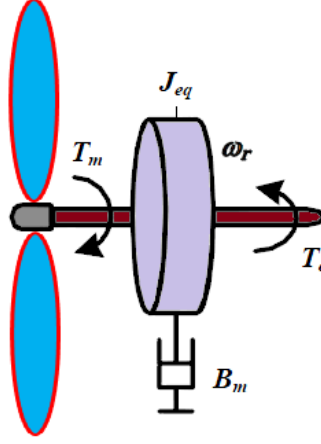


Fig. 2.4. One mass model of wind turbine

2.4. Pitch Controller Model

Wind power extraction by wind turbines depends on wind speed, and thus, output power of a wind generator always fluctuates due to variations in wind speed. For maintaining the output power of the generator below the rated level, the two pitch controllers are considered in this paper. Figs. 2.5 and 2.6 show the pitch control models for fixed speed and variable speed wind turbines, respectively. The control loop for the actuator of pitch control is represented by first order transfer function with an actuator time constant ($T_s=5$) and rate limiter of 10 deg/s [47]. A classic PI controller is used to manage tracking error. In fixed speed wind turbine, the pitch controller is used to keep the power output of SCIG (squirrel cage induction generator) under the rated power ($P_{IG} = 1$ pu), and in variable speed wind turbine, the pitch controller is used for keeping the rotational speed of the PMSG under its rated value ($\omega_r = 1$ pu).

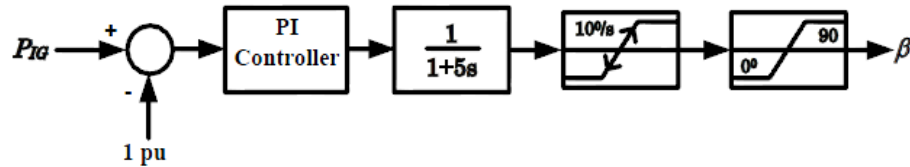


Fig. 2.5. Pitch controller for fixed speed wind turbine

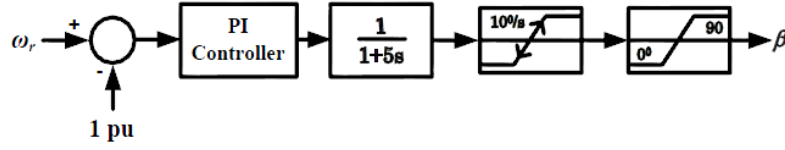


Fig. 2.6. Pitch controller for variable speed wind turbine

2.5. Fixed Speed Wind Generator

2.5.1. Basic of the Induction Machine

The induction machine consists of the stator and rotor windings. When balanced three-phase currents flow through the stator winding, a field rotating at synchronous speed, n_s , is generated [48]. The synchronous speed, n_s , in revolutions/minute is expressed as:

$$n_s = \frac{120 f_s}{p_f} \quad (2.11)$$

Where f_s (Hz) is the frequency of the stator currents, and p_f is the number of poles. If there is relative motion between the stator field and the rotor, voltages of frequency f_r (Hz) are induced in the rotor windings. The frequency f_r is equal to the slip frequency $s f_s$, where the slip, s , is given by:

$$s = \frac{n_s - n_r}{n_s} \quad (2.12)$$

Where n_r is the rotor speed in revolutions/minute. The slip is positive if the rotor runs below the synchronous speed and negative if it runs above the synchronous speed [48].

Figure 2.7 shows the schematic of the cross-section of a three-phase induction machine with one pair of field poles, and Figure 2.8 illustrates the stator and rotor electrical circuits. The stator consists of three-phase windings a_s , b_s and c_s distributed 120° apart in space. The rotor circuits have three distributed windings a_r , b_r and c_r . The angle θ is given as angle by which the axis of the phase a_r rotor winding leads the axis of phase a_s stator winding in the direction of rotation, and ω_r is the rotor angular velocity in electrical rad/s. The angular velocity of the stator field in electrical rad/s is represented by $\omega_s = 2\pi f_s$.

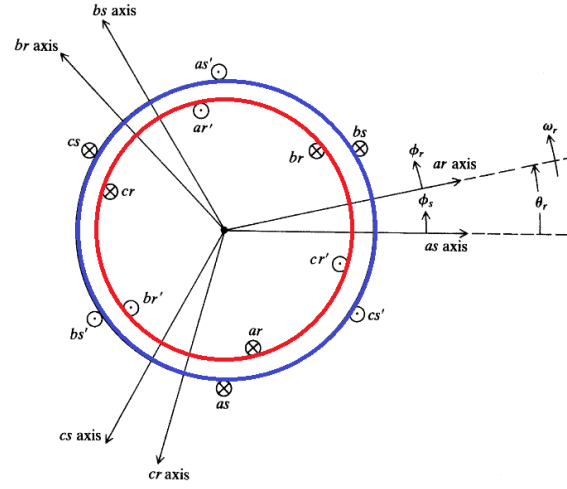


Fig. 2.7. Schematic diagram of a three-phase induction machine [48]

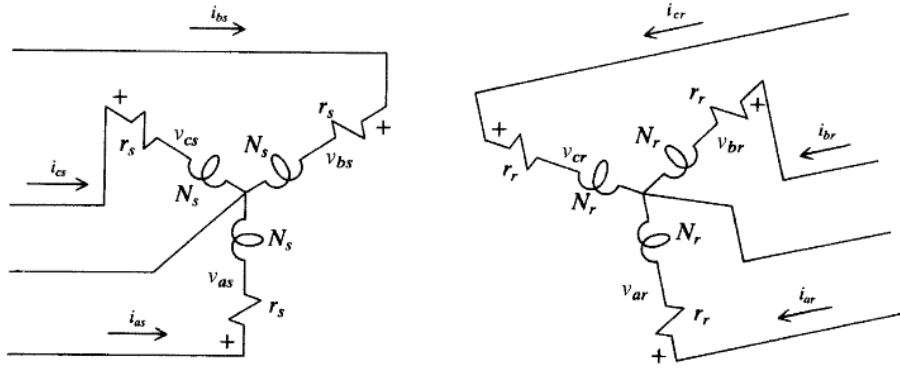


Fig. 2.8. Two-pole three-phase, wye connected symmetrical induction machine

Voltage is induced in the rotor phases by virtue of their velocity relative to the stator field, in accordance with Faraday's Law. The magnitude of the induced e.m.f, is proportional to the slip. If the rotor is stationary, then the induction machine may be regarded as transformer. Suppose the induced rotor voltage in each phase at standstill is V_r . Since the induced voltage is proportional to the rate of change of flux, the rotor voltage at a particular slip s will be, *rotor voltage* = sV_r .

2.5.2. Equivalent Circuit of Induction Generator

The single and double cage induction generators are used as fixed speed wind generators. The equivalent circuits of single and double cage induction generators are show in Figs. 2.9 and 2.10, respectively, where s denotes rotational slip [47],[49].

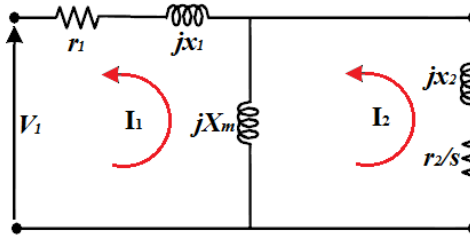


Fig. 2.9. Equivalent circuit of single cage induction generator

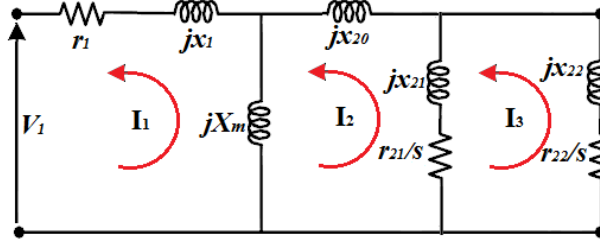


Fig. 2.10. Equivalent circuit of double cage induction generator

From the single cage equivalent circuit of an induction generator shown in Fig. 2.9, the loop equations can be derived as follows:

$$V_1 = -(r_1 + jx_m)I_1 + jx_m I_2$$

(2.13)

$$0 = jx_m I_1 - \left(\frac{r_2}{s} + jx_2 + jx_m\right)I_2 \quad (2.14)$$

From these two equations we can obtain the desired currents I_1 and I_2 . Again, from the equivalent circuit of a single cage induction generator, we can calculate the input power of the induction generator, $P_{IG_in\ Single}$, which is actually the output power of the wind turbine, as follows:

$$P_{IG_Single} = I_2^2 \frac{2(1-s)}{s} r_2 \quad (2.15)$$

From double cage equivalent circuit of the induction generator shown in Fig. 2.10, the loop equations can be derived as:

$$0 = jx_m I_1 - \left(\frac{r_{21}}{s} + jx_{21} + jx_{20} + jx_m\right)I_2 + \left(\frac{r_{21}}{s} + jx_{21}\right)I_3 \quad (2.16)$$

$$0 = \left(\frac{r_{21}}{s} + jx_{21} \right) I_2 - \left(\frac{r_{21}}{s} + \frac{r_{22}}{s} + jx_{21} + jx_{22} \right) I_3 \quad (2.17)$$

$$P_{IG_Double} = I_3 \frac{2(1-s)}{s} r_{22} + (I_3 - I_2)^2 \frac{2(1-s)}{s} r_{21} \quad (2.18)$$

From the equations above we can get the desired currents I_1 , I_2 , and I_3 . From the equivalent circuit of the double cage induction generator, we can calculate the input power of induction generator, $P_{IG_in_Double}$, as shown in Eq. (2.18). We can also calculate the output power of both single and double cage induction generators from the equivalent circuits shown in Figs. 2.9 and 2.10.

2.5.3. SCIG Wind Turbine Topology

A fixed speed wind turbine consists of a conventional, directly grid coupled squirrel cage induction generator (SCIG), which has some superior characteristics such as brushless and rugged construction, low cost, maintenance free, and operational simplicity. The slip and hence the rotor speed of a squirrel cage induction generator varies with the amount of power generated. These rotor speed variations are, however, very small, approximately 1 to 2 % of the rated speed. Therefore, this type of wind energy conversion system is normally referred to a fixed speed wind turbine generator system. The advantage of a fixed speed system is that it is relatively simple. Therefore, the list price of fixed speed turbine tends to be lower than that of variable speed turbines. However, fixed speed turbine must be more mechanically robust than variable speed turbines [50]. Because the rotor speed cannot be varied, fluctuations in wind speed translate directly into drive train torque fluctuations, causing higher structural loads than the case with variable speed operation. This partly cancels the cost reduction achieved by using a relatively cheap generating system.

A fixed speed wind turbine with SCIG is simplest electrical topology in a wind turbine concept. The schematic configuration of the fixed speed wind turbine is depicted in Fig. 2.11. It consists of SCIG directly connected to the grid, a soft-starter and a capacitor bank. The wind turbine transfers the kinetic energy of wind flow into mechanical energy. The SCIG transforms the mechanical power into electrical power and delivers the power directly to the grid system. Generally, the rotational speed of the generator is relatively high compared with that of wind turbine. Therefore, the wind turbine speed needs to be stepped up by using a multiple-stage gearbox with an appropriate gear ratio.

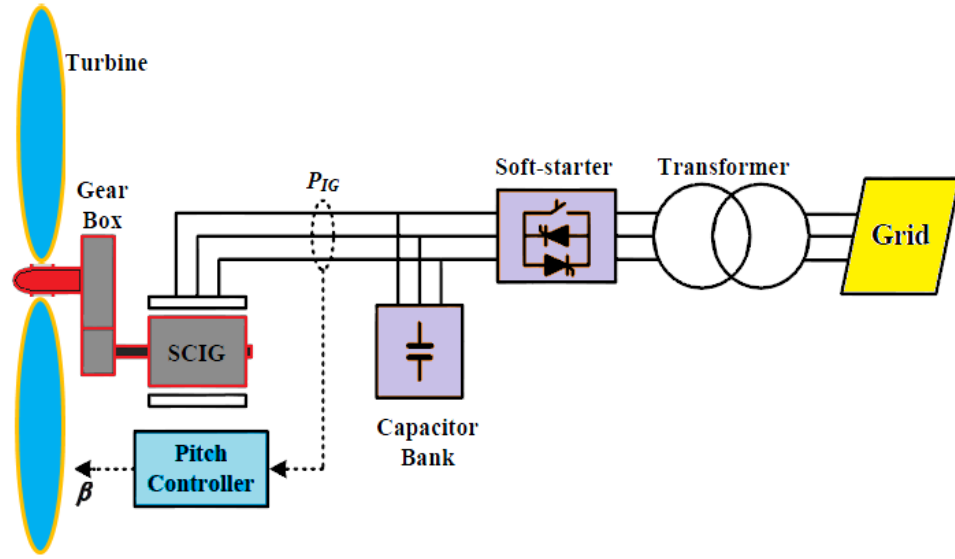


Fig. 2.11. Fixed speed wind turbine with SCIG configuration

The SCIG absorbs significant amount of reactive power from the grid. The reactive power consumption increases along with active power output. In order to compensate reactive power consumption a capacitor bank should be installed close to the generator terminal.

Since mechanical power is converted directly to electrical power by the generator, complex controller is not needed in the electrical part of a fixed speed wind turbine. However, a pitch controller is needed to regulate the pitch angle of the turbine blades (β) to keep power output of SCIG (P_{IG}) under the rated value. The advantages of a fixed-speed wind turbine are that it has a simple design with high reliability and has low investment and maintenance costs. However, low aerodynamic efficiency, high mechanical stress during gusty wind speeds, and difficulties in adapting to new grid compliances, such as fault ride-through and reactive power support, are the shortcomings of this concept.

2.6. Variable Speed Wind Turbine with PMSG

Another commercial trend of wind power generation is to use variable speed wind turbine (VSWT) driving a doubly fed induction generator (DFIG), wound field synchronous generator (WFSG) or permanent magnet synchronous generator (PMSG). The main advantage of variable speed operation is that more energy can be, in general, generated than that in the fixed-speed system. Although the electrical efficiency decreases due to the losses in the power electronic

converters that are essential for variable speed operation, the aerodynamic efficiency increases due to variable speed operation [50]. The aerodynamic efficiency gain can exceed the electrical efficiency loss, resulting in higher overall efficiency [51-52]. In addition, the mechanical stress is less, because the rotor can act as a flywheel (storing energy temporarily as a buffer), reducing the drive train torque variations. Noise problems are reduced as well, because the turbine runs at low speed. The main drawback of variable speed generating systems is that they are more expensive. However, using a variable speed generating system can also give major savings in other subsystems of the turbine such as lighter foundations in offshore applications, limiting the overall cost increase, etc.

2.6.1. PMSG Wind Turbine Topology

Typical configuration of a PMSG wind turbine is shown in Fig. 2.12. A direct-drive PMSG wind turbine uses a synchronous generator whose rotor is excited by permanent magnets and whose stator windings are connected to the grid through a full-rating power converter. The large number of poles mounted on the rotor allows the generator to operate at low speeds. This means that the gearbox can be omitted, and the generator is directly coupled to the wind turbine rotor.

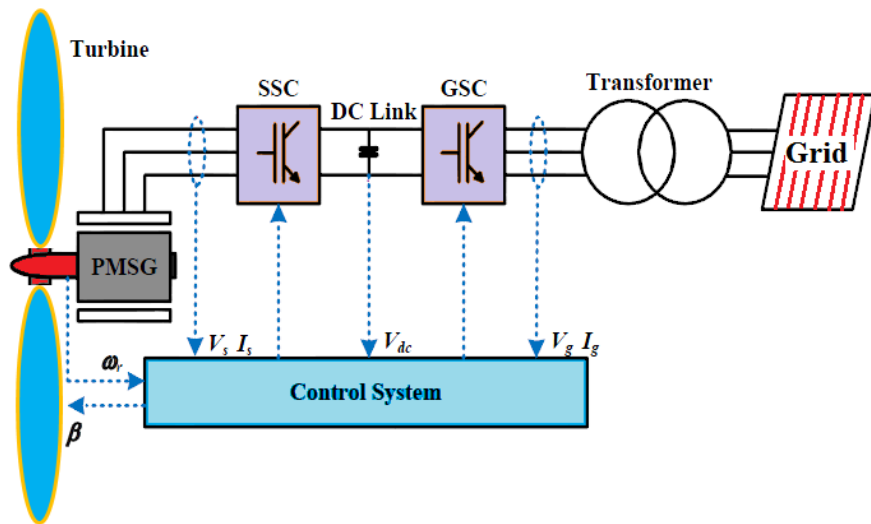


Fig. 2.12. Variable speed wind turbine with PMSG configuration

The back to back power converter consists of stator side converter (SSC) and the grid side converter (GSC) linked by a DC link circuit. The three-phase AC output of the generator is

converted to DC output, and then it is fed to an IGBT-based inverter. The GSC output is supplied to a step-up transformer, which delivers the energy to the grid system. The rating of the power converter depends on the rated power of the generator. The full scale power converters control the generated power and the power flow to the grid. In addition, it decouples the electrical grid frequency and the mechanical rotor frequency, and thus the variable speed generation can be possible.

2.6.2. PMSG based Wind Turbine Model [53]

The electrical model of PMSG wind turbine can be represented by the equivalent circuit shown in Fig. 2.13 [53]. The equivalent circuit model is divided in three parts; generator side, DC-link circuit, and grid side.

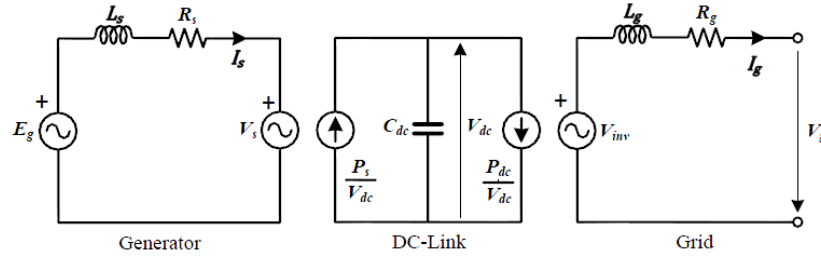


Fig. 2.13. Equivalent circuit of PMSG based wind turbine [53]

2.7. VSC-HVDC System

HVDC technology has been utilized in the electric power system for about sixty years since the first commercial link was put into operation between Sweden mainland and the island of Gotland in 1954. Today, it can be categorized in two types based on the switching devices employed in the converter, CSC-HVDC (Current Source Converter High Voltage Direct Current) and VSC-HVDC (Voltage Source Converter High Voltage Direct Current). CSC uses thyristor valves as switching devices. It is a kind of Line Commutated Converter (LCC) because thyristor can only be switched off when the current through it passes zero, and therefore, it requires line voltage for commutation. CSC-HVDC is suitable for high voltage bulk power and long distance transmission projects without the effect of capacitance along the long transmission line [54]. The typical examples are the Ultra HVDC (UHVDC) projects commissioned recently in China, which transmit about 6000MW power from hydro plants to the load area about 2000 km away through

two overhead lines with ± 800 kV dc voltage. Other applications include e.g. connection of two unsynchronized ac grids, or even grids with different system frequency.

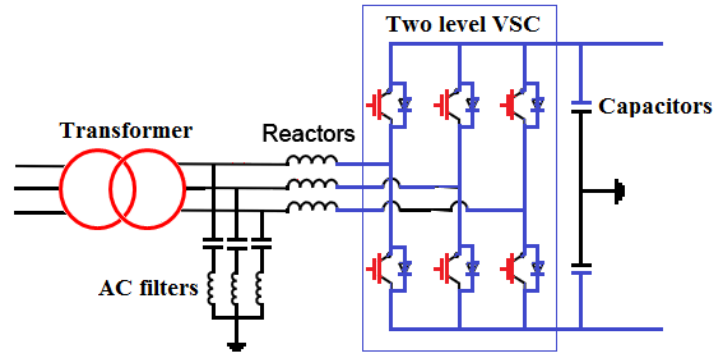


Fig. 2.14. Typical configuration of VSC-HVDC with two-level converter.

The configuration of VSC-HVDC system using two-level VSC is shown in Figure 2.14. Insulated Gate Bipolar Transistor (IGBT) is commonly used with Pulse-Wide Modulation (PWM) control method in VSC-HVDC projects. The features of the VSC-HVDC are independent control of both active and reactive power, supply of passive networks and black-start capability, high dynamic performance and multi-terminal possibility.

2.8. Chapter Summary

In this chapter, the basic theory of energy extraction from wind is described briefly. Then, wind turbine, drive train and pitch angle control models of wind turbine generator system are presented. The fixed speed and variable speed wind turbine topology overview and electrical modeling system are explained and at the end of the chapter VSC-HVDC is briefly explained.

Chapter 3

Cooperated Stabilizing Control of PMSG based Grid Connected Wind Farm

This chapter proposes a control system design for cooperated stabilizing control of PMSG based grid connected wind farm. In this study, a wind farm composed of PMSGs and SCIGs is considered to be connected to multi-machine power system. Though outputs of the SCIG based wind turbines are collected on AC network, PMSG based wind turbines are integrated in DC network with single grid side converter. In order to contribute to frequency and voltage stabilizing control, controller system of the inverter is modified in order for its active and reactive powers to be delivered to the grid easily and effectively. Simulation analysis is performed by using PSCAD/EMTDC, in which comparative analysis between proposed control strategy and conventional strategy is performed.

3.1. Introduction

The rapid increase in installation of large-scale wind farm into the grid system would have a serious impact on the system stability due to the variation of generated power from wind generators [14]. This chapter investigates wind farm penetration effect on power system frequency characteristics, especially frequency drop when unexpected generation loss due to a fault in the grid system or load increase occurs. In general, governor droop characteristic and inertias of conventional power plants have a main impact on system frequency performance in severe network disturbance [55]. Frequency and voltage stabilities have become the main aspects that should be considered from a viewpoint of the security of electric power system. During severe network disturbance such as a short circuit fault, the terminal voltage of wind farm decreases significantly and active power from wind farm cannot be supplied to the grid system. Under such condition, large oscillation occurs in the power system frequency due to the loss of active power. Moreover, existence of Squirrel Cage Induction Generator (SCIG) based fixed speed wind generators in the wind farm can lead the power system to become weak due to their low fault ride through capability under network disturbance [56-58]. The SCIG absorbs large reactive power when a short circuit fault occurs in the grid system [29]. If reactive power is insufficient, the rotational speed of the

induction generator will be increased significantly because the developed torque of the generator decreases while the wind turbine continues to drive the SCIG.

Flexible AC Transmission System (FACTS) devices are often installed at wind farm for stabilizing its dynamic characteristics [59-60]. However, the installation of FACTS devices at a wind farm increases the system overall cost. Combined installation of PMSG (Permanent Magnet Synchronous Generator) and SCIG in a wind farm can be a good solution, because the PMSG can provide the required reactive power of SCIG during fault condition. Therefore, in this chapter control system design for cooperated stabilizing control of PMSG based grid connected wind farm is discussed.

The PMSG is attractive type of wind turbine concept because it is connected to the power grid system through the full power rating back to back converter. The back to back converter totally decouples the generator from the grid, and the converter permits very flexible control of active and reactive powers in cases of normal and disturbed grid conditions [47],[61]. Back to back converter consists of generator side converter and grid side converter linked by DC circuit with a capacitor. Accordingly, installation of DC network in PMSG based wind farm is possible. In this chapter, control strategy of DC network in PMSG based wind farm is discussed. The modified controller system of the inverter is proposed in order for its active and reactive powers to be delivered to the grid easily and effectively.

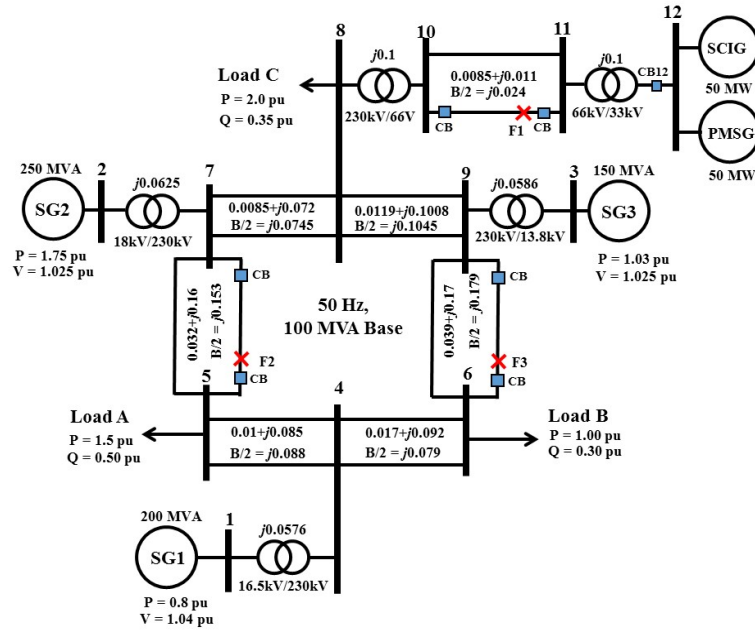


Fig. 3.1. Multi-machine power system model with wind farm connected

3.2. Power System Model

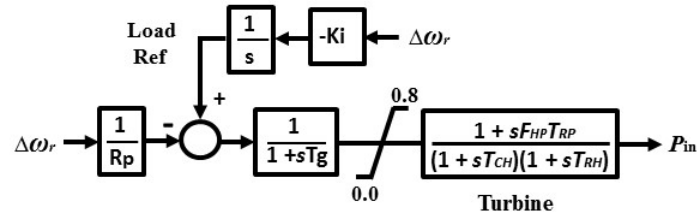
The model system used in this study is shown in Fig 3.1, in which the 9-bus main system consists of three conventional power plants, three static loads (Load A, Load B, and Load C), and a wind farm. The conventional power plants are composed of two thermal power plants (SG1 and SG2) and a hydro power plant (SG3). SG1 is operated under Automatic Generation Control (AGC), SG2 and SG3 are operated under Governor Free Control. The wind farm consists of two types of wind generators, i.e., five variable speed PMSGs each rated at 10 MW and fixed speed SCIG rated at 50 MW. Wind farm is connected to the main system through 66kV double circuit transmission line. Parameters of the three synchronous generators are shown in Table 3.1.

Table 3.1. Parameters of synchronous generators

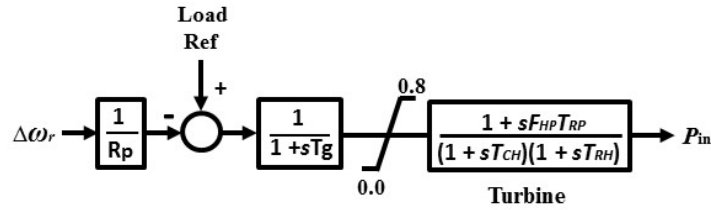
Synchronous Generator			
Gen. name	SG1 (AGC)	SG2 (GF)	SG3 (GF)
Power	200 MVA	250 MVA	150 MVA
R_a	0.003 pu		0.005 pu
L_l	0.1 pu		0.1 pu
X_d	2.11 pu		1.2 pu
X_d'	0.35 pu		0.35 pu
T_{do}'	8.6 s		8.17 s
X_d''	0.21 pu		0.3 pu
T_{do}''	0.03 s		0.03 s
X_q	2.02 pu		0.7 pu
X_q''	0.21 pu		0.3 pu
T_{qo}''	0.03 s		0.07 s
H	4.0 s		4.8 s

3.3. Governor and AVR model

Fig. 3.2 shows thermal governor systems used in SG1 and SG2, where $R_p = 0.05$, $T_g = 0.2s$, $F_{HP} = 0.3$, $T_{RH} = 7.0s$, and $T_{CH} = 0.3s$ [55]. These are typical values for the turbine system. The governor system for SG1 is equipped with integral controller as AGC system. The AGC controls power reference according to deviation of generator rotational speed.



(a) System for SG1 with AGC



(b) System for SG2 without AGC

Fig. 3.2. Thermal governor model

The schematic diagram of hydro turbine and its governor system used in SG3 are shown in Fig. 3.3. The hydraulic turbine model is equipped with governor system including transient droop compensator, where $R_p = 0.05$, $T_g = 0.2s$, $T_R = 5.0s$, $R_T = 0.38$, and $T_w = 1s$ [55].

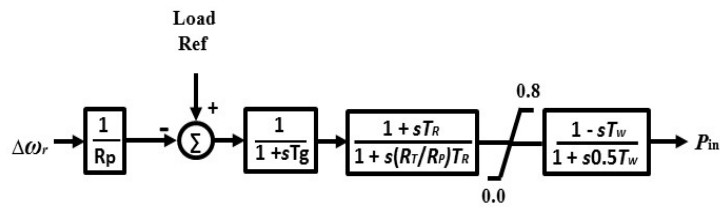


Fig. 3.3. Hydro governor model

Automatic Voltage Regulator (AVR) model in PSCAD/ EMTDC package [62] is used here. Fig. 4 shows the exciter model considered for all synchronous generator. The field voltage (E_f) is controlled by the AVR system to maintain the terminal voltage (V_t) at reference voltage (V_{ref}).

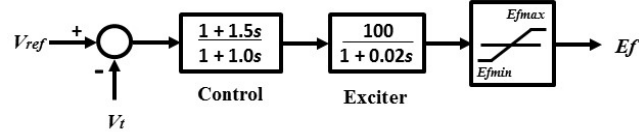


Fig. 3.4. AVR model

Table 3.2. Parameters of PMSG and SCIG

Wind Generator			
SCIG		PMSG (each)	
Power	50 MVA	Power	10 MVA
$R1$	0.066 pu	R_s	0.01 pu
$R21$	0.298 pu	Lls	0.06 pu
$R22$	0.018 pu	X_d	0.9 pu
$X1$	0.046 pu	X_q	0.7 pu
Xm	3.86 pu	$Flux$	1.4 pu
$X21$	0.122 pu	H	4.0 s
$X22$	0.105 pu		
H	3.0 s		

3.4. Wind Farm Model

Configuration of proposed wind farm model is shown in Fig. 3.5. The wind farm consists of five PMSGs with total capacity of 50 MW and one SCIG rated at 50 MW. PMSGs are connected to Bus 12 through a converter, 3kV DC cable, a main inverter and a 1.8kv/33kv transformer. Each PMSG is equipped with over-voltage protection system with variable load installed at output side of the converter. The variable load is used to absorb energy from the PMSG during fault condition to damp over-voltage on the DC line. The main inverter controls the DC line voltage and terminal voltage of Bus 12 to be rated values (3.0 kV). SCIG is connected to Bus 12 through a 0.69kV/33kV

transformer and single transmission line. A capacitor bank is installed at the terminal of SCIG to compensate the reactive power consumption by the induction generator. Parameters of PMSG and SCIG are shown in Table 3.2.

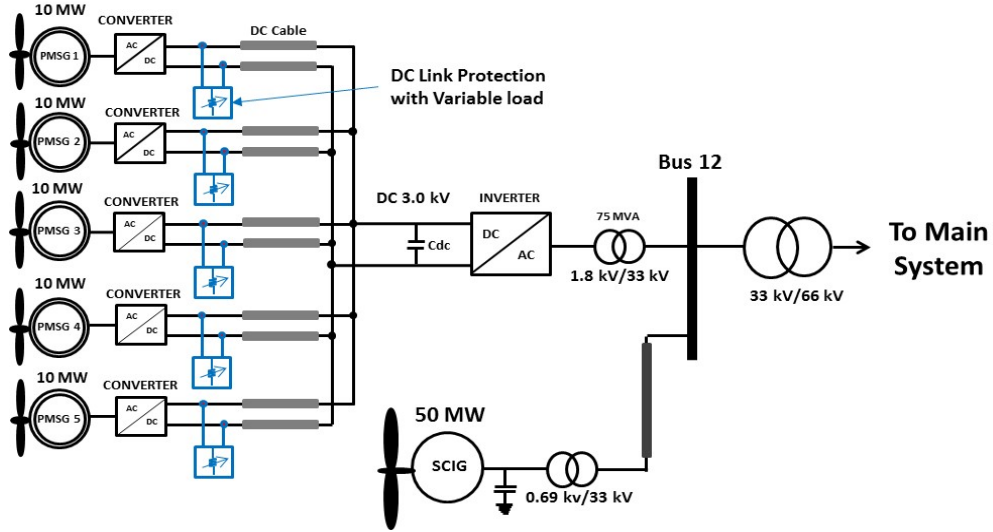


Fig. 3.5. Layout of wind farm

A configuration of PMSG based wind turbine and its control system is shown in Fig. 3.6. The wind turbine directly drives the rotor of PMSG. The stator of PMSG is connected to a converter. The converter transforms three phase voltage of PMSG into DC voltage. Three phase stator current (I_s) as well as active power (P_s) and reactive power (Q_s) are detected on the stator of the PMSG. The rotational speed (ω_r) is detected from the rotor. The active power and reactive power of PMSG are controlled by the converter.

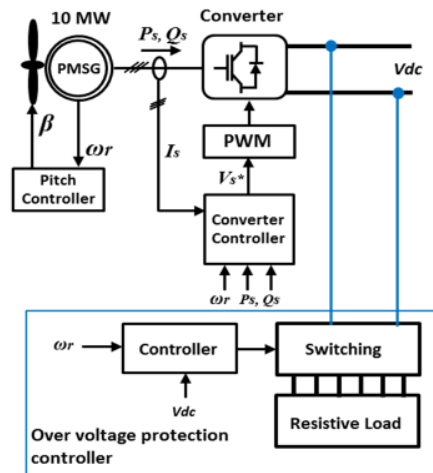


Fig. 3.6. Block diagram of PMSG

Detailed scheme of converter controller is depicted in Fig. 3.7. Aim of the converter controller is to control active and reactive power output of the PMSG. Three phase stator current of PMSG is transformed into d-axis and q-axis components by using Park transformation. The rotor angle position (θ_e) obtained from the rotor speed of PMSG is used in the transformation between abc and dq variables. The active power (P_s) and reactive power (Q_s) of the PMSG are controlled by the q-axis current (I_{sq}) and the d-axis current (I_{sd}), respectively. The active power reference (P_s^*) is obtained by the combination of MPPT and the proposed primary load frequency control. The reactive power reference (Q_s^*) is set to zero for unity power factor operation.

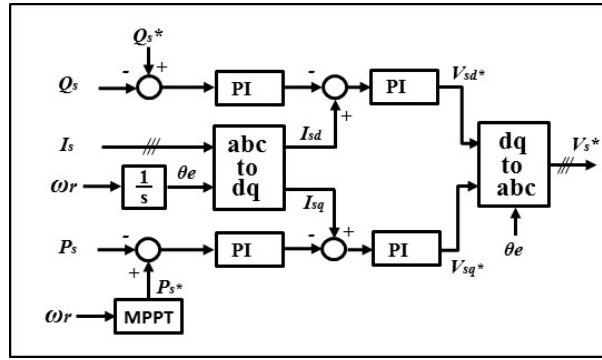


Fig. 3.7. Converter controller of PMSG

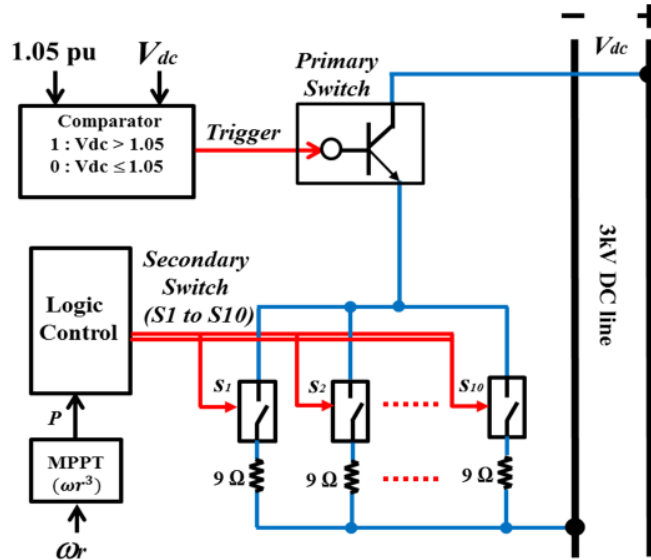


Fig. 3.8. Over-voltage protection system of DC line circuit (proposed)

Over-voltage protection controller is activated when DC voltage increases due to a short circuit fault in the grid system. Fig. 3.8 depicts detailed scheme of the over-voltage protection controller. Main part of the protection system consists of logic controller, switches, and resistive loads. When DC circuit voltage increases more than 1.05 pu, the primary switch will be triggered for absorbing the energy from PMSG. At the same time the secondary switches will be triggered by the logic controller to connect the resistive load. The secondary switches are selected by using program logic as presented in Table 3.3, where '1' and '0' indicate 'on' and 'off', respectively. 'on' and 'off' of the secondary switches depend on generated power (P) from the PMSG. The MPPT method can be used to calculate the power of PMSG.

Table 3.3. Logic control of over voltage protection system

Logic	switch number									
	$s1$	$s2$	$s3$	$s4$	$s5$	$s6$	$s7$	$s8$	$s9$	$s10$
$0 < P \leq 1.5$	1	0	0	0	0	0	0	0	0	0
$1.5 < P \leq 2.5$	1	1	0	0	0	0	0	0	0	0
$2.5 < P \leq 3.5$	1	1	1	0	0	0	0	0	0	0
$3.5 < P \leq 4.5$	1	1	1	1	0	0	0	0	0	0
$4.5 < P \leq 5.5$	1	1	1	1	1	0	0	0	0	0
$5.5 < P \leq 6.5$	1	1	1	1	1	1	0	0	0	0
$6.5 < P \leq 7.5$	1	1	1	1	1	1	1	0	0	0
$7.5 < P \leq 8.5$	1	1	1	1	1	1	1	1	0	0
$8.5 < P \leq 9.5$	1	1	1	1	1	1	1	1	1	0
$9.5 < P \leq 10$	1	1	1	1	1	1	1	1	1	1

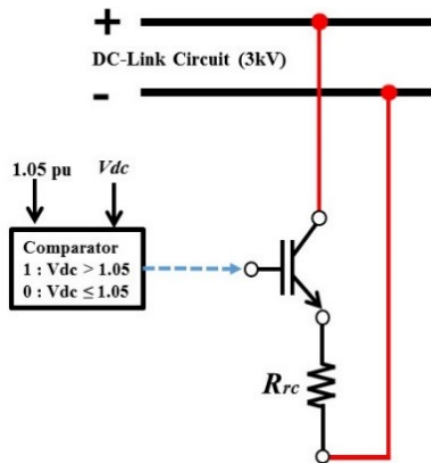


Fig. 3.9. DC-link protection system (conventional)

The control scheme of the DC-link conventional protection system used in this paper is shown in Fig. 3.9. The protection system consists of a switch and constant breaking resistance. The switch

circuit activates the DC-link protection when DC-link circuit voltage increases more than 1.05 pu due to a fault in the grid system, and then, the DC link circuit voltage is applied to the breaking resistance (R_{rc}) to consume the excess energy generated from the PMSG.

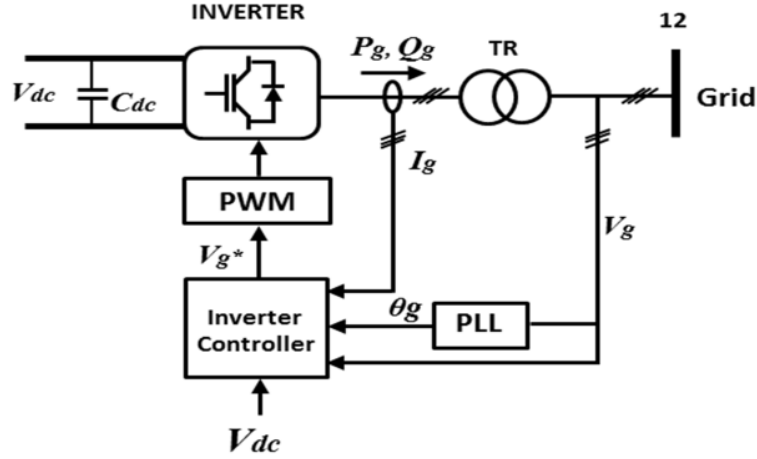


Fig. 3.10. Block diagram of inverter

Block diagram of the inverter and its control system are shown in Fig.3.10. The inverter converts DC voltage into three phase AC voltage. The inverter is connected to the grid through a step up transformer (TR). Three phase grid current is detected at low voltage side of the transformer and three phase grid voltage is detected at high voltage side of the transformer. In order to synchronize frequency between the inverter output and the grid system, Phase Lock Loop (PLL) is used. The inverter controls the grid voltage (V_g) and DC line voltage (V_{dc}) at rated values by controlling the d-axis (I_{gd}) and the q-axis (I_{gq}) currents, respectively. Detailed scheme of the inverter controller is shown in Fig.3.11.

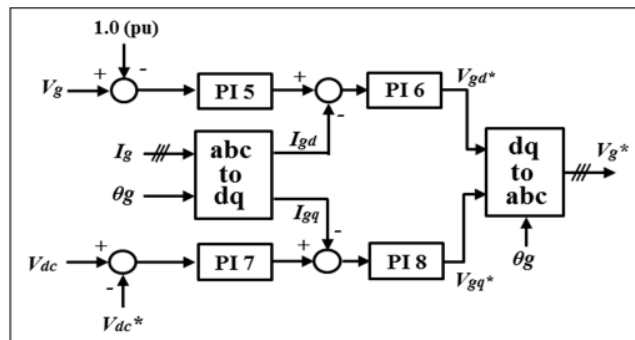


Fig. 3.11. Inverter control system

3.5. Wind Turbine Model

Extracted power from wind energy can be calculated as follows [63]:

$$P_w = 0.5 \rho \pi R^2 V_w^3 C_p(\lambda, \beta) \quad (3.1)$$

where P_w is the captured wind power (W), ρ is the air density (Kg/m³), R is the radius of rotor blade (m), V_w is wind speed (m/sec), and C_p is the power coefficient. The value of power coefficient is depending on tip speed ratio (λ) and blade pitch angle (β) of the wind turbine. Power coefficient of wind turbine can be calculated as follows [63]:

$$C_p(\lambda, \beta) = c_1 \left(\frac{c_2}{\lambda_i} - c_3 \beta - c_4 \right) e^{\frac{-c_5}{\lambda_i}} + c_6 \lambda \quad (3.2)$$

with

$$\frac{1}{\lambda_i} = \frac{1}{\lambda - 0.08 \beta} - \frac{0.035}{\beta^3 + 1} \quad (3.3)$$

And

$$\lambda = \frac{\omega_r R}{V_w} \quad (3.4)$$

where c_1 to c_6 are characteristic coefficients of wind turbine ($c_1=0.5176$, $c_2=116$, $c_3=0.4$, $c_4=5$, $c_5=21$ and $c_6=0.0068$) [64], and ω_r is rotational speed of turbine in rad/sec. Fig. 3.12 depicts the characteristic between the turbine power output and the rotor speed for different wind speeds where the blade pitch angle is set at 0 deg.

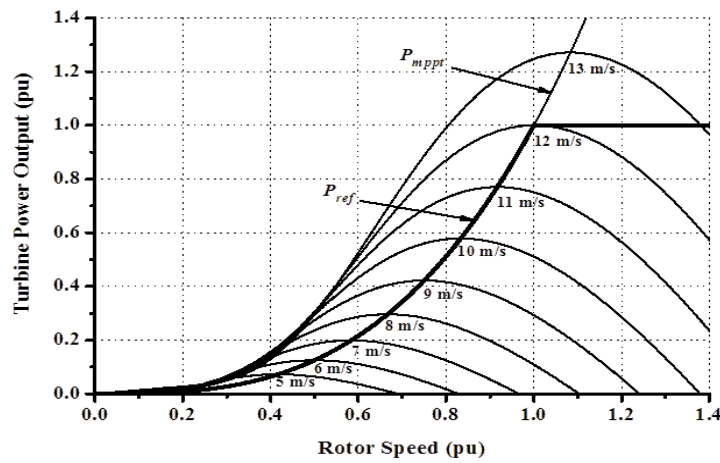


Fig. 3.12. Wind turbine characteristic

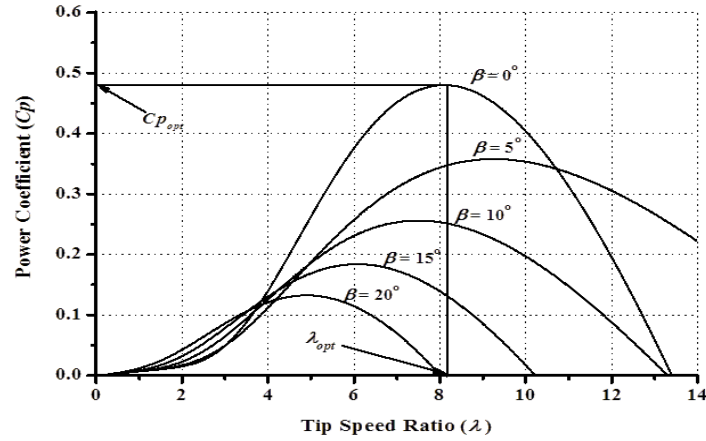


Fig. 3.13. $C_p - \lambda$ characteristic for different pitch angle

The $C_p - \lambda$ characteristics for different values of β are shown in Fig. 3.13. The optimum power coefficient is 0.48 at $\lambda = 8.1$.

3.6. Simulation Results

Simulation analysis has been performed on the power system model shown in Fig. 3.1 by using PSCAD/ EMTDC package software. The symmetrical three line to ground fault at the transmission lines in three locations (F1, F2, and F3) shown in Fig.3.1 are considered as network disturbance. The fault occurs at 1.1 sec; the circuit breakers (CBs) on the faulted line are opened at 1.2 sec, and at 2.0 sec the CBs are re-closed. The wind speeds for both types of wind generators are kept constant at the rated wind speed, assuming that the wind speed does not change so much in the short time interval. Two cases are investigated to compare the dynamic responses in transient condition between the proposed control strategy and the conventional strategy. Fig. 3.14 shows the wind farm model system used in the conventional control strategy and referred as Case 1, while the proposed control strategy of wind farm shown in Fig. 3.5 is referred as Case 2. In Case 1, the conventional protection system shown in Fig. 3.9 is added to the DC-link circuit. The pulse signal to trigger the IGBT is activated when V_{dc} exceeds 1.05pu, and thus the switch is turn on and the energy is dissipated in the breaking resistance.

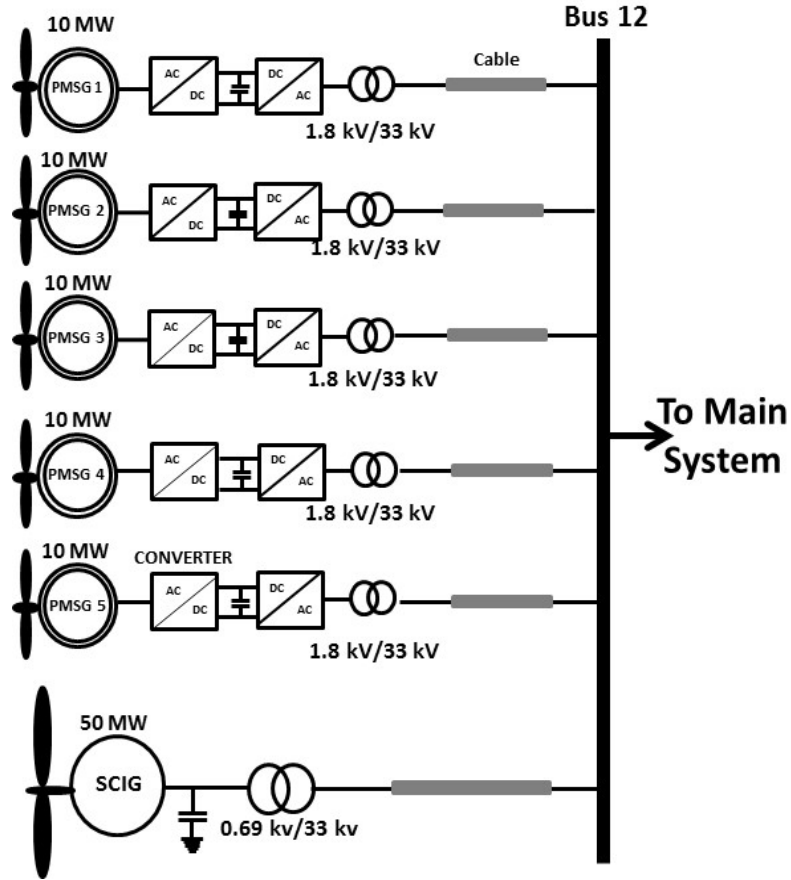


Fig. 3.14. Wind farm model in Case 1

The terminal voltage responses of wind farm at Bus 12 for three fault locations are shown in Fig. 3.15. It can be seen that the voltage can return back to the initial value in Case 2. However, in Case 1 the voltage cannot return back to the initial value. Therefore, the wind farm is disconnected from the system by opening CB12 at 2.5 sec. Rotational speed of SCIG is shown in Fig. 3.16. It can also be seen that the rotational speed of SCIG increases significantly in Case 1 because active power output of the SCIG cannot be recovered after the fault as depicted in Fig. 3.17. Responses of real and reactive power outputs of PMSG based wind farm are shown in Fig. 3.18. Figs 3.19 and 3.20 show real power output and rotational speed of the conventional power plants (SGs), respectively. It can be seen that the real power and rotational speed of the SGs can return back to the initial condition in Case 2. However, the real power of the SGs in Case 1 increases significantly after the wind farm is disconnected. It is clearly understandable that the system becomes unstable in Case 1, which can also be seen from Fig. 3.21 where the system frequency collapses in Case 1 after the wind farm is disconnected.

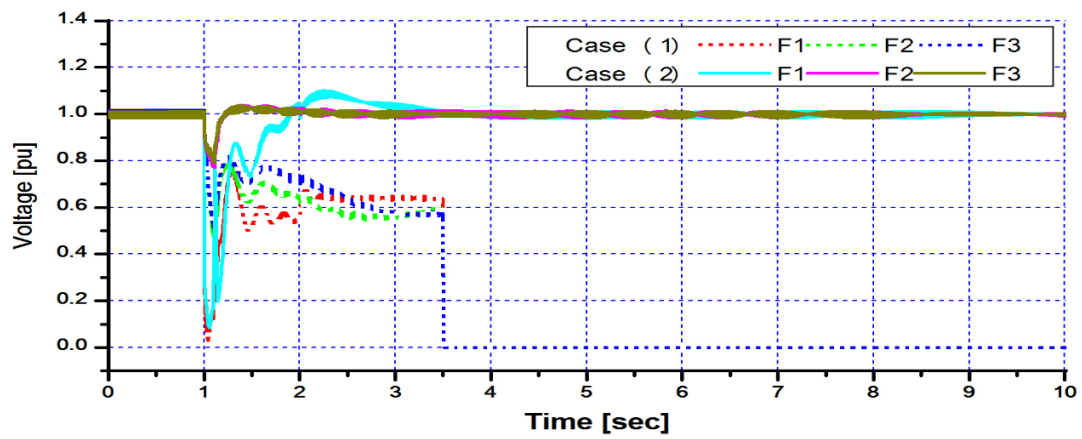


Fig. 3.15. Terminal voltage at Bus 12

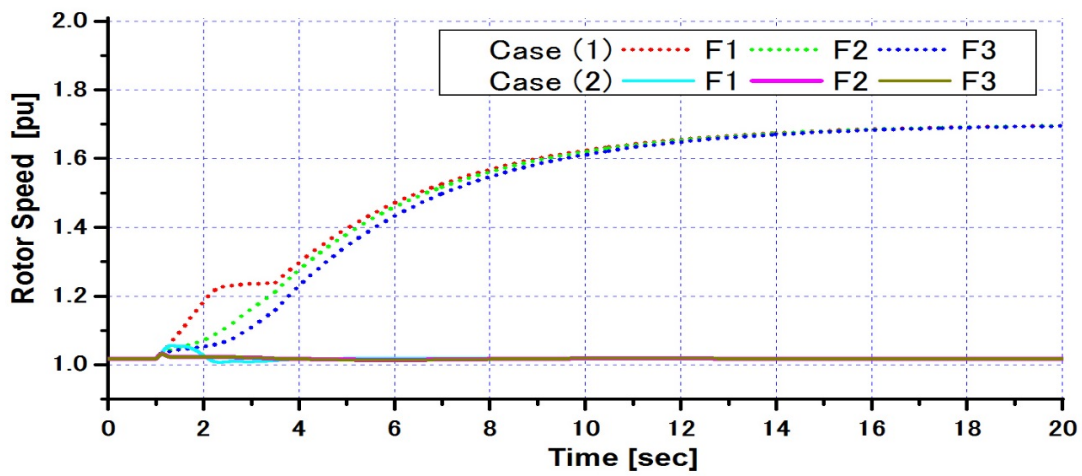
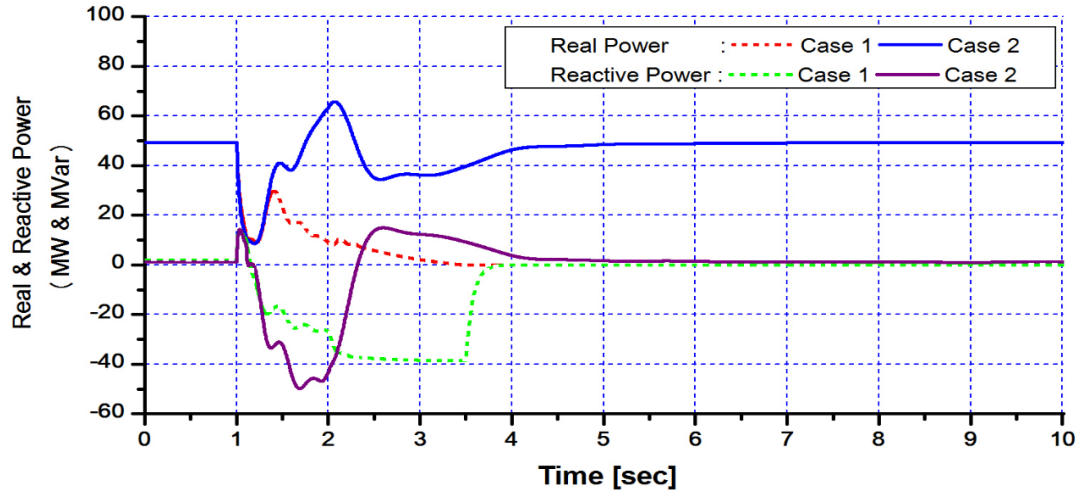
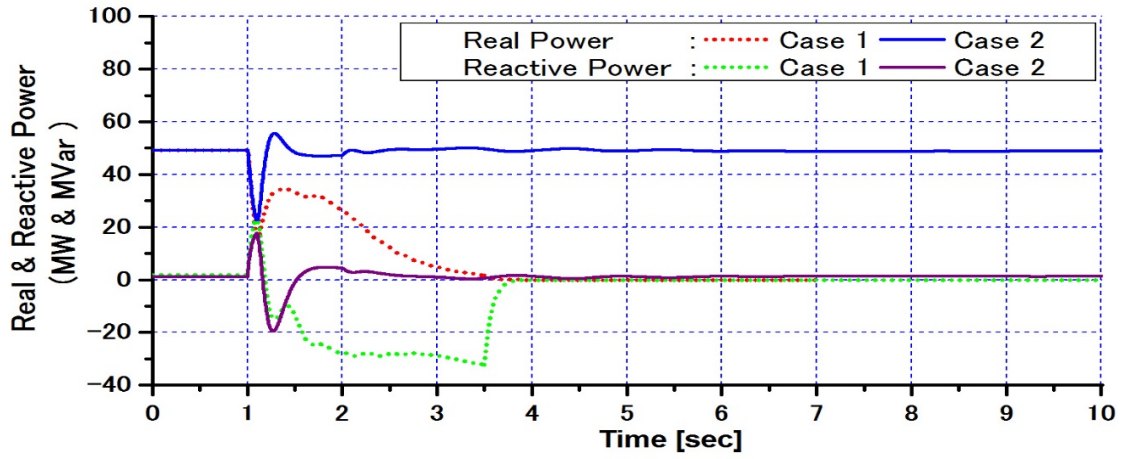


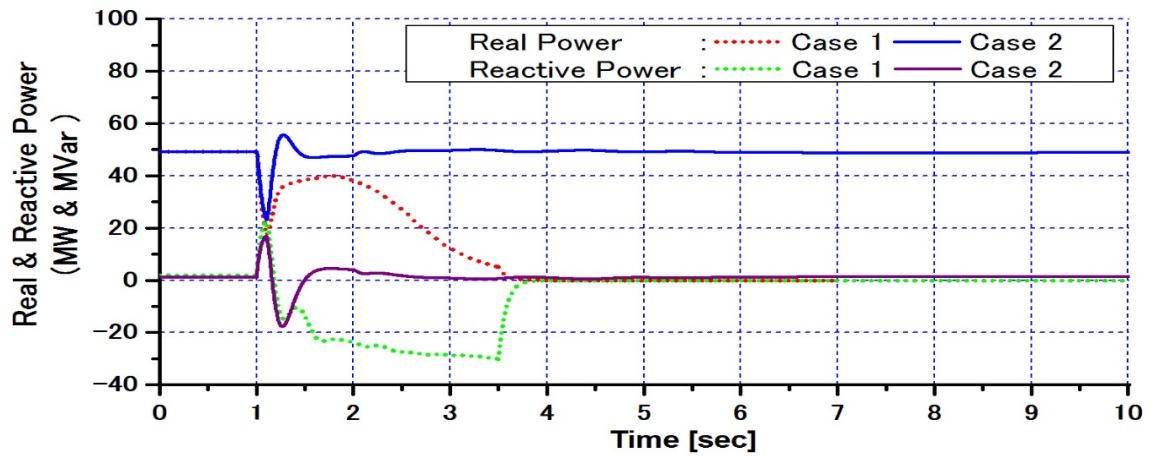
Fig. 3.16. Rotational speed of SCIG



(a) F1

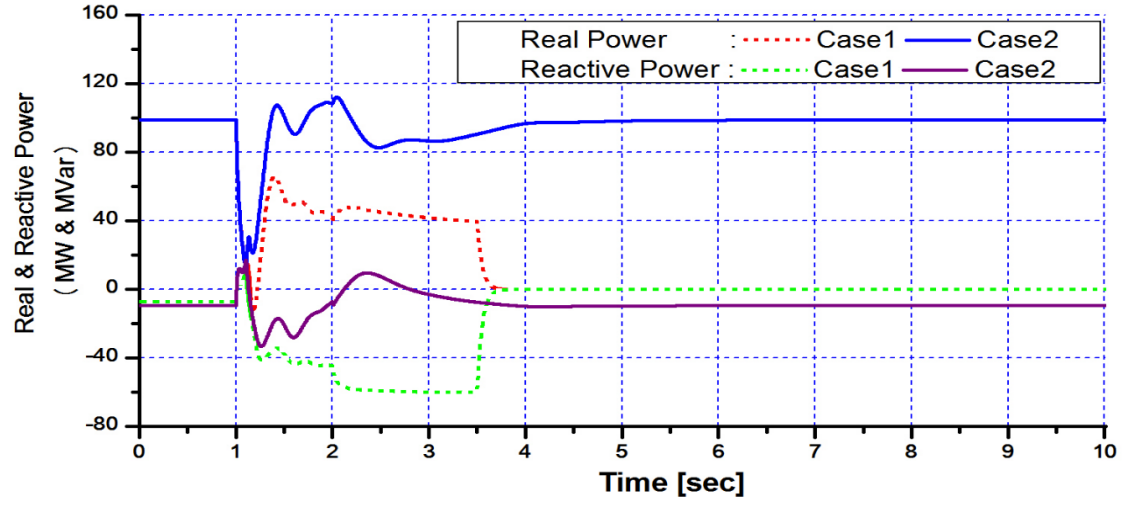


(b) F2

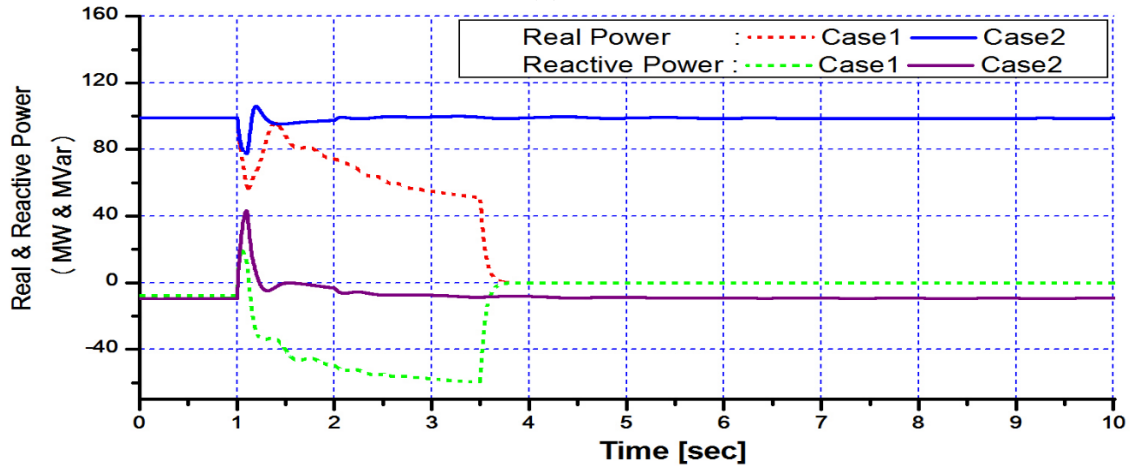


(c) F3

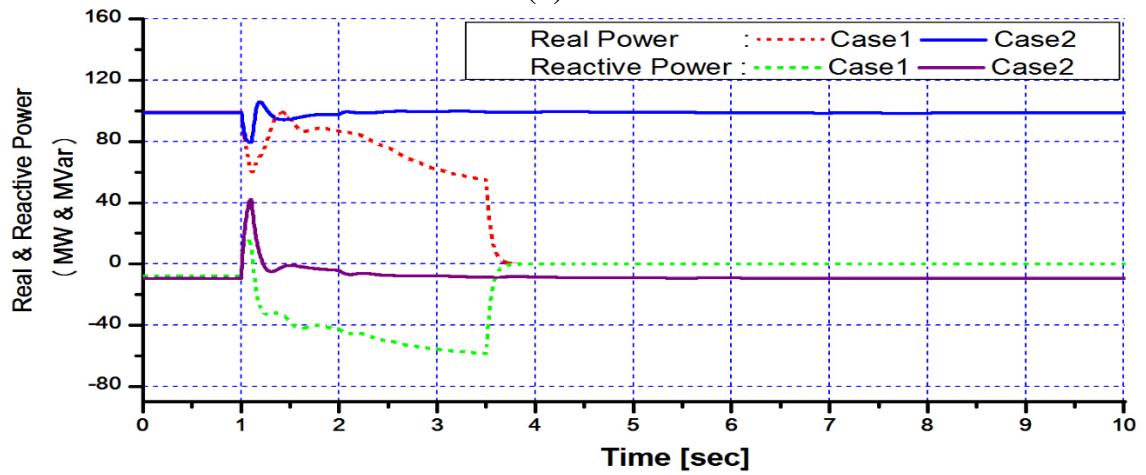
Fig. 3.17. Real and reactive power output of SCIG based wind farm



(a) F1

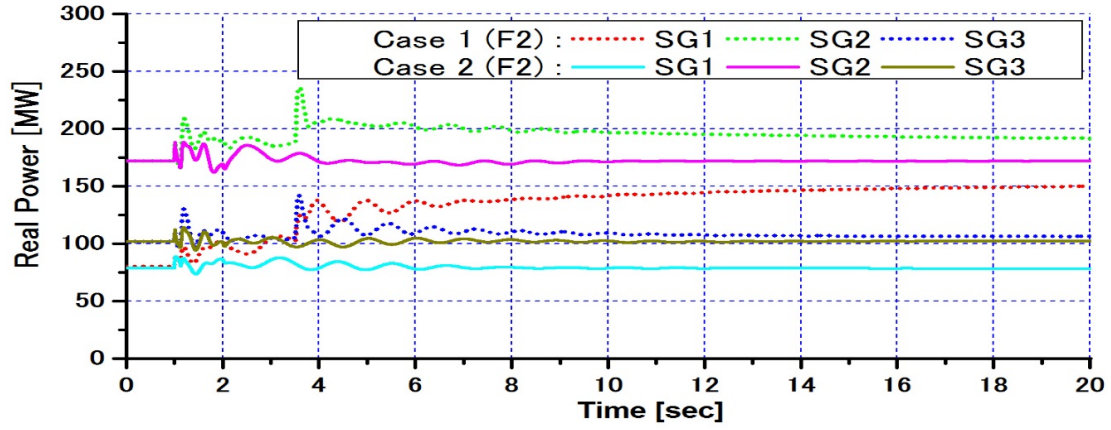


(b) F2

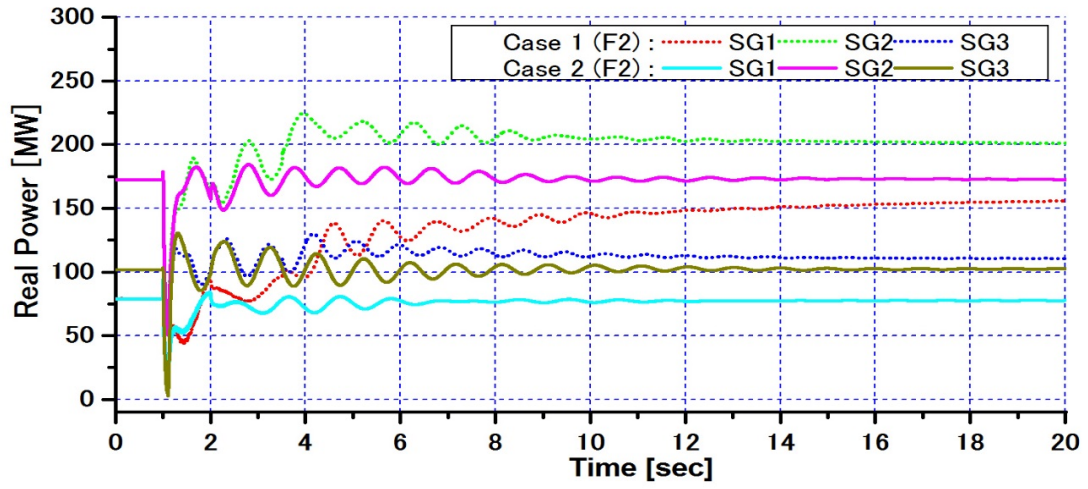


(c) F3

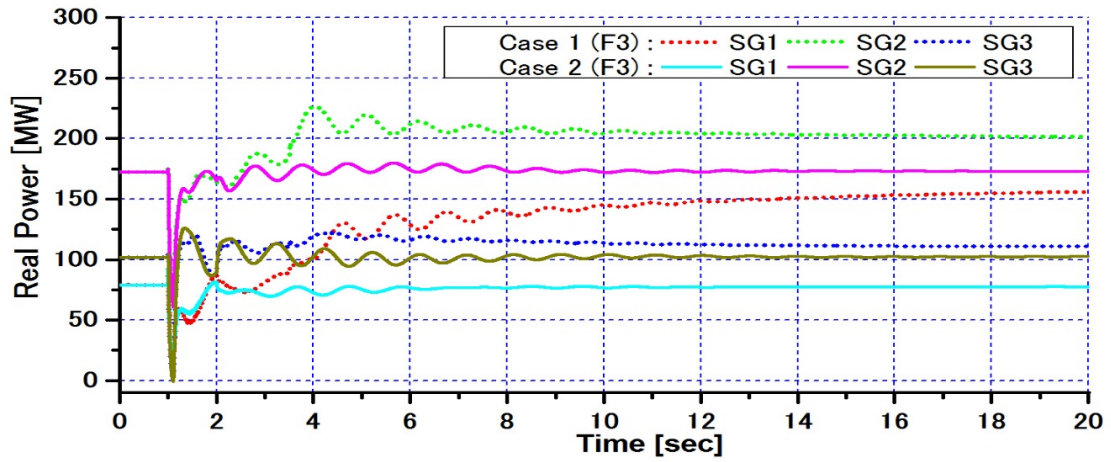
Fig. 3.18. Real and reactive power outputs of PMSG based wind farm



(a) F1

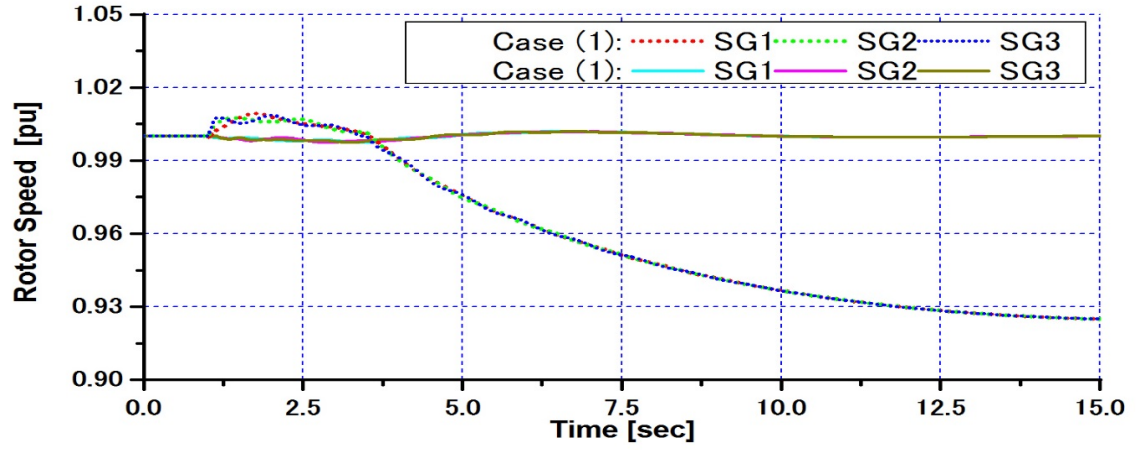


(b) F2

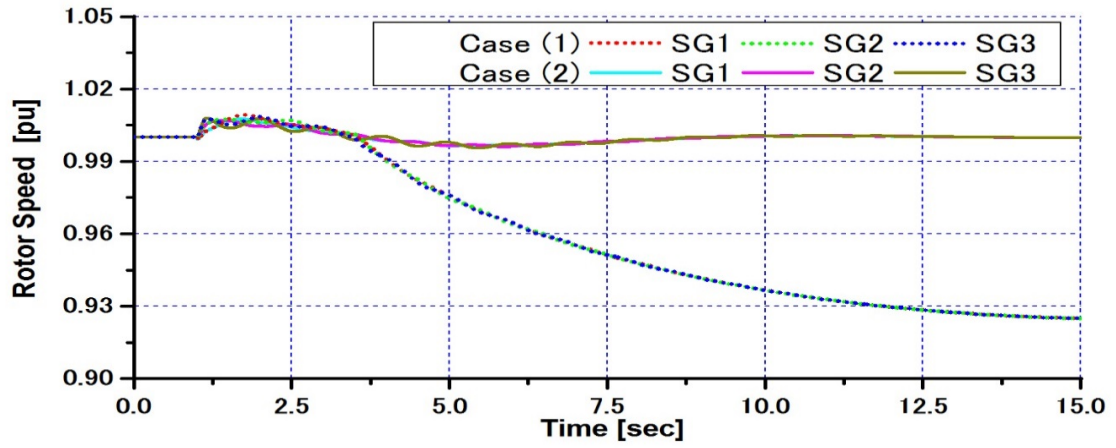


(c) F3

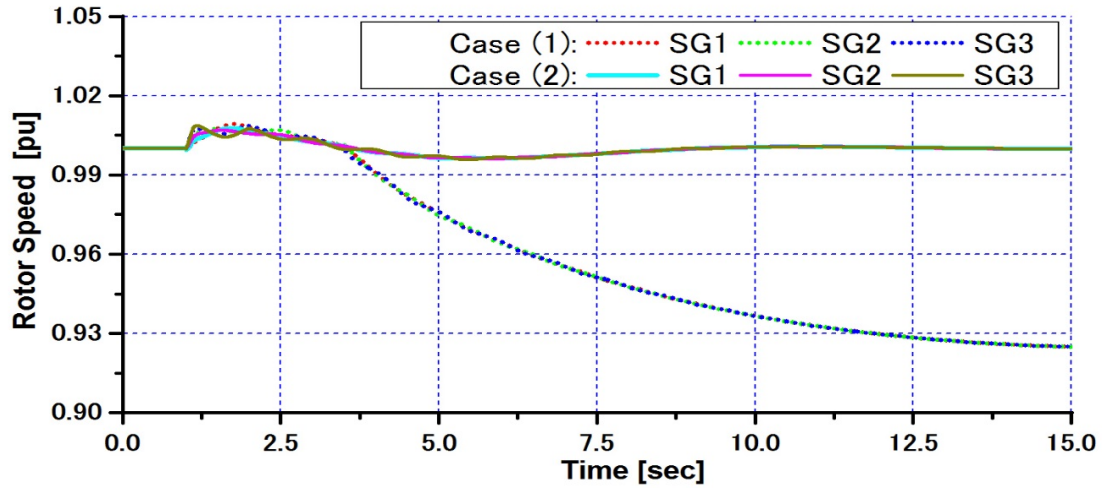
Fig. 3.19. Real power output of SGs



(a) F1



(b) F2



(c) F3

Fig. 3.20. Rotational speed of SGs

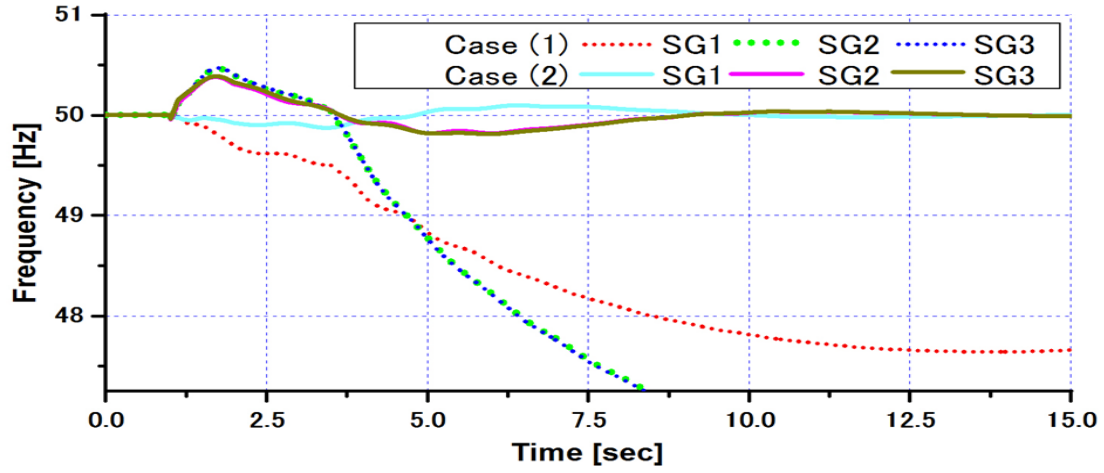


Fig. 3.21. Frequency response of the power system

3.7. Chapter Summary

A new control system for cooperated stabilizing control of PMSG based grid connected wind farm has been proposed. The simulation results show the proposed control system can enhance the fault ride through capability of the wind farm and also the transient stability of the grid system during a severe 3LG fault. Therefore it can be concluded that the proposed control strategy can contribute to enhance the stability of wind farm and connected power system during a network disturbance.

Chapter 4

Enhancement of DC-Link Protection of PMSG based Wind Turbine under Network Disturbance by using New Buck Controller System

In this chapter an improvement of DC-Link protection of PMSG based wind turbine under network disturbance by using new buck controller system is proposed. Protection system for DC-link circuit of back-to-back converter of PMSG (Permanent Magnet Synchronous Generator) based wind turbine is essential part for the system to ride through a network fault in grid system. Voltage on the DC-link circuit can be increased significantly due to power unbalance between stator side converter and grid side converter. Increase of DC-link circuit voltage can lead to a damage of IGBT of the converter and control system failure. The buck converter is used to control supplied voltage of a braking resistor to dissipate energy from the wind generator during network disturbance. In order to investigate effectiveness of the proposed DC-link protection system, fault analysis is performed in the simulation study by using PSCAD/EMTDC software program. In addition, comparative analysis between the proposed protection system and the conventional protection system using DC chopper is also performed.

4.1. Introduction

In many countries utilization of wind power is being encouraged by way of government's policy to establish the real commercial generation projects [65, 66]. Large scale of wind farms are planned in many countries not only for reducing the production of CO₂, SO₂ and NO_x but also for economic competition [66].

Over recent years, PMSG (Permanent Magnet Synchronous Generator) based variable speed wind turbine has become one of the most popular types of wind turbine generator. In this concept, PMSG is directly driven by a wind turbine without gear and is connected to the AC power grid through the power converter. Permanent magnet machines are characterized as having large air gaps, which reduce flux linkage even in machines with multi-magnetic poles [67-68]. PMSG system equipped with full rating power electronic converters has strong fault ride through capability during a network disturbance.

Currently, most of PMSG system studies consider normal operation, for example, realization

of maximum power point tracking. Studying on the PMSG system protection is not so much [28], meanwhile, enhancement of FRT (fault ride-through) capability is required for operating of wind farm. The wind farm should stay online during and after a network disturbance [69]. Therefore, enhancement of protection system of the wind generator is very important to be studied. When a fault occurs in the grid, a voltage dip appears at the terminal of wind generator and then the active power delivered to the grid is also reduced. As the generator side converter is decoupled with the grid, generator continues to generate the active power and thus the DC-link voltage increases due to the energy unbalance between the generator side converter and the grid side converter.

Usually, a simple DC chopper with a braking resistance is inserted into the DC-link circuit to dissipate the active power produced by PMSG in such a way that the active power balance in the DC-link circuit is maintained [29, 30, 31]. However, it can have a problem if the active power coming from the PMSG is not balanced against the capacity of braking resistor. This is because the capacity of resistor in the protection system with a simple DC chopper is constant (uncontrolled). In order to solve the problem new topology of DC-link protection of PMSG by using buck converter is proposed in this paper.

4.2. PMSG Based Wind Turbine

A configuration of PMSG based wind turbine is shown in Fig. 4.1. The wind turbine directly drives the rotor of PMSG without a gear box. The stator winding of PMSG is connected to the grid system through fully rated power of back-to-back converter and a step up transformer (TR). The back-to-back converter consists of SSC (stator side converter) and GSC (grid side converter) linked by DC circuit. Typically, SSC controls active power (P_s) and reactive power (Q_s) of the generator by controlling its stator current (I_s). On the other hand, grid side converter maintains the DC-link voltage (V_{dc}) across DC capacitor (C_{dc}) to be constant and controls the reactive power (Q_g) injected to grid system by controlling the converter grid current (I_g) [70]. Both converters are constructed from IGBTs circuit of which switching is controlled by PWM (pulse wide modulation) technique. SSC is operated under variable frequency depending on the rotational speed of generator (ω_r) and GSC is operated under constant frequency depending on the grid system (50 Hz or 60 Hz). In order to synchronize frequency between the grid side converter output and the grid system, PLL (phase lock loop) is used [62]. The PLL generates a phase output signal (θ_g). A pitch controller is equipped with the wind turbine to control pitch angle of wind turbine blades (β)

when the rotational speed increases over the generator's maximum speed. DC-link protection circuit is installed parallel with the DC capacitor. The DC protection circuit limits the transient over-voltage of the DC-link circuit due to network disturbance such as a short circuit. The DC-link protection circuit protects both IGBTs of back-to-back converter and DC capacitor.

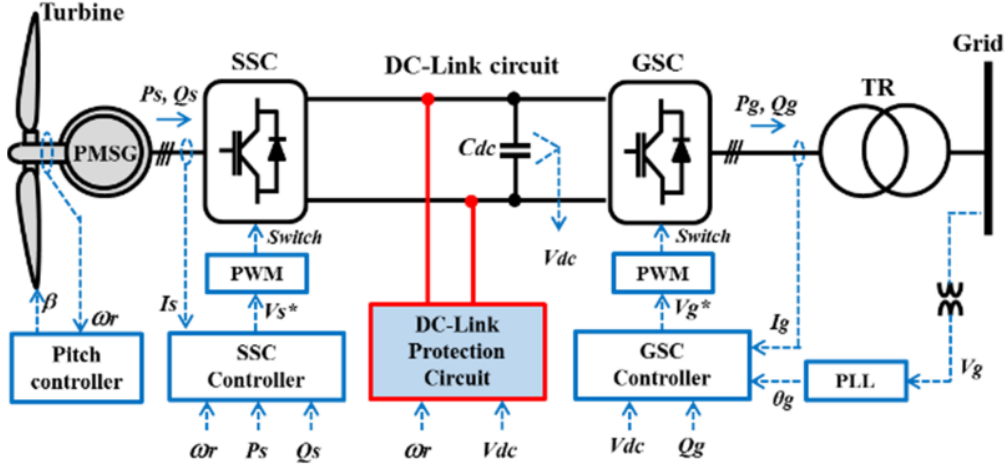


Fig.4.1. Configuration of PMSG based wind turbine.

4.2.1 Aerodynamic Model

The mathematical model expressing mechanical power extraction from wind can be written as follows [43]:

$$P_w = 0.5 \rho \pi R^2 V_w^3 C_p(\lambda, \beta) \quad (4.1)$$

where, P_w is the captured wind power (W), ρ is the air density (kg/m^3), R is the radius of rotor blade (m), V_w is wind speed (m/sec), and C_p is the power coefficient.

The power coefficient is depending on tip speed ratio (λ) and blade pitch angle (β) of the wind turbine. The power coefficient of the turbine can be obtained as follows:

$$C_p(\lambda, \beta) = c_1 \left(\frac{c_2}{\lambda_i} - c_3 \beta - c_4 \right) e^{\frac{-c_5}{\lambda_i}} + c_6 \lambda \quad (4.2)$$

with

$$\frac{1}{\lambda_i} = \frac{1}{\lambda - 0.08 \beta} - \frac{0.035}{\beta^3 + 1} \quad (4.3)$$

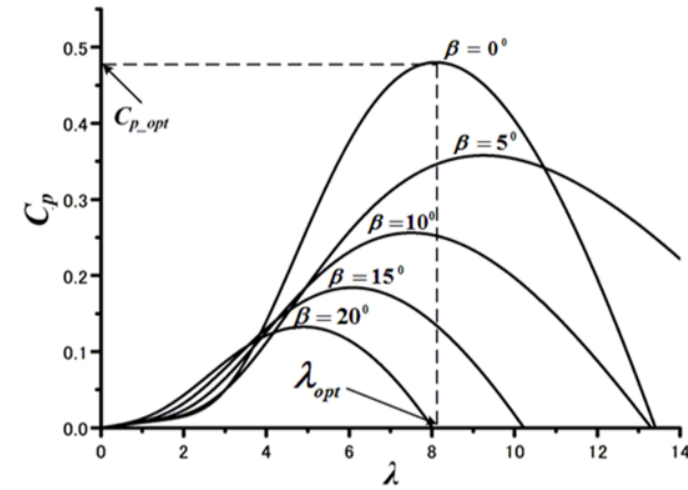
and

$$\lambda = \frac{\omega_r R}{V_w} \quad (4.4)$$

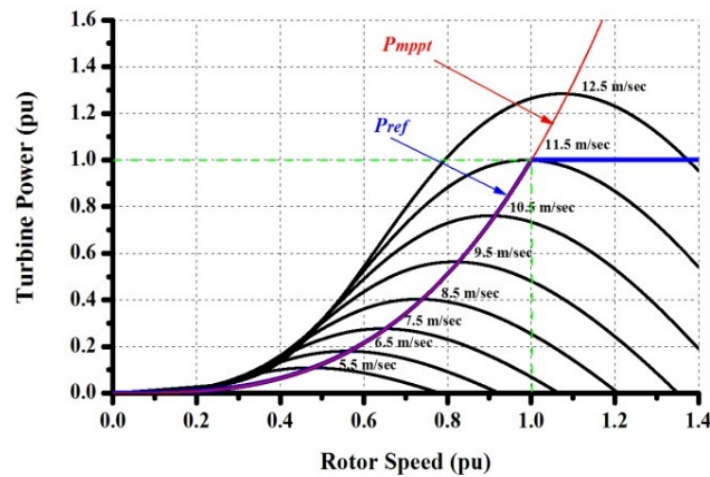
The characteristic coefficients of wind turbine, c_1 to c_6 , are $c_1 = 0.5176$, $c_2 = 116$, $c_3 = 0.4$, $c_4 = 5$, $c_5 = 21$, and $c_6 = 0.0068$ [64], and ω_r is rotational speed of turbine in rad/sec. The C_p - λ characteristic for different values of the pitch angle β is shown in Fig. 4.2a. The maximum value of C_p ($C_{p_opt} = 0.48$) is achieved for $\beta = 0^\circ$ and $\lambda = 8.1$. This value of λ is defined as the optimal value (λ_{opt}). Fig. 4.2b depicts the turbine output power as a function of the rotor speed with the blade pitch angle $\beta = 0^\circ$.

In variable speed wind turbines, the rotational speed of wind turbine is controlled to follow the MPPT (maximum power point trajectory) as follows:

$$P_{mppt} = 0.5 \rho \pi R^2 \left(\frac{\omega_r R}{\lambda_{opt}} \right)^3 C_{p_{opt}} \quad (4.5)$$



(a) C_p - λ characteristic for different pitch angle



(b) Power characteristic

Fig.4.2. Characteristics of wind turbine

4.2.2. Mechanical Model

The rotating mass of mechanical wind turbine system consists of wind turbine rotor, generator, and a gear box. It is known that the single rotating mass or one-lump mass is sufficient as shaft model for analyzing the impact of wind speed fluctuations [71, 72]. When the effect of a severe network disturbance in the power system is analyzed, however, at least two mass shaft model should be considered [55, 73]. Wind turbine rotor, generator, and a gear box can be represented as two mass inertia model. State space equations of the two mass drive train model are expressed as follows:

$$\frac{d}{dt}(\delta_t - \delta_g) = (\omega_t - \omega_g) \quad (4.6)$$

$$\frac{d}{dt}\omega_t = \left(\frac{1}{2H_t}\right) \left(T_m - D(\omega_t - \omega_g) - K(\delta_t - \delta_g)\right) \quad (4.7)$$

$$\frac{d}{dt}\omega_g = \left(\frac{1}{2H_g}\right) \left(D(\omega_t - \omega_g) + K(\delta_t - \delta_g) - T_e\right) \quad (4.8)$$

where,

H_t, H_g : Moments of inertia of wind turbine rotor and generator;

T_m, T_e : Wind turbine aerodynamic and electromagnetic torques;

ω_t, ω_g : Wind turbine rotor and generator speeds;

δ_t, δ_g : Angular positions of wind turbine rotor and generator rotor;

D_{shaft} : Damping coefficient;

K_{shaft} : Spring constants.

4.2.3. Pitch Control Model

Fig. 4.3 depicts a pitch controller system of wind turbine [71, 74]. The pitch controller of variable speed wind turbine usually regulates rotational speed of the rotor not to be over its setting value. The control loop of the pitch actuator is represented by a first-order transfer function with time constant (T_β) and the pitch rate limiter in this study. In this model, the blade pitch angle of wind turbine is kept to zero degree when the rotational speed is less than the setting value ($\omega_{set} = 1.21$ pu).

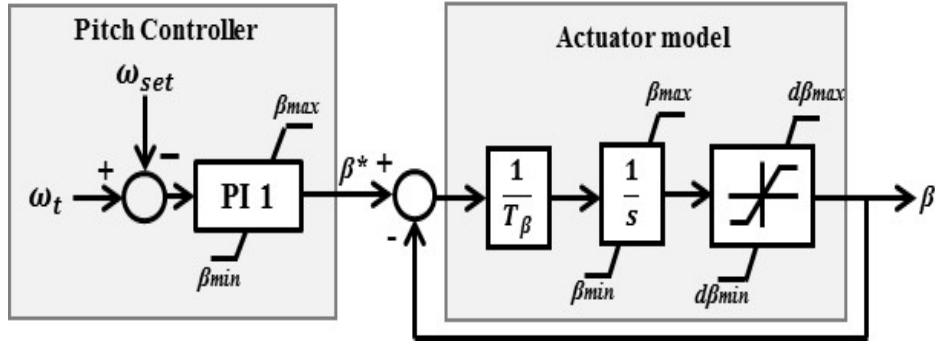


Fig. 4.3. Pitch controller model.

4.2.4. Permanent Magnet Synchronous Generator (PMSG) Model

Differential equations of permanent magnet synchronous machine can be expressed in the dq rotor reference frame, where all quantities in the rotor reference frame are referred to the stator [64]. The equations are expressed as follows:

$$L_{ds} \frac{di_{ds}}{dt} = V_{ds} - R_s i_{ds} + \omega_s L_{qs} i_{qs} \quad (4.9)$$

$$L_{qs} \frac{di_{qs}}{dt} = V_{qs} - R_s i_{qs} + \omega_s L_{ds} i_{ds} - \omega_s \psi_m \quad (4.10)$$

where, L_{ds} and L_{qs} are inductances of stator winding, R_s is the stator winding resistance, V_{ds} and V_{qs} are stator voltages, I_{ds} and I_{qs} are stator currents, ω_s is angular frequency of the stator, and ψ_m is the permanent magnet flux linkage.

4.2.5. Converter Controller System

Block diagram of SSC controller is depicted in Fig. 4.4. The aim of the SSC controller is to control active and reactive power output of PMSG. The active power and reactive power of the PMSG are controlled by the q-axis current (I_{sq}) and the d-axis (I_{sd}) current, respectively. The active power reference (P_s^*) is obtained by MPPT controller. The reactive power reference (Q_s^*) is set to zero for unity power factor operation.

Fig. 4.5 shows a block diagram of the GSC controller. The controller is used to control the reactive power output of GSC and DC-link voltage by controlling the d-axis (I_{gd}) and the q-axis (I_{gq}) output currents of GSC. The reactive power reference (Q_g^*) is set to zero and the DC voltage reference (V_{dc}^*) is set to 3.0 kV (rated value).

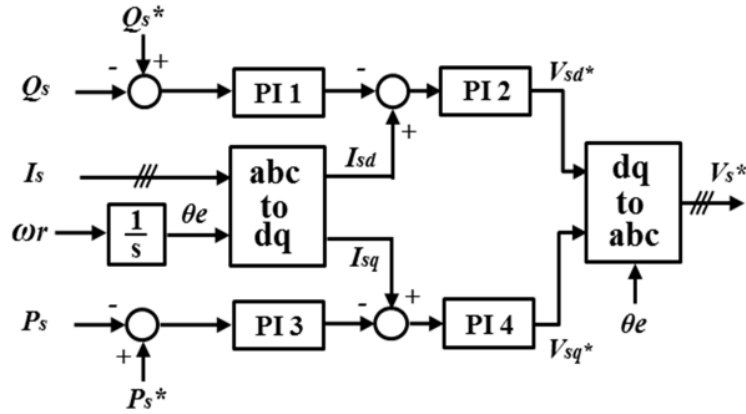


Fig. 4.4. Stator side converter controller system

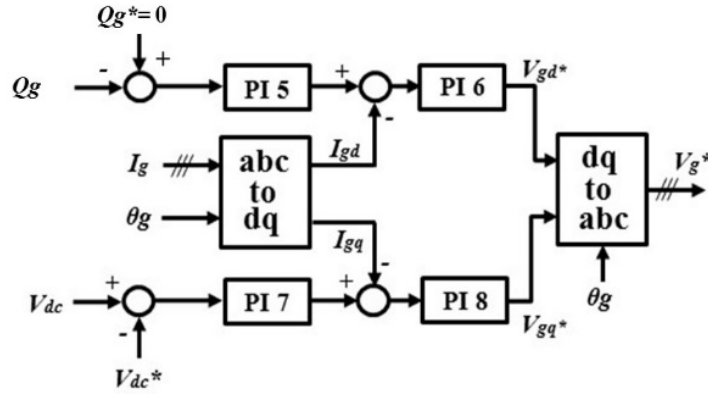


Fig. 4.5. Grid side converter controller system

4.3. DC-Link Protection System

During a network disturbance like a short circuit fault, output power of the PMSG at the grid side converter decreases and then over-voltage can appear in DC-link circuit of the back-to-back power converter of PMSG. During a fault condition, the DC-link voltage can suddenly increase due to the energy imbalance between the stator side converter and the grid side converter. The voltage increase can be controlled by inserting a braking resistor in the DC-link circuit to dissipate the excess energy through a power electronic switch as shown in Fig. 4.6. However, dissipated energy in the braking resistor cannot be controlled, and hence, energy imbalance between SSC and GSC can still appear. This can appear due to the imbalance between the output power from the generator and the power capacity of the resistor.

The detailed control scheme of the DC-link protection system proposed in this paper is shown in Fig. 4.7. The protection system consists of main switch circuit and buck converter circuit. Main switch circuit is used to activate the DC-link protection when DC-link circuit voltage increases more than 1.05 pu due to a fault in the grid system. The buck converter is used to control DC voltage (V_{rc}) across the breaking resistance (R_{rc}) depending on power generated from the PMSG (P). The power output of PMSG is determined from its rotational speed through maximum power point tracking controller. By using the information, generated power from PMSG and consumed power in the breaking resistance can be balanced, and then, dynamic stability of the PMSG can be enhanced.

Fig. 4.8 illustrates the basic principle of the buck-chopper composed of IGBT as a switch breaker [75]. During the period T_{on} the chopper is operated, and the source voltage will be connected to the load (R_{rc}) terminals. Furthermore, during the period T_{off} , the chopper is off, the current i_0 in R_{rc} will flow into the commutation diode (D_F), the load terminals are connected briefly through D_F , and V_{rc} becomes zero. Thus, the average value of the DC voltage at the load can be determined by the following equation.

$$e_o = V_{dc} \alpha \quad (4.11)$$

$$\alpha = D = \left(\frac{T_{on}}{T_{on} + T_{off}} \right) = \left(\frac{T_{on}}{T} \right) = f \cdot T_{on} \quad (4.12)$$

where,

e_o : DC voltage on the load;

V_{dc} : Voltage source;

α, D : Duty cycle;

T_{on} : Period of switch-on;

T_{off} : Period of switch-off;

f : Frequency;

T : Period.

If a fault occurs in the grid system, the grid side converter has a voltage dip on the grid side voltage. Therefore power sent from the converter to the grid is influenced. After the disturbance is cleared, the converter voltage returns to the normal, and then the active power will be supplied to the grid again. Power transferred from the GSC to the grid is given by Eq. (4.13) [76].

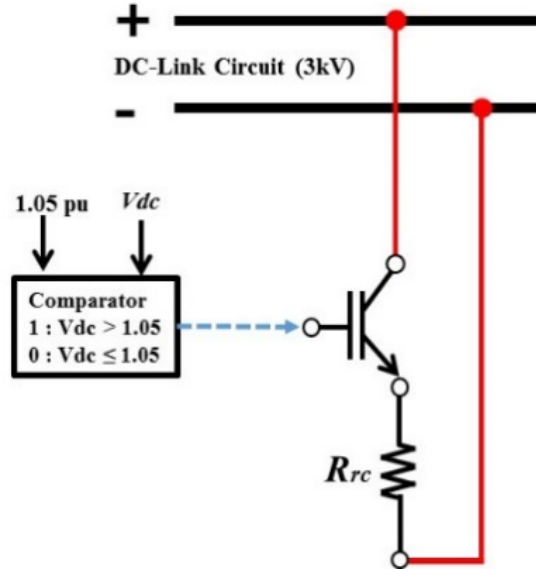


Fig. 4.6. Conventional DC-link protection system.

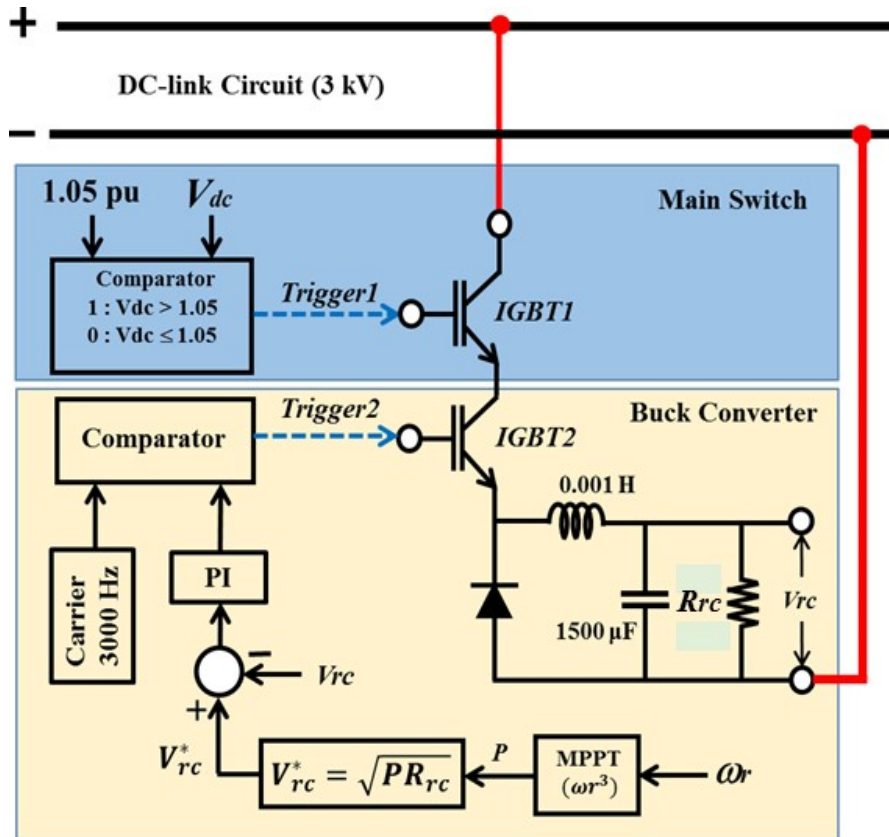


Fig. 4.7. Proposed DC-link protection system.

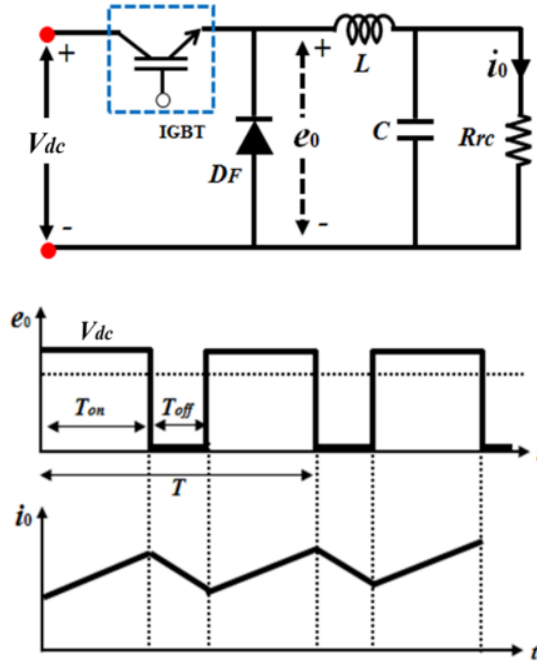


Fig. 4.8. Basic chopper step-down circuit

$$P_{cg} = \frac{V_c * V_g}{X_{ph}} \sin(\delta_c - \delta_g) \quad (4.13)$$

where,

P_{cg} : Power transferred from the converter to the grid;

V_c, δ_c : Converter terminal voltage (magnitude and phase of the fundamental component);

V_g, δ_g : Grid terminal voltage (magnitude and phase of the voltage grid);

X_{ph} : Reactance between V_c and V_g .

When V_g decreases to 0, the active power cannot be transferred to the grid, and then over-voltage as given in Eq. (4.14) appears in the DC-link circuit.

$$V_{dc} = \sqrt{\frac{2}{C_{dc}} \int (P_{WT} - P_{cg}) dt} \quad (4.14)$$

DC over-voltage can be controlled within a safe level if the excess power is discarded in several ways, for example, chopper controlled resistor. Resistor of the chopper can be determined as follows:

$$R_{rc} = \frac{V_{rated}^2}{P_{rated}} \quad (4.15)$$

$$I_{chop} = \frac{1.05 V_{rated}}{R_{chop}} = \frac{1.05 P_{rated}}{V_{chop}} = 1.05 I_{rated} \quad (4.16)$$

4.4. Simulation Analysis

4.4.1. Power System Model

The power system model considered in this analysis is shown in Fig. 4.9. A wind farm with power capacity of 25 MW composed of five PMSGs each rated at 5 MW is connected to a large power system through a 33 kV/66 kV, 25 MVA main transformer and 66 kV double circuit transmission line. The grid frequency is 50 Hz and system base is 25 MVA.

The parameters of PMSG based wind turbine are presented in Table 4.1. Temporary three-line to ground fault (3 LG) for 5 cycles (0.1 sec) is considered as network disturbance. The fault occurs at 1.0 sec. In this study, the different wind speed data are applied to each wind turbine as shown in Fig. 4.9.

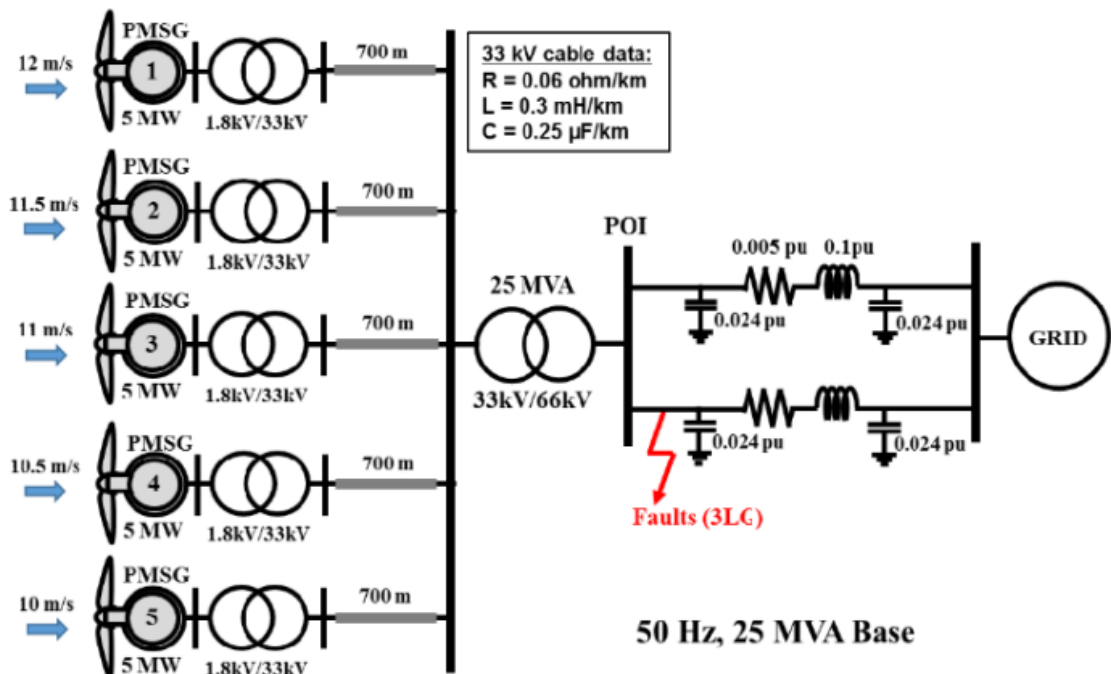


Fig. 4.9. Power system model

Table 4.1. Parameters of PMSG based wind turbine.

Generator parameter	Value	Drive train parameter	Value
Power	5 MW	H_g	0.45 s
Voltage	1,800 V	H_t	3.0 s
Frequency	20 Hz	D	1.5
R_s	0.017 pu	K	296
L_{ds}	0.96 pu		
L_{qs}	0.76 pu		
ψ_m	1.4		

4.4.2. Simulation Results

The proposed controller has been investigated through simulation analyses performed by using PSCAD/EMTDC. Two cases are considered as scenarios to confirm the effectiveness of the proposed control system. In Case 1, the proposed controller system shown in Fig. 4.7 is used for DC-link protection system. In Case 2, the DC link protection is performed by using conventional system shown in Fig. 4.6. In both scenarios wind speeds for each wind generator are kept constant to the values shown in Fig. 4.9 and value of R_{rc} is set at 1.0 pu.

Comparative simulation analysis of PMSG's dynamic responses has been performed between the proposed method (Case 1) and conventional method (Case 2), and the results are shown in the figures. Figs. 4.10-4.12 show the responses of DC-link circuit voltage during (3 LG) three lines to ground fault. In the simulation analysis, wind speeds of PMSG1, PMSG3, and PMSG5 are 12 m/sec, 11 m/sec, and 10 m/sec, respectively. It is seen from the figures that excess DC-link voltage can be well controlled in the proposed method. Figs. 4.13-4.15 show the rotor speed responses of PMSGs for Case 1 and Case 2, from which it is seen that transient oscillation of the rotor speed can be well controlled in the proposed method. Figs. 4.16-4.19 show responses of active and reactive power outputs of all the PMSGs, respectively. From the figures, it is seen that power drop and power swing during the fault can be reduced more significantly in the proposed method than the conventional method.

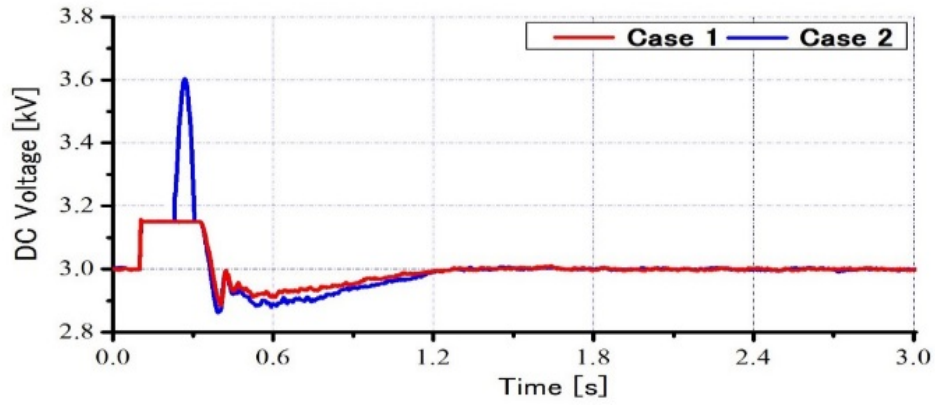


Fig. 4.10. DC-link voltage response of PMSG1 (12 m/sec)

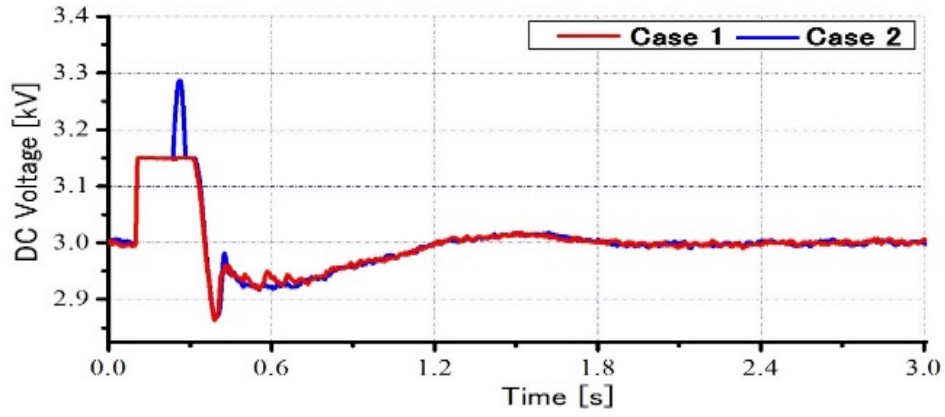


Fig. 4.11. DC-link voltage response of PMSG3 (11 m/sec)

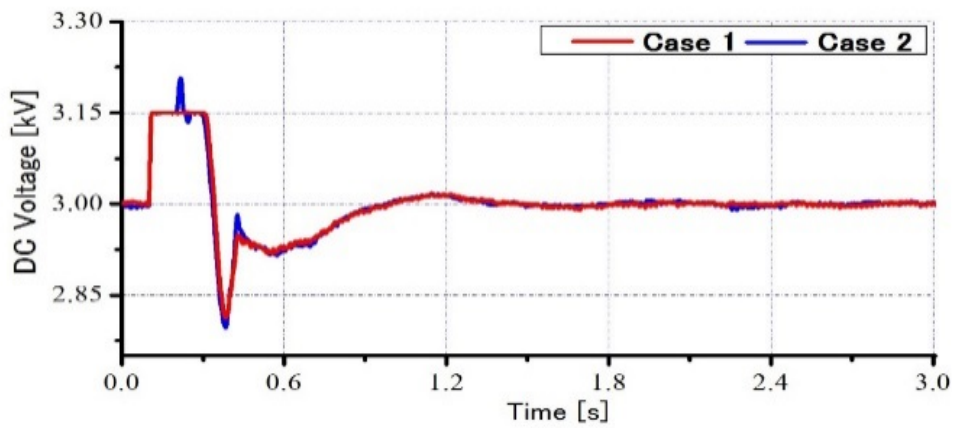


Fig. 4.12. DC-link voltage response of PMSG5 (10 m/sec)

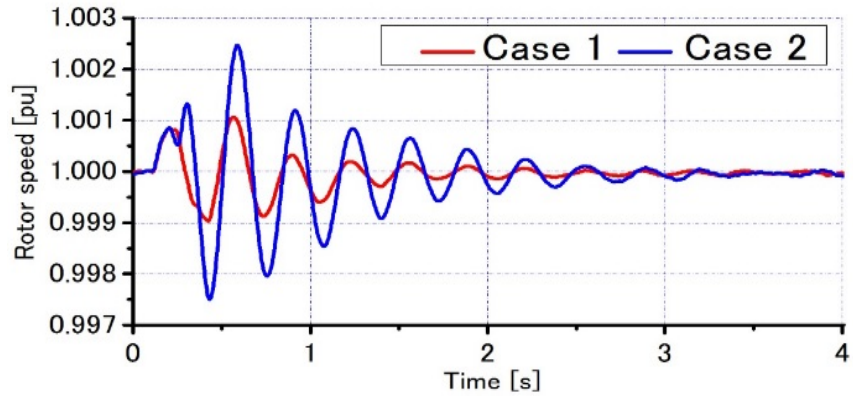


Fig. 4.13. Rotor speed response of PMSG1 (12 m/sec)

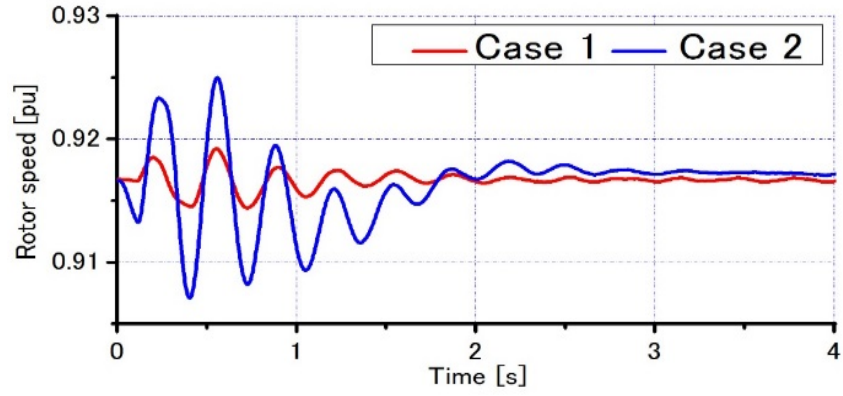


Fig. 4.14. Rotor speed response of PMSG3 (11 m/sec)

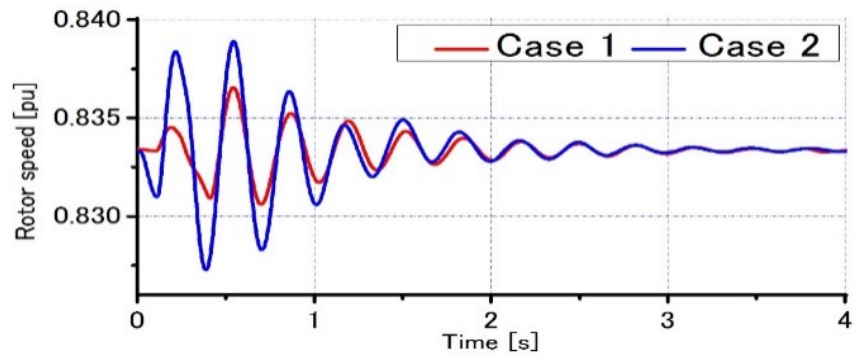


Fig. 4.15. Rotor speed response of PMSG5 (10 m/sec)

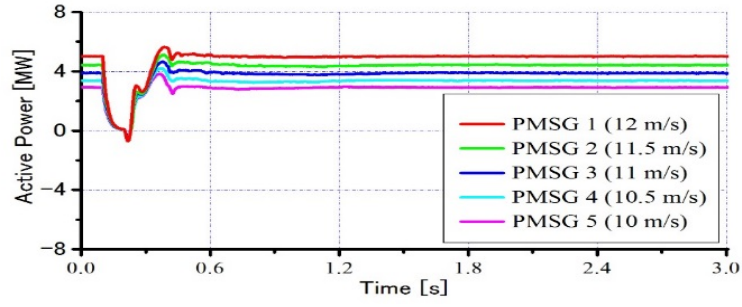


Fig. 4.16. Active power output of PMSGs in Case 1 (proposed method)

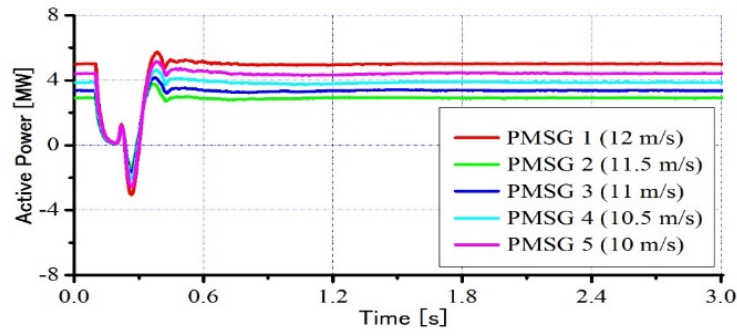


Fig. 4.17. Active power output of PMSGs in Case 2 (conventional method)

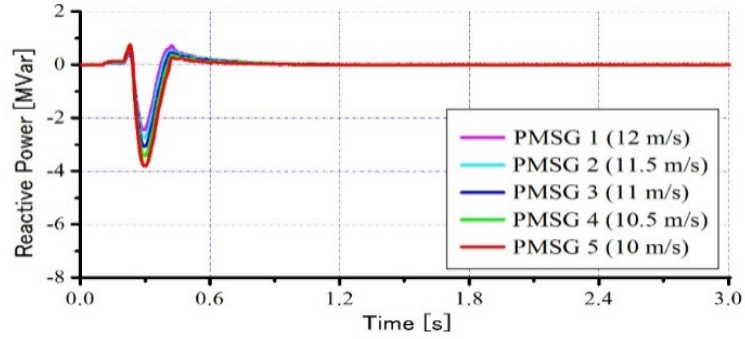


Fig. 4.18. Reactive power output of PMSGs in Case 1 (proposed method)

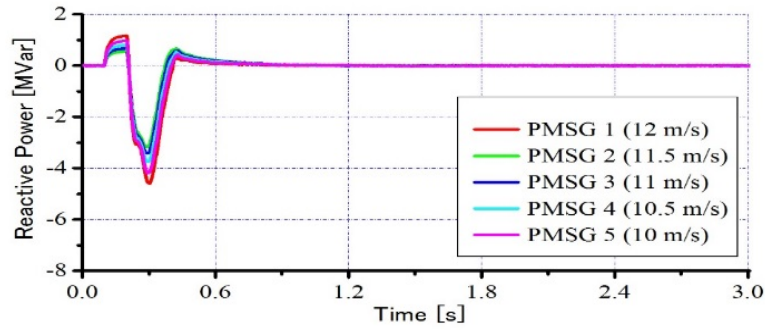


Fig. 4.19. Reactive power output of PMSGs in Case 2 (conventional method)

4.5. Chapter Summary

A new DC-link protection scheme using buck converter has been proposed for permanent magnet wind generator and its performance under network disturbance condition has been investigated through simulation analyses using PSCAD/EMTDC. Comparative simulation analysis has been performed for severe three-line to ground (3 LG) fault between the proposed DC-link protection system and the conventional protection system. From the simulation results, it is shown that the proposed method can control well the DC-link voltage as well as other dynamic responses of PMSG such as rotor speed and active power output. Therefore it can be concluded that the dynamic performance of PMSG can be enhanced by the proposed DC-link protection system.

Chapter 5

Wind Turbines Cluster System Composed of Fixed Speed Wind Generators Controlled by Cluster Converter based VSC-HVDC System

This chapter presents wind turbines cluster system composed of Squirrel Cage Induction Generators (SCIGs) controlled by cluster converter based VSC-HVDC System. The wind turbine cluster systems (multiple clusters) are installed in an offshore wind farm and connected to onshore system through a Voltage Source Converter based High Voltage Direct Current (VSC-HVDC) transmission line. A control scheme of cluster converter and VSC-HVDC converter systems are developed so that power production by SCIGs can be delivered to the onshore system effectively. In this study dynamic behavior of the wind turbines has been investigated by simulation study performed by using PSCAD/EMTDC for fluctuating wind speed and short circuit fault. Simulation results show that the proposed cluster system composed of SCIGs has high performance under transient and steady state conditions.

5.1. Introduction

Offshore wind farms have been introduced in many countries to harness the energy of strong, consistent winds over the oceans. Offshore wind farms have some advantages over onshore wind farms. They provide renewable energy, do not consume water, provide a domestic energy source, and do not emit any environmental pollutants. Compared to onshore winds the offshore winds blow stronger and more uniformly. Accordingly, offshore winds can generate much smoother electricity. Moreover, offshore wind power plants have more steady operation than onshore plants [77].

2015 was a notable year for offshore wind generator installation because of the total offshore wind installed capacity of over 12 GW. 11,034 MW, about 91% of them, has been installed in Europe. The remaining 9% of installed capacity is located in Asia, where China is leader in offshore wind capacity installed, followed by Japan and South Korea [78].

Offshore wind farm can be connected to onshore power system using HVAC transmission technology if the wind power plant is near the onshore. But HVDC technology may be more

attractive for the transmission of bulk power over long distances. HVDC becomes a more economical solution than HVAC in the case of transmission over a certain distance called "break-even". The break-even distance is between 500-800 km for overhead lines and around 50 km for submarine cables [79]. There are two kinds of technologies used in HVDC transmission system; thyristor based LCC (Line Commuted Converter) and transistor based VSC (Voltage Source Converter) [35, 36, 80]. VSC-HVDC provides some advantages compared with the LCC-HVDC such as black start capability, independent control of active and reactive powers, multi-terminal configuration, and high dynamic performance [27]. It can be also said that application of VSC-HVDC technology to offshore wind farm can enhance performance and stability of the wind farm.

Doubly Fed Induction Generator (DFIG) or Permanent Magnet Synchronous Generator (PMSG) based variable speed wind turbine is actually used in offshore wind farm with HVDC transmission system. These wind generator concepts require power converter for each individual wind generator. From the economical point of view, it will be desirable if the individual power converter of each wind generator can be eliminated and the wind farm can be controlled by using cluster VSC converter. Commonly a group of generators in an offshore wind farm is electrically connected to an offshore substation, and then connected to the onshore system [81]. Therefore the cluster VSC converter can be located on the substation platform.

The main purpose of grouping of wind turbine generators into clusters system is to reduce the number of power electronic converters that can potentially fail. Therefore the overall number of converter failures in a wind farm can be reduced. In addition, higher technical availability of the wind turbines for power production can be achieved. Moreover, the provision of redundant converters can be avoided (no more power converter installed on the individual wind turbine).

In this chapter, Fixed Speed Wind Turbine-Squirrel Cage Induction Generator (SCIG) based wind farm which is connected to onshore power system through the VSC-HVDC transmission system is considered. In comparison with DFIG and PMSG, SCIG has some superior characteristics such as a simple design with high reliability, brushless and rugged construction, low investment and maintenance cost, and operational simplicity [82]. In addition, the SCIG needs no individual power converter in its operation. Although SCIGs have almost no Low Voltage Ride through (LVRT) capability, the LVRT capability of the SCIG based wind farm can be enhanced if the wind farm is connected to onshore main grid through VSC-HVDC line and controlled by the proposed cluster VSC converter system.

The control methods of wind turbine cluster based SCIG has been reported in some papers [35], [83]. The papers focus on controlling the cluster SCIGs in variable frequency operation. The operating frequency of the cluster's wind farm is estimated by using "Magnetic Angle Estimator" or "Angle and Flux Estimator". In Ref. [35] the torque of the cluster wind farm generator is controlled based on the average mechanical speed calculated from mechanical speeds of the SCIGs. In Ref. [83], the average mechanical speed is used to control the output power of SCIG by using maximum power point tracking (MPPT) method. From the control mechanism in the papers it can be said that the supplied voltage and frequency to the SCIGs are not constants (variable) during their operation. However, from practical point of view SCIG based fixed speed wind turbine as well as squirrel cage induction generator is designed and manufactured to be operated under specific rated voltage and frequency. Variations in operating point of supplied voltage and frequency of the machines can affect the machine's performances negatively and can reduce the machine's life time. In addition, the performance of terminal voltage on the cluster wind farm side was not reported in the papers. It should be noted that the SCIG absorbs inconstant amount of reactive power for its excitation. The amount of the reactive power consumption depends on active power production captured from varying wind speed which can lead to the voltage fluctuation. Furthermore, the reactive power compensator is not considered in the papers. Reactive power compensator is very important for SCIG based wind turbine during its operation. If the reactive power is not compensated, the SCIGs needs to absorb the reactive power from the cluster converter. Consequently, capacity of the cluster converter becomes larger than the total capacity of SCIGs, because, when the SCIGs are generating maximum active power, the cluster converter needs to inject the maximum active power to HVDC network while at the same time the cluster converter also needs to supply the reactive power to the SCIGs. Moreover, installation of the communication bus sensors between wind generators and the cluster converter can make the control mechanism of the cluster converter more complex.

According to the disadvantages stated above, it is proposed in this chapter that SCIGs of the cluster wind farm are operated under constant voltage and frequency based on the rated values for optimizing the SCIGs performance. Complex controller is not needed in the electrical part of the SCIG. Proposed cluster converter controller is designed based on the simple way, but robust under disturbance and effective to control voltage, frequency, active and reactive powers of the cluster wind farm.

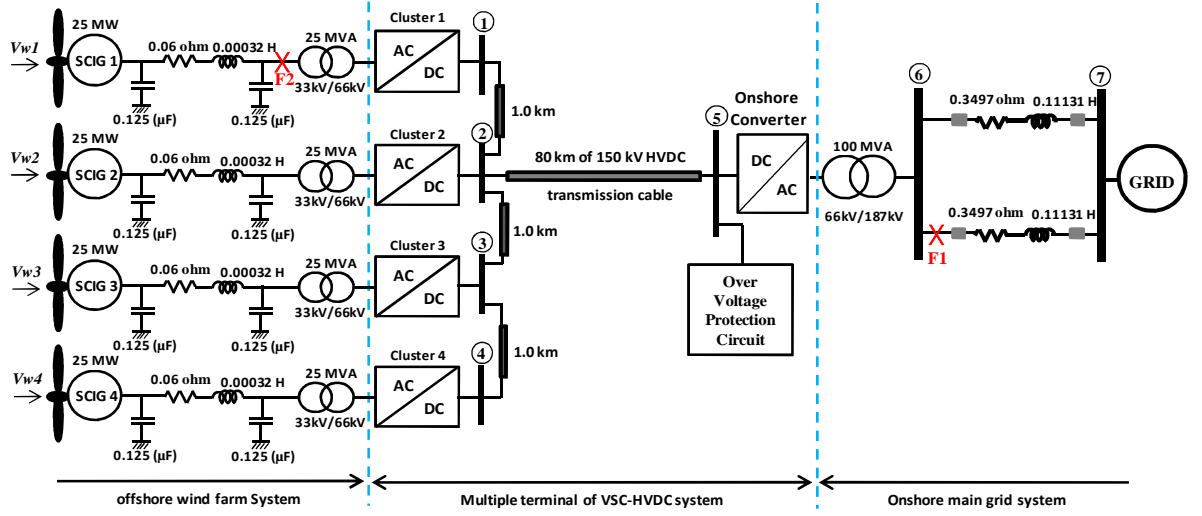


Fig. 5.1. SCIG based offshore wind farm with cluster converter system

5.2. Offshore Wind Farm Model

Fig. 5.1 shows the proposed offshore wind farm model system used in the simulation analyses. Total capacity of the wind farm is 100 MW. The wind farm consists of four clusters of FS WT-SCIG. This configuration provides an advantage that a smaller number of converters, which could potentially fail, are required.

In simulation analysis, the wind generators in the same cluster are aggregated in 25 MW of single machine representation for simplicity. The wind generators are operated at frequency of 50 Hz. The capacity of 25 MW of the cluster wind farm is adopted referring to the floating substation capacity (25MVA) which was developed in the Fukushima floating offshore wind farm project in Japan. The aggregated representation of wind generators is very common in simulation analyses [84]-[85]. The aggregated 25 MW SCIG is connected to AC/DC cluster converter through collector system ($R_{eq}=0.06$ ohm, $L_{eq}=0.00032$ H, $B_{eq}/2=0.125$ uF) and 33kV/66kV step up transformer. The cluster converter is connected through 1.0 km cable to 150 kV HVDC power cable. The cluster converter system is part of multiple terminal VSC-HVDC system. It is assumed that the DC terminal bus of cluster converter 2 (Bus 2) is nearest to onshore main converter, and then the offshore cluster converter system is connected from terminal 2 to the main converter through 80 km/150 kV HVDC transmission cable. Through the main converter the power from the wind farm is transmitted to the onshore main grid system via a 66kV/187kV step up transformer,

and a double circuit transmission line. The submarine cable data is shown in Table 5.1.

On the DC network the over-voltage protection system is installed at the main onshore converter (Bus 5). Over-voltage could occur on the DC network when the difference between the power from offshore wind farm and the power transmitted to the onshore system becomes large. The HVDC over-voltage protection system is very effective on the system stability when severe network disturbance such as short circuit fault occurs in the onshore main grid system. The over-voltage control system can maintain the HVDC circuit voltage during network disturbance. Detailed configuration of the proposed control system of cluster converter, onshore converter, and the protection system will be explained later.

Table 5.1. Submarine cable data

Rated Voltage (kV)	Resistance (Ω/km)	Inductance (mH/km)	Capacitance ($\mu\text{F}/\text{km}$)
150	0.047	0.6	0.15

5.3. FSWT-SCIG Model

5.3.1. Basic Configuration

A fixed speed wind turbine with SCIG is the simplest electrical topology in wind turbine concepts. The schematic configuration of the fixed speed wind turbine is depicted in Fig. 5.2. It consists of SCIG directly connected to the grid, a soft-starter, and a capacitor bank. The wind turbine transfers the kinetic energy of wind flow into mechanical energy. The SCIG transforms the mechanical power into electrical power and delivers the power directly to the grid system. Generally, the rotational speed of the generator is relatively high compared with that of wind turbine. In order to operate the induction machine as a generator, the rotor speed should be rotate over its synchronous speed. Therefore, the generator speed needs to be stepped down by using a multiple-stage gearbox with an appropriate gear ratio.

The SCIG absorbs significant amount of reactive power from the grid. The reactive power consumption increases as active power output increases. In order to compensate reactive power consumption a capacitor bank needs to be installed close to the generator terminal. The capacity of capacitor bank is chosen so that the power factor of the wind power station becomes unity during

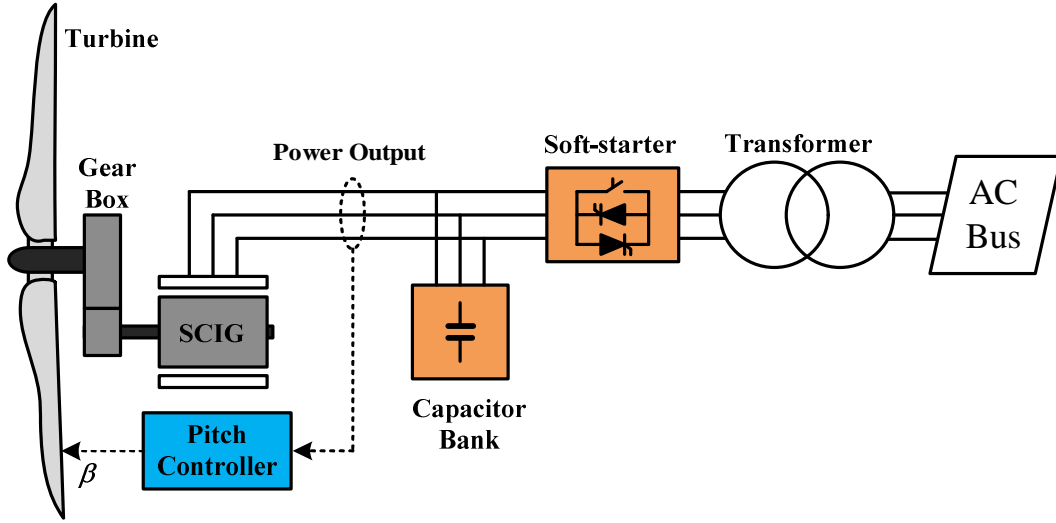


Fig. 5.2. Configuration of fixed speed wind turbine with SCIG

the rated condition. When the SCIG produces maximum (rated) active power, the SCIG also consumes maximum reactive power. According to this condition the value of the capacitor bank is chosen, and hence necessary reactive power for excitation can be totally compensated by the capacitor bank. The reactive power as well as the active power will be fluctuating due to variation of wind speed. However, excessive reactive power on the cluster network is absorbed by the cluster converter in order to maintain the terminal voltage at the rated value.

Actually the rated voltage of SCIG is low, and hence a step up transformer is required in order to connect the generator to the collector network system of the wind farm of medium voltage.

Since mechanical power is converted directly to electrical power by the generator, complex controller is not needed in the electrical part of a fixed speed wind turbine. However, a pitch controller is needed to regulate the pitch angle of the turbine blades (β) to keep output power of SCIG under the rated value.

5.3.2. Wind Turbine Model

Wind turbine model is based on steady state aerodynamic power characteristic. The power from wind energy can be calculated as follows [63].

$$P_w = 0.5 \rho \pi R^2 V_w^3 C_p(\lambda, \beta) \quad (5.1)$$

where P_w is the captured wind power (W), ρ is the air density (Kg/m^3), R is the radius of rotor blade (m), V_w is wind speed (m/sec), and C_p is the power coefficient. The value of C_p is depending on tip speed ratio (λ) and blade pitch angle (β) of the wind turbine. C_p of the turbine can be obtained by eq. (2):

$$C_p(\lambda, \beta) = c_1 \left(\frac{c_2}{\lambda_i} - c_3 \beta - c_4 \right) e^{\frac{-c_5}{\lambda_i}} + c_6 \lambda \quad (5.2)$$

with

$$\frac{1}{\lambda_i} = \frac{1}{\lambda - 0.08 \beta} - \frac{0.035}{\beta^3 + 1} \quad (5.3)$$

and

$$\lambda = \frac{\omega_r R}{V_w} \quad (5.4)$$

where c_1 to c_6 are characteristic coefficients of wind turbine ($c_1=0.5176$, $c_2=116$, $c_3=0.4$, $c_4=5$, $c_5=21$ and $c_6=0.0068$) [64], and ω_r is rotational speed of turbine in rad/sec. The C_p - λ characteristic for different values of β (the pitch angle) is shown in Fig. 5.3. The maximum value of C_p ($C_{p_opt} = 0.48$) is achieved for $\beta = 0.8$ and $\lambda = 8.2$. This value of λ is defined as the optimal value (λ_{opt}).

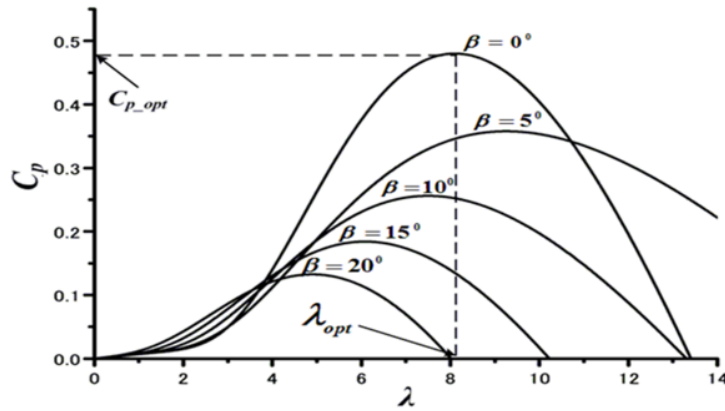


Fig. 5.3. C_p - λ characteristic for different pitch angle

5.3.3. Pitch Controller Model

Fig. 5.4 shows the model of blade pitch controller system for fixed speed wind turbine based SCIG [86]. In fixed speed wind turbine, the pitch control system is used to control power output of induction generator not to exceed the rated power. The pitch actuator is represented by a first-order transfer function with time constant of 5.0s and the pitch rate and angle limiters. A PI controller is used to control the pitch angle effectively.

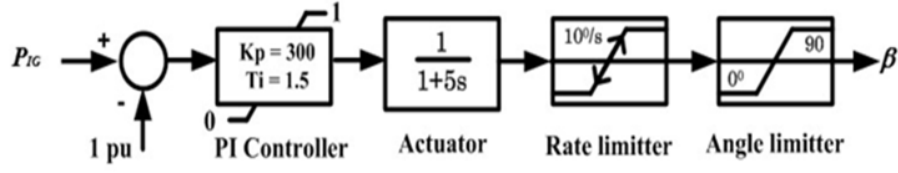


Fig. 5.4. Pitch controller for fixed speed wind turbine

5.3.4. Drive Train Model

The drive train of a wind turbine generator system consists of the following elements: a blade-pitching mechanism with a spinner, a hub with blades, a rotor shaft and a gearbox with breaker, and generator [87]. Depending on the complexity of the study, the complexity of the drive train modeling differs. For example, when the problems such as torsional fatigue are studied, dynamics of all parts have to be considered. For these reasons, two-lumped mass or more sophisticated models are required. However, when the study focuses on the interaction between wind farms and grid system, the drive train can be treated as one-lumped mass model with acceptable precision for the sake of time efficiency [86], [87]. In the present study, it is modelled by the following equation:

$$\frac{d\omega_r}{dt} = \frac{T_e - T_m}{J_{eq}} - \frac{B_m}{J_{eq}} \omega_r \quad (5.5)$$

where ω_r is the mechanical angular speed (rad/s) of the generator, B_m is the damping coefficient (Nm/s), T_e is the electromechanical torque (Nm), T_m is the mechanical torque of the wind turbine, and J_{eq} is the equivalent rotational inertia of the generator (kg.m²). The one mass model of wind turbine is shown in Fig. 5.5.

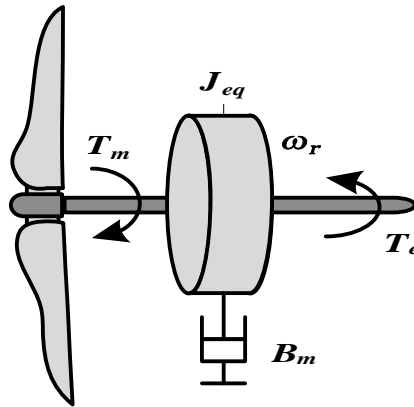


Fig. 5.5. One mass model of wind turbine

5.3.5. SCIG Modeling

The SCIG model used in this study is adopted from PSCAD/EMTDC library SCIG model [62]. The equation used to express this model consists of the double cage equivalent circuit of an induction generator shown in Fig. 5.6 and all parameters of the generator are shown in Table 5.2. Circuit equations for the double cage induction generator can be obtained as equations (5.6) to (5.7) [49].

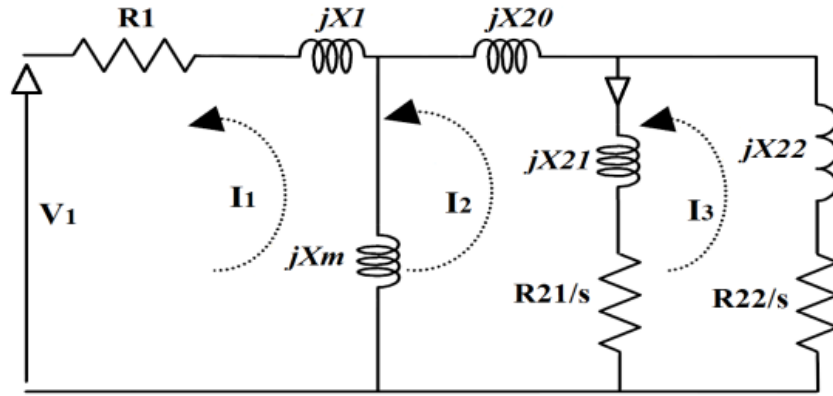


Fig. 5.6. Induction machine equivalent circuit

$$0 = jx_m I_1 - \left(-\frac{R_{21}}{s} + jx_{21} + jx_{20} + jx_m\right) I_2 + \left(-\frac{R_{21}}{s} + jx_{21}\right) I_3 \quad (5.6)$$

$$0 = \left(\frac{R_{21}}{s} + jx_{21}\right) I_2 - \left(-\frac{R_{21}}{s} + \frac{R_{22}}{s} + jx_{21} + jx_{22}\right) I_3 \quad (5.7)$$

Table 5.2. Generator Parameters

SCIG	Rating	25 MW
	R1	0.01 (pu)
	X1	0.1 (pu)
	Xm	3.5 (pu)
	R21	0.035 (pu)
	R22	0.014 (pu)
	X21	0.030 (pu)
	X22	0.089 (pu)
	H	1.5 s

5.4. Multi- Terminal VSC-HVDC for Cluster SCIG based Wind Farm

5.4.1. Basic Configuration

VSC-HVDC has become the preferred solution for grid connected large offshore wind farms compared to HVAC or LCC-HVDC because of several technology advantages provided by VSCs. Therefore, guidelines and recommendation for control strategies of multi terminal VSC-HVDC connection of offshore wind farms are highly needed for the HVDC and wind turbine generator industries.

In a VSC-HVDC with multi terminals, the system has more than two converters connected to provide additional reliability through the ability to compensate for the loss of any single converter of the system. Typically, one of the converters regulates the DC voltage and the other converters control the power flow. Model system of the multi-terminal VSC-HVDC for cluster SCIG based wind farm used in this study is presented in Fig. 5.1. Commonly, practical VSC-HVDC applications have been based on two or three-level technology which enables switching two or three levels to the AC terminal of the converter. For such converter topologies a large number of semiconductor devices with blocking capability of a few kilovolts are connected in series up to several hundred per converter arm depending on the DC voltage [89-90]. However, in this simulation analysis the converter system topology for VSC-HVDC is represented by three levels IGBT switch converter model controlled by PWM technique for simplicity.

The circuit configuration of three-level PWM is shown in Fig. 5.7. This application reviews those three levels converter topology often referred to as Neutral Point Clamped (NPC) converter. The converter uses twelve switches and six additional diodes. Each leg has four IGBTs connected in series. The applied voltage on the IGBT is one-half of that in the conventional two level converters. The bus voltage is split in two by the connection of equal series connected bus capacitors. Each leg is completed by the addition of two clamp diodes. To generate the switching pulses for the converters, two carrier waveforms are simultaneously compared with a sinusoidal waveform at the fundamental frequency. The switching states for the four switches of each phase and the input phase voltages for the AC/DC converters are described in Table 5.3. The detailed model and control strategies are explained in the following.

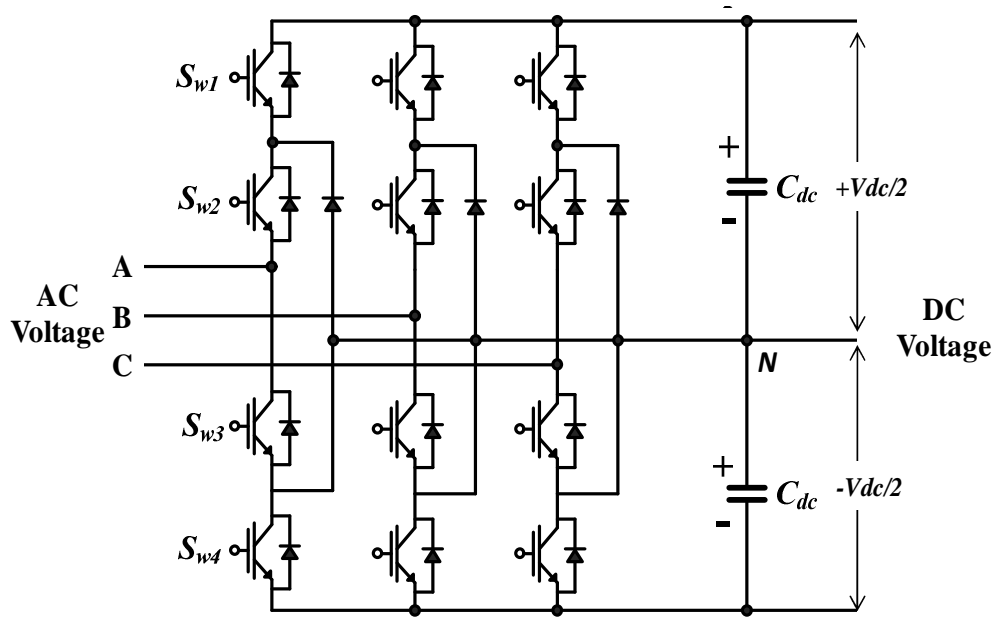


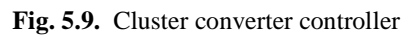
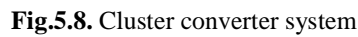
Fig. 5.7. Circuit configuration of three level converters

Table 5.3. Switching state of three level converter

Input Voltage	Switching states			
	S_{w1}	S_{w2}	S_{3w}	S_{w4}
$+V_{dc}/2$	1	1	0	0
0	0	1	1	0
$-V_{dc}/2$	0	0	1	1

5.4.2. Cluster Converter for SCIG based Wind Farm

Scheme of the cluster converter system is described in Fig. 5.8. The output power generated by the cluster circuit of SCIG is collected in the AC terminal bus, and then the power is transferred to HVDC circuit through the 33kV/66kV transformer and AC/DC cluster converter. Three phase voltage (V_{cl}) and current (I_{cl}) are collected respectively from low voltage side and high voltage side of the transformer. The cluster controller is used to control the voltage reference (V_{cl}^*) for the converter system.



67

this method the reactive power on the cluster circuit system is controlled by the cluster converter automatically.

Detailed scheme of cluster converter controller is depicted in Fig. 5.9. Aim of the cluster controller is to control the converter voltage to be its reference (V_{cl}^*). Three phase voltage from AC terminal bus (V_{cl}) is extracted into positive sequence voltage in polar form (magnitude and phase) by using the “Vabc to V1” block. The voltage angle reference for cluster system (θ_{cl}) is obtained from virtual PLL in which the operating frequency of cluster wind farm is set at 50 Hz. The transformation block computes the direct (d) axis and quadratic (q) axis quantities in a two-axis rotating reference frame for a three-phase sinusoidal signal⁽²²⁾. The following park transformation is used:

$$V_d = \frac{2}{3} (V_a \cos(\theta) + V_b \cos(\theta - 2\pi/3) + V_c \cos(\theta + 2\pi/3)) \quad (5.8)$$

$$V_q = \frac{2}{3} (V_a \sin(\theta) + V_b \sin(\theta - 2\pi/3) + V_c \sin(\theta + 2\pi/3)) \quad (5.9)$$

where, θ is rotation speed (rad/s) of the rotating frame. V_d and V_q are the d-axis and the q axis components of the voltage, respectively. In this control system V_d and V_q is used to represent the rectangular coordinates of the positive-sequence component in which the magnitude and angle of V_1 are calculated as follows:

$$|V_1| = \sqrt{V_d^2 + V_q^2} \quad (5.10)$$

$$\angle V_1 = \tan^{-1}(V_q / V_d) \quad (5.11)$$

Three phase current taken from the converter (I_{cl}) can be transformed into d-axis and q-axis current components by using eq. (5.8) and eq. (5.9), respectively. The active power from the cluster wind farm can be controlled through the angle of the cluster terminal voltage, and hence the d-axis current (I_{cld}) is used to control the voltage phase constant at 0° . On the other hand, the reactive power on the cluster wind farm network can be controlled by its magnitude, and hence the q-axis current (I_{cdq}) is used to control the voltage magnitude at 1.0 pu.

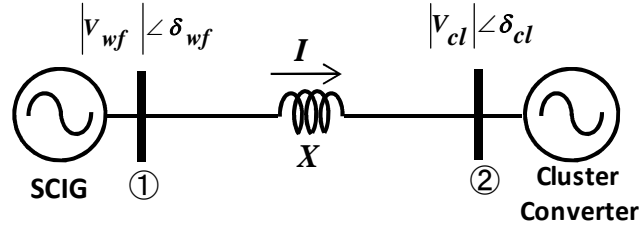


Fig. 5.10. Cluster converter controller

$$P_{12} = \frac{|V_{wf}| |V_{cl}|}{X} \sin(\delta_{wf} - \delta_{cl}) \quad (5.12)$$

$$Q_{12} = \frac{|V_{wf}|}{X} \left[|V_{wf}| - |V_{cl}| \cos(\delta_{wf} - \delta_{cl}) \right] \quad (5.13)$$

Taking into account those stated above, interaction between SCIG's terminal voltage and cluster converter's terminal voltage is investigated by using a single-phase equivalent circuit shown in Fig. 5.10. The transmission line is represented by reactance (X). The active power and reactive power at the sending end can be expressed by Eqs. (5.12) and (5.13) respectively. From eq. (5.12), it is seen that small change in δ_{wf} or δ_{cl} will have significant impact on the active power flow. Therefore, the active power flow on the transmission line is controlled by angle difference between both terminal bus voltages ($\delta = \delta_{wf} - \delta_{cl}$). The active power flows from the wind farm bus to the cluster converter bus if V_{wf} leads V_{cl} and δ is positive. On the other hand, it is seen from eq. (5.13) that ⁽²³⁾ the reactive power flow on the transmission line can be controlled by magnitude difference of the bus voltages. Based on this concept, the magnitude and angle of terminal bus of cluster converter are controlled to be constant value of 1.0 pu and 0 deg respectively as if it were an infinite bus.

5.4.3. Onshore Converter Model

Fig. 5.11 shows a block diagram of the onshore converter. The converter system transfers the DC voltage of HVDC circuit to AC voltage on the onshore grid system. The converter is composed of two level IGBT switch devices controlled by PWM technique. The aim of the onshore converter is to maintain the HVDC circuit voltage at rated value and to control reactive power output to zero for unity power factor operation.

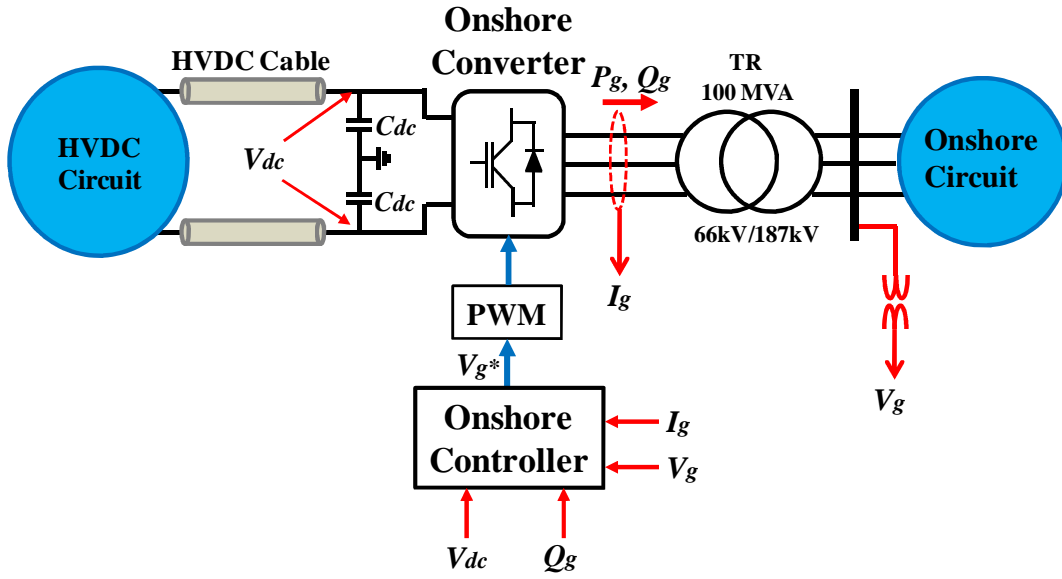


Fig. 5.11. Onshore converter system

Detail of the onshore converter controller scheme is shown in Fig. 5.12. Three phase output current of the converter is transformed into components on the d-q rotating reference frame. When grid voltages on the stationary reference frame are transformed into the d-q rotating reference frame, V_{gd} becomes constant and V_{gq} becomes zero. Therefore, the active and reactive power delivered to the grid can be controlled by the d-axis current (I_{gd}) and the q-axis current (I_{gq}), respectively. The voltage of DC-link capacitor (V_{dc}) is maintained constant in order to transmit the active power from HVDC circuit to the onshore system effectively. For unity power factor operation, the q-axis current reference signal is set to zero so that the reactive power delivered to the grid becomes zero. The phase angle (θ_g) of the grid system is obtained from the terminal voltage (V_g) by using the PLL technique.

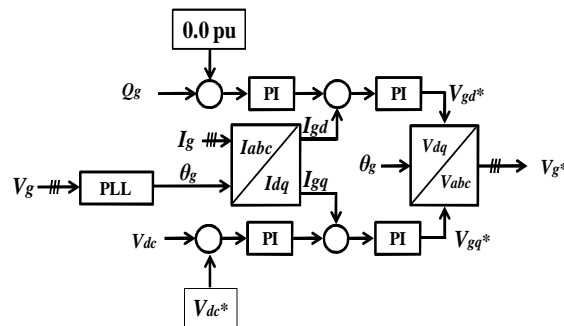


Fig. 5.12. Onshore converter controller system

5.4.4. Over-Voltage Protection Circuit of HVDC System

When a severe network disturbance such as short circuit fault occurs in the onshore grid system, the onshore converter cannot transmit the active power from the HVDC circuit to the onshore circuit, resulting in over-voltage in the HVDC circuit. The over-voltage occurs due to unbalance between the power generated from the wind farm and the power transferred to the onshore system. This may hamper normal operation of the converter. Therefore, the DC voltage of the HVDC circuit should be maintained within the permissible range.

The over-voltage protection circuit of HVDC is located at the DC side of the onshore converter as shown in Fig.5.13. The braking chopper is embedded in the HVDC circuit in order to protect the DC capacitor (C_{dc}) during fault situation. The chopper is activated when the DC voltage increases over the predefined limit and the excess active power is dissipated in the resistance (R_c) during a fault in the onshore grid system.

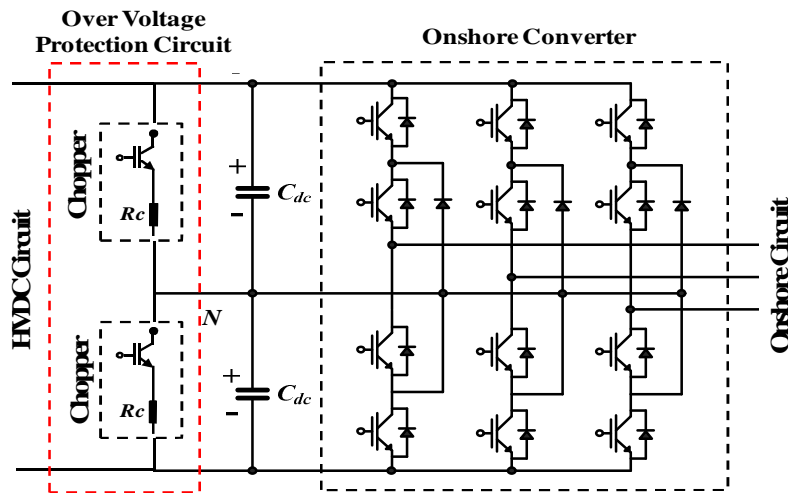


Fig. 5.13. Over voltage protection system

5.5. Simulation Results

The performance, robustness, and effectiveness of the control system for a wind farm are commonly evaluated in the transient and the steady state conditions. Currently, the grid code prosecutes that the wind generators should be remained stay online during a network disturbance, because out of synchronism of a large number of wind generators has serious impact on power system stability. It can be said that control system of wind farm should be robust to the disturbances and also be effective in controllability.

Simulation analyses have been performed for the power system model shown in Fig. 5.1 by using PSCAD/EMTDC. Transient and steady state conditions are considered in the analyses for investigating the dynamic characteristics of the proposed system. Aim of the investigation is to demonstrate the performance of the SCIG based wind farm controlled by the proposed cluster converter based VSC-HVDC system.

5.5.1. Transient stability analysis

In order to show the effectiveness of the proposed system on the transient stability, two locations of disturbance are taken into account in the simulation analysis. In this transient stability analysis, the wind speeds for the wind generators are kept constant ($V_{w1} = 12$ m/s, $V_{w2} = 11.5$ m/s, $V_{w3} = 11$ m/s, $V_{w4} = 10.5$ m/s) assuming that the wind speed does not change dramatically within this small time duration.

In the first case, the disturbance occurs at point F1 on the transmission line in the onshore area. The symmetrical three lines to ground fault is considered as the fault. The fault occurs at 0.1 sec; the circuit breakers (CB) on the faulted line are opened at 0.2 sec, and at 1.0 sec the CBs are re-closed. The voltage performance of each cluster is shown in Fig. 5.14. Active and reactive power outputs of the wind farm from each cluster are shown in Figs. 5.15 and 5.16, respectively. It can be seen that the voltages and powers of the wind farm are not significantly fluctuated. The voltage and power fluctuations are very small. During the fault condition the power from the wind farm is sent to the HVDC circuit continuously, meanwhile the power sent to the onshore system decreases significantly due to the fault. As a result, the voltage on the HVDC circuit increases significantly. When the DC voltage reaches 155 kV the over-voltage protection circuit of the HVDC system is activated by triggering the chopper IGBT gates. Then the active power from the wind farm is absorbed by the breaking resistor (R_c). Therefore the DC voltage of HVDC circuit can be maintained constant. The voltage response on the HVDC circuit is shown in Fig. 5.17. Active and reactive powers sent to the onshore system are shown in Fig. 5.18. From Fig. 5.18 it is seen that the active power delivered from the onshore converter decreases significantly due to voltage drop caused by the tree lines to ground fault. However, after fault clearance the onshore converter can control the active power return back to initial condition within 0.5 second. In addition, though active and reactive powers of the onshore converter change significantly due to

the fault, the DC voltage on the HVDC line can be controlled within a small range about the initial value.

In the first case, the simulation analysis shows the performance of the onshore converter and the dc voltage protector, because the disturbance in this case has impact only on the onshore converter and dc protector. However, because the cluster converters are also connected to the system in this case, the simulation analysis is required to confirm whether the disturbance has significant impact on the wind farm or not. From the simulation results it can be seen that the grid side disturbance has no significant influence on the wind generator performance. Therefore the expected result can be obtained in this case that the disturbance on the onshore system does not have so significant influence on the offshore wind farm.

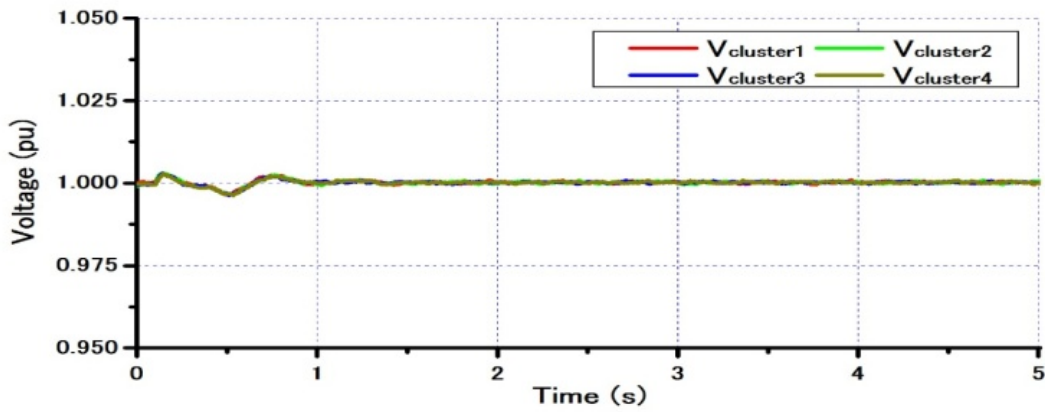


Fig. 5.14. Voltage response on each cluster circuit (F1)

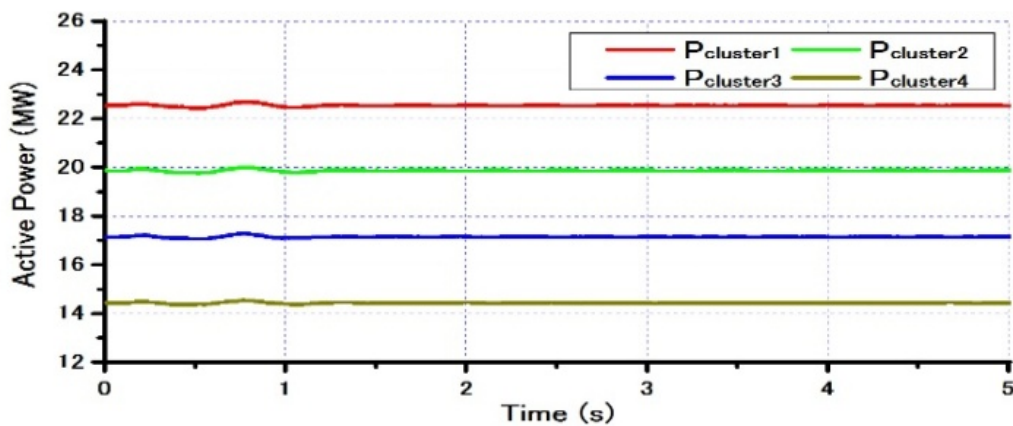


Fig. 5.15. Active power output of each cluster (F1)

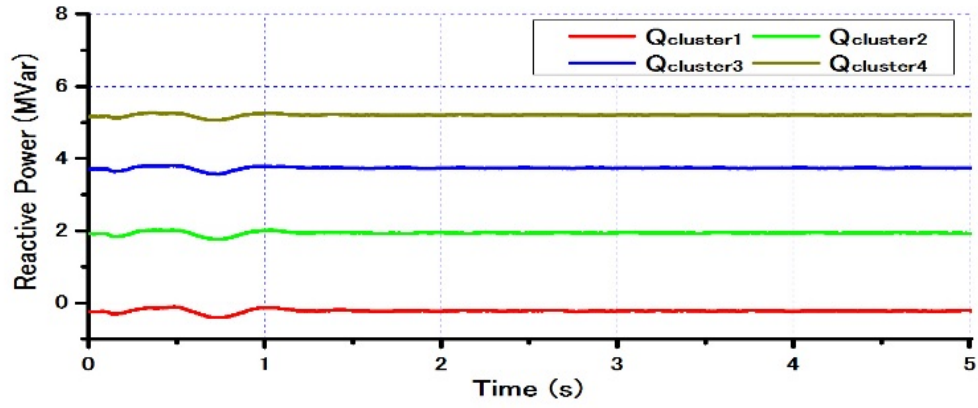


Fig. 5.16. Reactive power output of each cluster (F1)

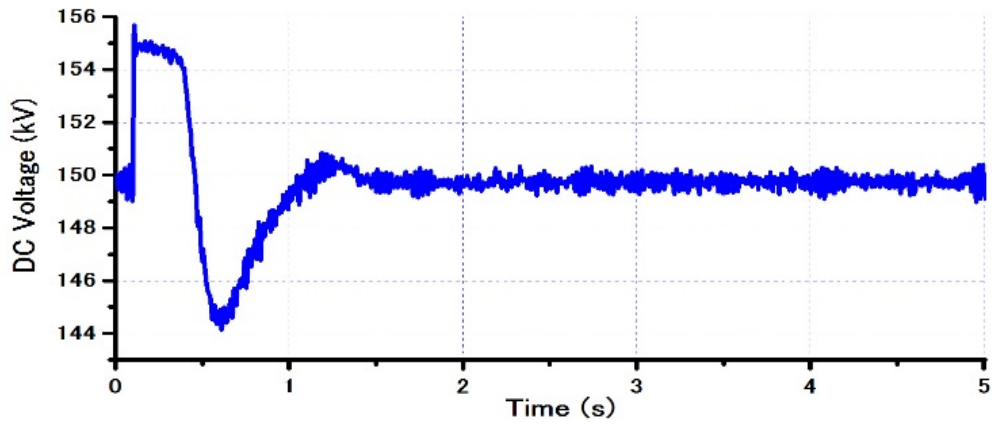


Fig. 5.17. Voltage response on HVDC circuit (F1)

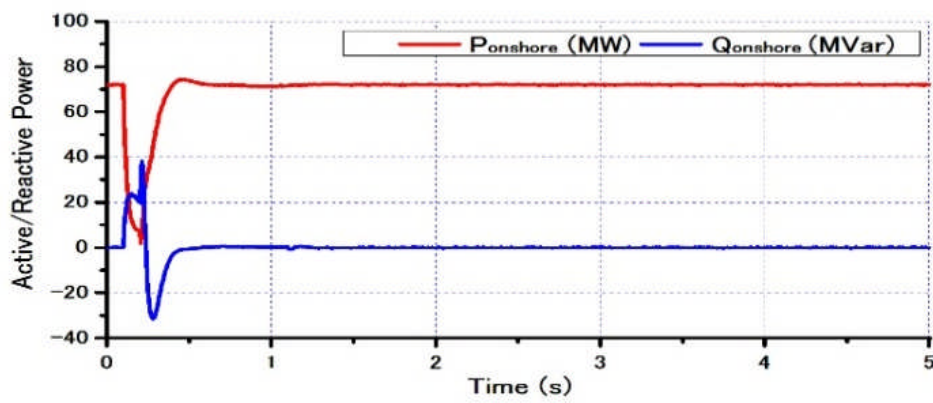


Fig. 5.18. Active and reactive power output of onshore converter (F1)

As a second case, disturbance at point F2 in the wind farm cluster 1 circuit is considered. From practical point of view a fault on offshore system is rare but possible. In this study a fault on the offshore circuit is also taken into account for investigating the advantage of the proposed control method of cluster converter system. In addition, the comparative analysis between the proposed cluster converter based offshore wind farm and the conventional wind farm without cluster converter shown in Fig. 5.19 is performed. In this scenario temporary short circuit between A-phase and B-phase for 3 cycles (0.06 s) is considered as the disturbance.

The simulation analysis in the second case is required to answer the question why the converter should be clustered. From practical point of view an offshore wind farm with a huge number of wind generators should be installed in several groups or clusters for easy operation and maintenance. The wind generator in a group or a cluster is connected to a substation and then connected to the main station. The main idea in this study for clustering wind farm is to locate the offshore converters in the sub stations; hence a large capacity of single converter in main station can be distributed into several cluster converters of small capacity and also the main platform station of offshore wind farm can be neglected.

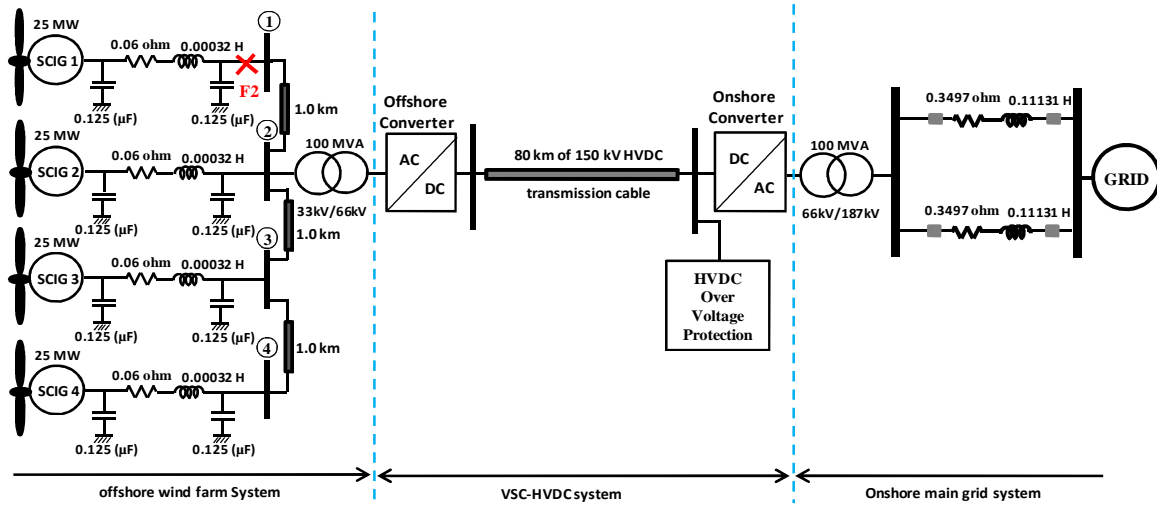
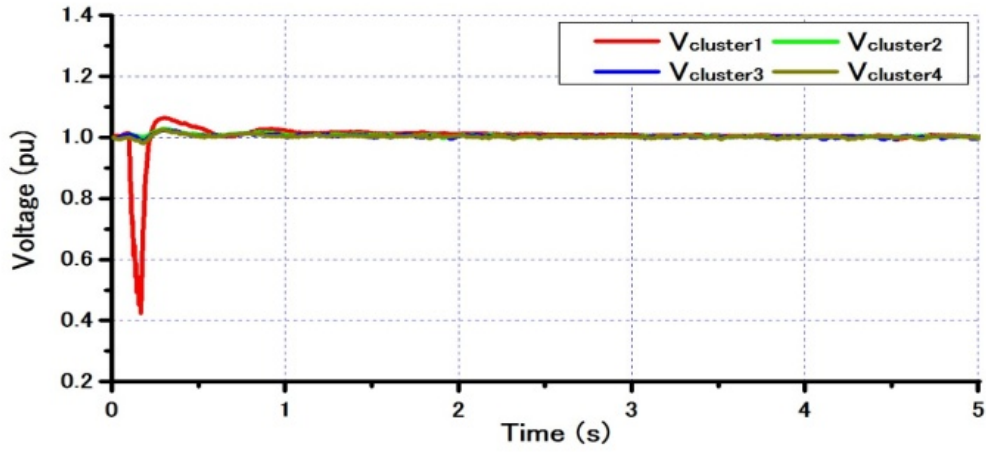


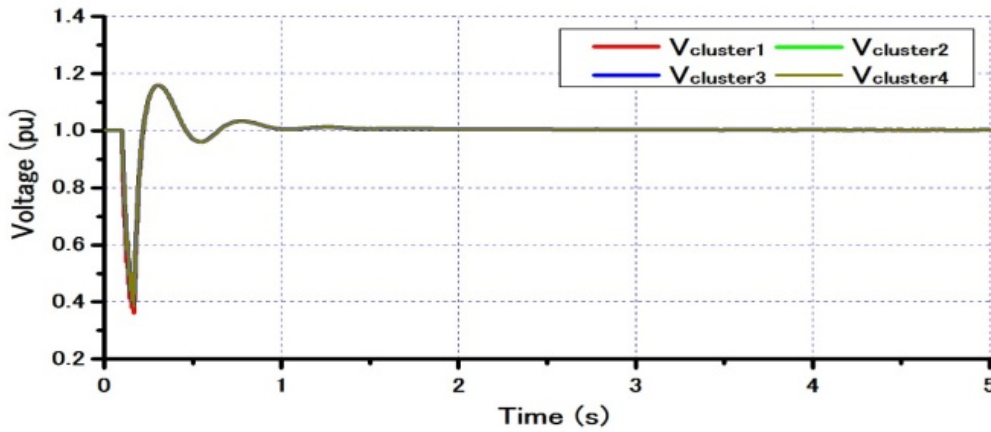
Fig. 5.19. SCIG based offshore wind farm without cluster converter

The simulation results for the disturbance at F2 are shown in Fig. 5.20 to Fig. 5.24. Voltage response of each cluster circuit is shown in Fig. 5.20. Active and reactive power outputs of the wind farm are shown in Figs. 5.21 and 5.22, respectively. From the results it can be seen that the short circuit on the cluster 1 does not have so significant impact on neighbor clusters (Clusters 2,

3, and 4) in the case of the proposed cluster converter system. It is seen that the voltage of other clusters are almost constant. However, in the case of the wind farm without cluster converter, the fault on the cluster circuit 1 has significant impact on the neighbor cluster circuits. Therefore it is concluded that the proposed cluster converter system can minimize the spread of the fault effect to neighbor cluster circuits



(a) proposed cluster converter

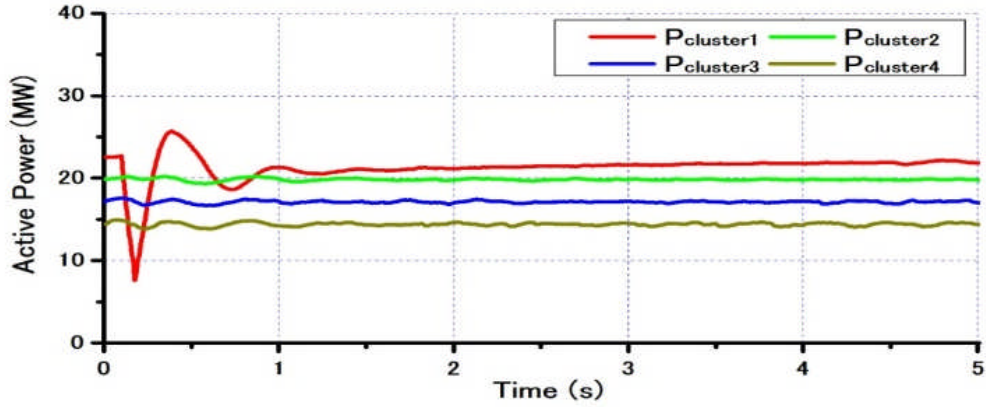


(b) without cluster converter

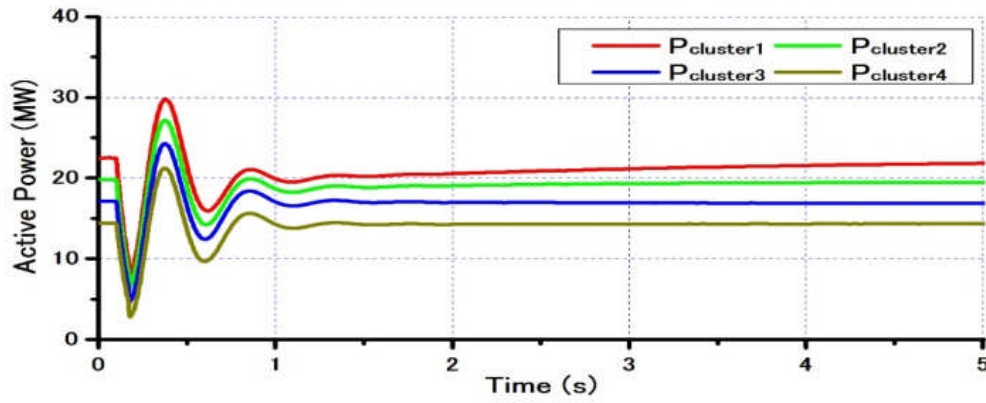
Fig. 5.20. Voltage responses of cluster circuit (F2)

Voltage response of the HVDC circuit is shown in Fig. 5.23. During the fault at F2, the voltage of HVDC circuit in the case of the proposed cluster converter system decreases to 130 kV, because the wind farm absorbs large amount of reactive power (See Fig. 5.22) for recovering

electromagnetic torque of the wind generators. However, the cluster converter is designed to maintain the cluster circuit's voltage constant at rated voltage, and hence the voltage can return back to initial condition. On the other hand, voltage of the HVDC circuit in the case of the wind farm without cluster converter decreases more.

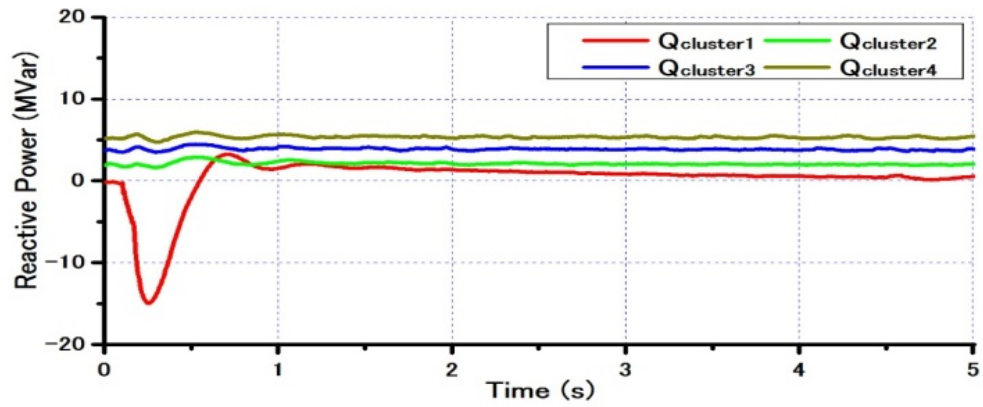


(a) proposed cluster converter

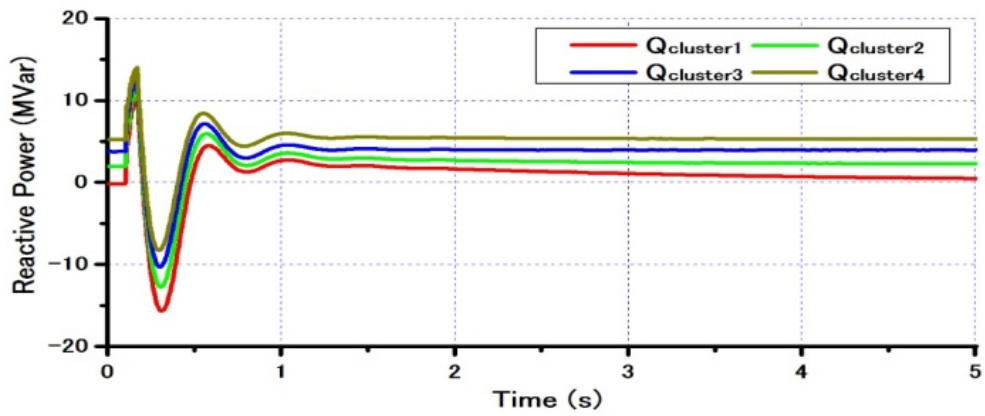


(b) without cluster converter

Fig. 5.21. Active power output of cluster wind farm (F2)

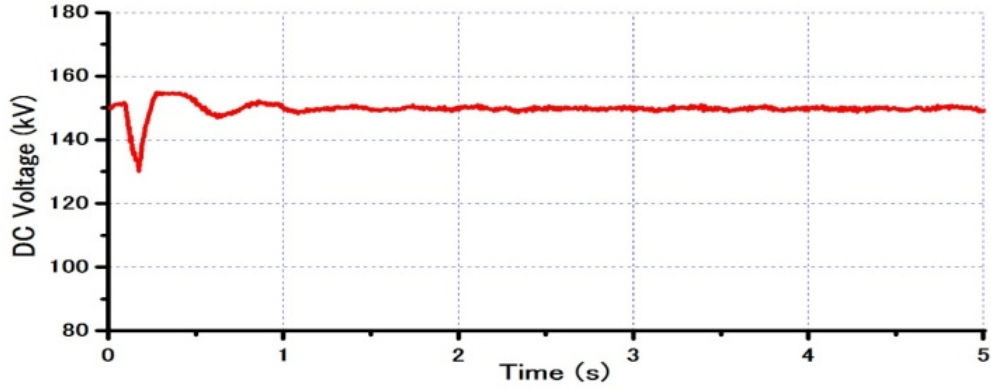


(a) proposed cluster converter

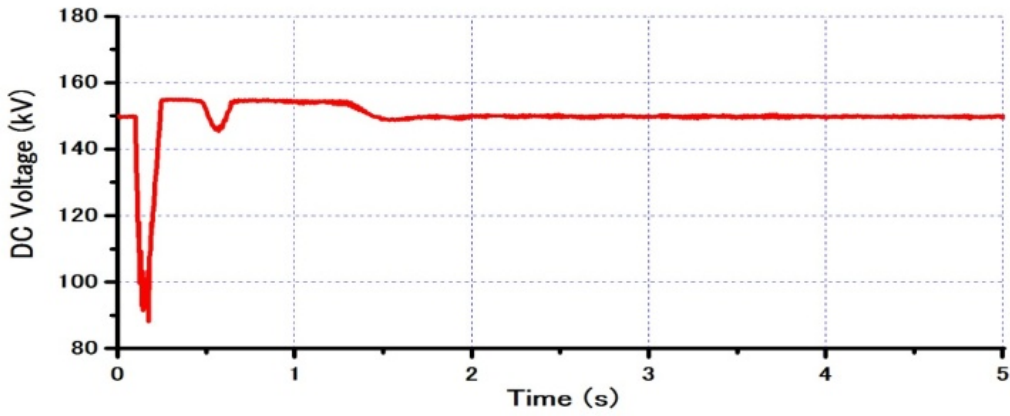


(b) without cluster converter

Fig. 5.22. Reactive power output of cluster wind farm (F2)



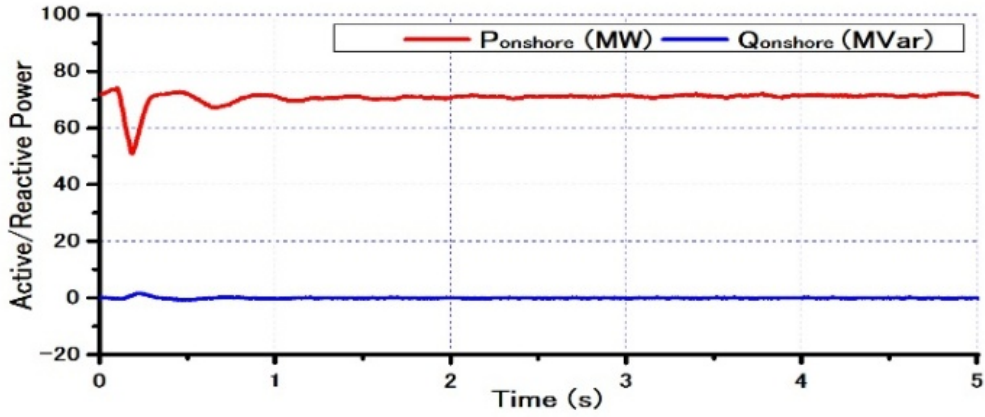
(a) proposed cluster converter



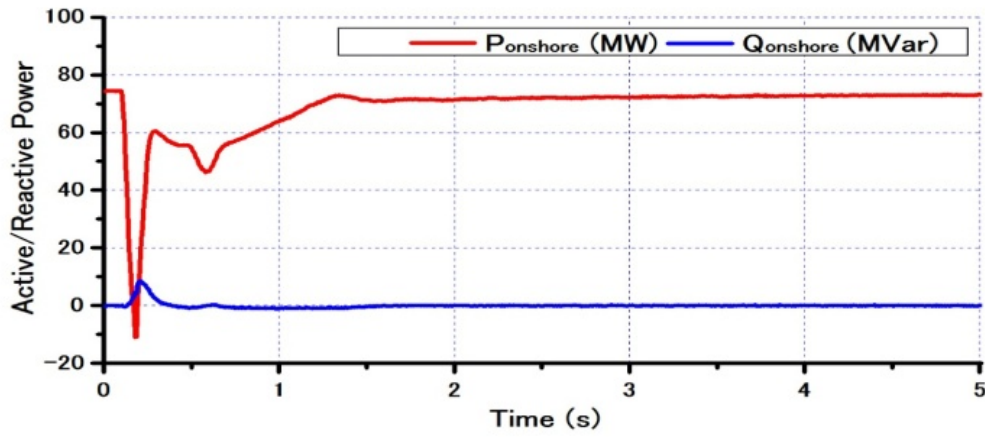
(b) without cluster converter

Fig. 5.23. Voltage response of HVDC circuit (F2)

Finally, Fig. 5.24 shows active and reactive powers sent to the onshore system. As can be seen from the simulation results in this case, responses of the state variables without the cluster are recovered to the normal operation within 1 second. This is because the control mechanism is similar to that of the cluster converter system. However, the significant difference is shown in Fig. 5.24. It is clearly seen that the effect of the fault on the active power sent to the onshore grid is smaller in the case of the proposed system than in the case of wind farm without cluster converter. The contribution of the cluster system is to minimize the decrease of active power injection to the grid system. Therefore, sudden loss of large amount of active power in the power system can be reduced significantly.



(a) proposed cluster converter



(b) without cluster converter

Fig. 5.24. Active and reactive power output of onshore converter (F2)

5.5.2. Steady state performance analysis

To evaluate the steady state performance of the proposed system, responses for the wind speed data as shown in Fig. 5.25 is investigated. Each wind speed is fluctuating randomly but the wind speed for wind farm cluster 1 is set to decrease gradually to zero and then gradually increases as shown in the figure. The reason to adopt such wind speed data is to confirm controllability of the cluster converter system under low or zero wind speed. Fig. 5.26 shows the rotational speed of SCIGs. Figs. 5.27 and 5.28 show the active and reactive power output of the wind farm clusters, respectively. It can be seen that the rotational speed of SCIG-1 connected to Cluster 1 decreases below the synchronous speed (1.0 pu) when the wind speed is at low or zero level and its active

power output becomes negative. In this situation SCIG-1 is operating in motor mode and under this condition large reactive power is absorbed by the cluster converter in order to maintain the cluster terminal voltage at constant value. From these results, it can be concluded that the cluster converter can work well in motor mode as well as in generator mode of the SCIG.

Voltage responses of the wind farm clusters are shown in Fig. 5.29, from which it is seen that the voltages are maintained constant at rated voltage, 1.0 pu (33 kV). The voltage of HVDC circuit is also maintained constant at 150 kV as shown in Fig. 5.30. Finally, the total active power transmitted from the wind farm clusters to the onshore system is shown in Fig. 5.31, and it is seen the power can be sent effectively with unity power factor through the onshore converter system.

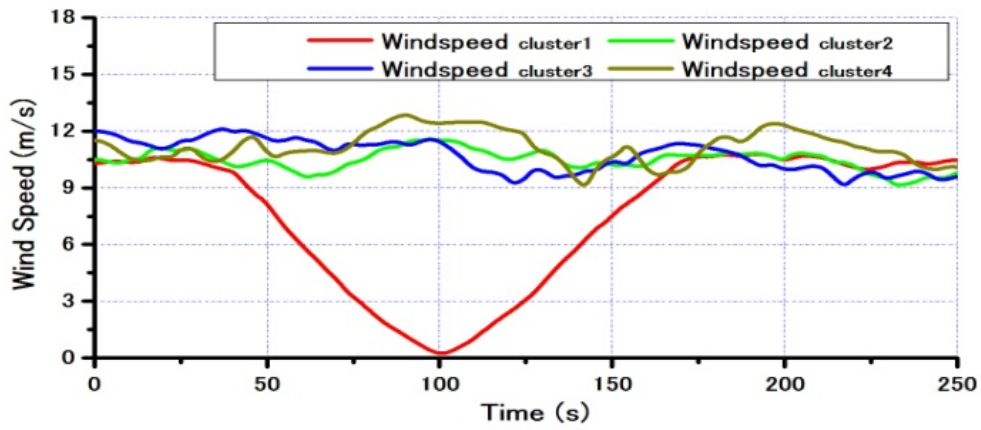


Fig. 5.25. Wind speed data (steady state)

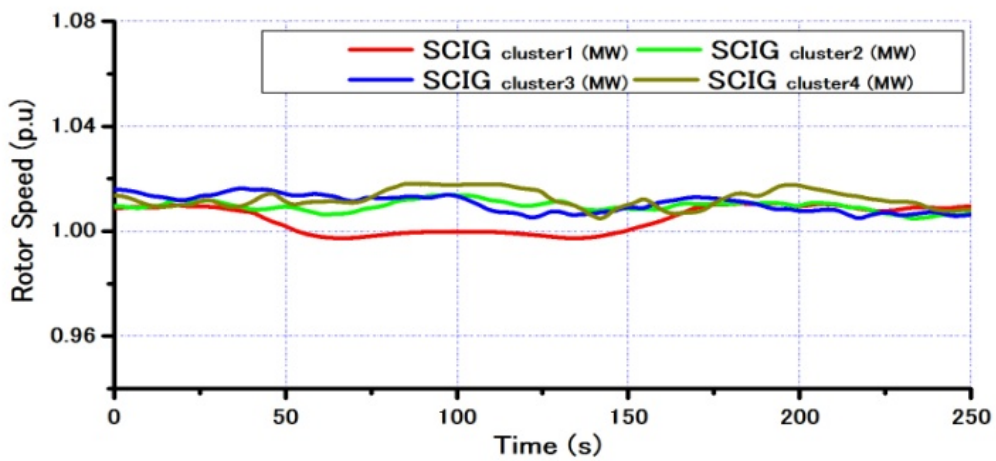


Fig. 5.26. Rotor speed of SCIGs (steady state)

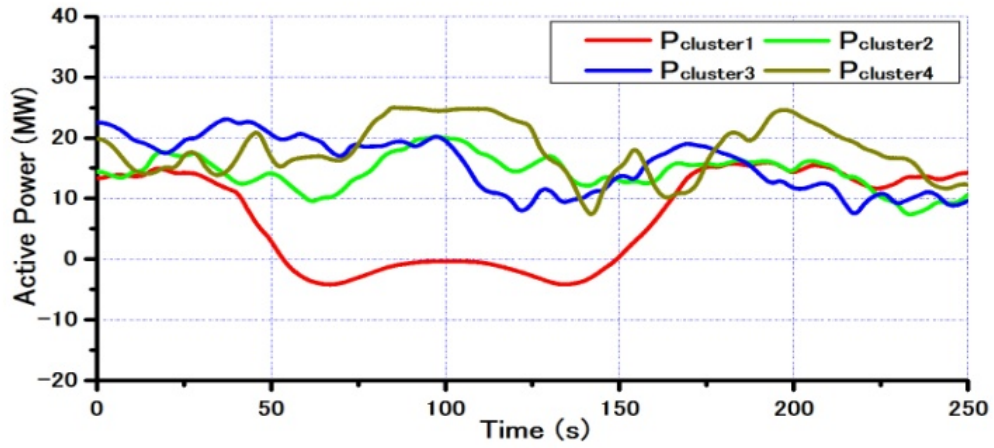


Fig. 5.27. Active power output of cluster wind farm (steady state)

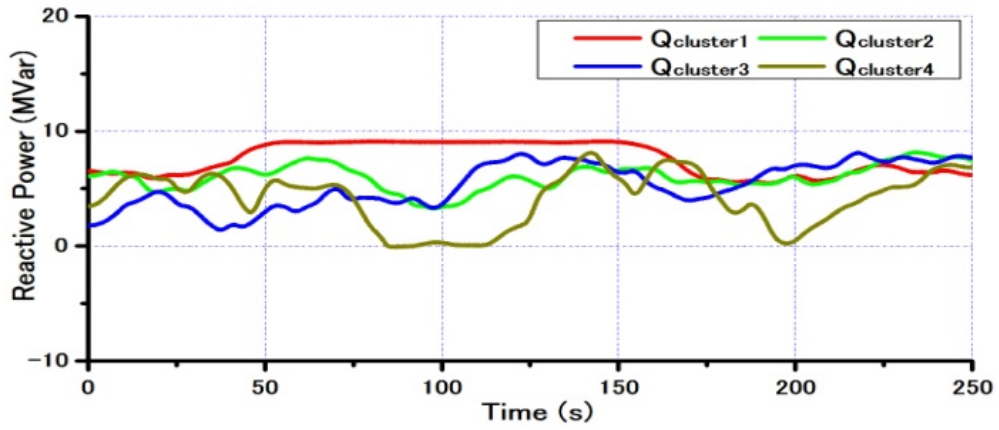


Fig. 5.28. Reactive power output of cluster wind farm (steady state)

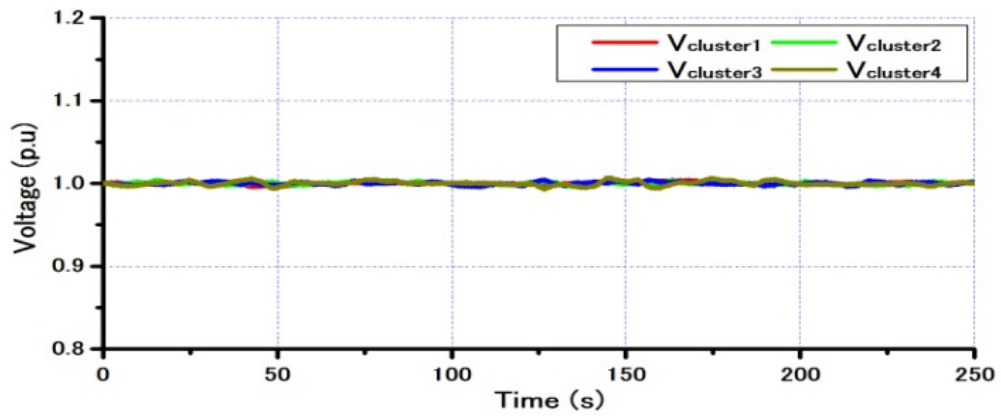


Fig. 5.29. Voltage responses of cluster circuit (steady state)

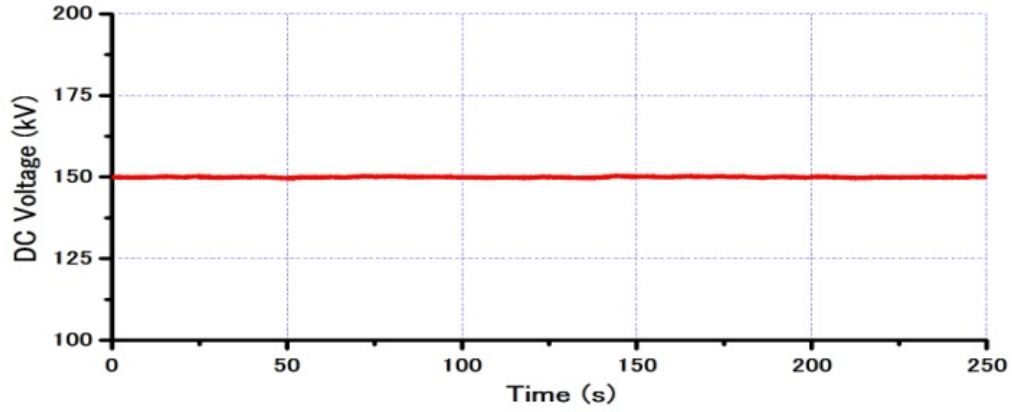


Fig. 5.30. Voltage response of HVDC circuit (steady state)

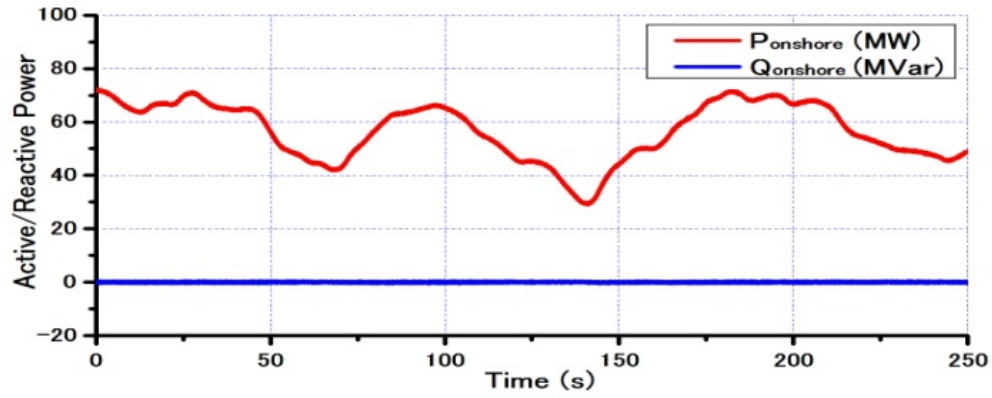


Fig. 5.31. Active and reactive power output of onshore converter (Steady state)

5.6. Chapter Summary

The new wind turbine cluster system composed of Squirrel Cage Induction Generators (SCIGs) controlled by cluster converters with VSC-HVDC system has been proposed and investigated. The dynamic and steady state characteristics of the proposed system have been analyzed through simulation studies by using PSCAD/MTDC. From the simulation results it can be concluded that the proposed system can enhance the performance and stability of the SCIG based offshore wind farm under both transient and steady state conditions.

Chapter 6

Conclusions

The rapid increase in installation of large-scale wind farms into the grid system would have a serious impact on the system stability due to the variation of generated power from wind generators. The wind farm penetration can have a serious effect on power system frequency characteristics, especially frequency drop when unexpected generation loss due to a fault in the grid system or load increase occurs. Frequency and voltage stabilities have become the main aspects that should be considered from a viewpoint of the security of electric power system. During severe network disturbance such as a short circuit fault, the terminal voltage of wind farm decreases significantly and active power from wind farm cannot be supplied to the grid system. Under such condition, large oscillation occurs in the power system frequency due to the loss of active power. New studies must be performed in order to evaluate the behavior of the wind farms after severe faults and improve the design of the wind farms in an efficient and economical way. Therefore, the interaction between wind farm and grid system from points of view of transient and steady state characteristics has become a very important issue to be analyzed.

Chapter 2 describes about wind turbine generation system. A brief introduction of basic principles of energy extraction from wind is presented. Then, drive train and pitch angle control models of wind turbine generator system are presented. The topological overview and modeling are presented for both fixed speed and variable speed wind turbine generator systems. And this chapter also gives overview and a brief introduction of basic principles the VSC-HVDC system.

In Chapter 3, a model system is considered in which a wind farm composed of Permanent Magnet Synchronous Generator (PMSGs) and Squirrel Cage Induction Generators (SCIGs) is connected to multi-machine power system. Though outputs of the SCIG based wind turbines are collected on AC network, PMSG based wind turbines are integrated in DC network with single grid side converter. The fixed speed wind turbines with SCIGs (FSWT-SCIGs) are widely used in wind farm due to their advantages of mechanical simplicity, robust construction, and lower cost. However, the FSWT-SCIG directly connected to the grid does not have any LVRT (Low Voltage Ride Through) capability or FRT (Fault Ride Through) capability when a short circuit occurs in the grid system. Moreover, under steady state condition its reactive power consumption cannot be controlled and hence terminal voltage of the wind generator leads to large fluctuation. Combined

installation of PMSG and SCIG in a wind farm can be considered a good solution, because the PMSG can provide the required reactive power of SCIG during fault condition. Therefore, in this chapter new control system for cooperated stabilizing control of PMSG based grid connected wind farm is proposed, in which, in order to contribute to frequency and voltage stabilizing control, controller system of the inverter of PMSG is modified in order for its active and reactive powers to be delivered to the grid easily and effectively. The simulation analyses show the proposed control system can enhance the fault ride through capability of the wind farm and also the transient stability of the grid system during a severe 3LG fault. Therefore it can be concluded that the proposed control strategy can contribute to enhance the stability of wind farm and connected power system during a network disturbance.

In Chapter 4, a control strategy of DC-link protection of PMSG based wind turbine by using new control system of buck converter is proposed and investigated. During a network disturbance like a short circuit fault, output power of the PMSG decreases at the grid side converter and then over-voltage can appear in DC-link circuit of the back-to-back power converter of PMSG due to the energy imbalance between the stator side converter (SSC) and the grid side converter (GSC). The voltage increase can be controlled by inserting a braking resistor in the DC-link circuit to dissipate the excess energy through a power electronic switch. However, dissipated energy in the braking resistor cannot be controlled, and hence, energy imbalance between SSC and GSC can still appear. This is due to the imbalance between the output power from the generator and the power capacity of the resistor. Increase of DC-link circuit voltage can lead to a damage of IGBT of the converter and control system failure. In order to investigate effectiveness of the proposed DC-link protection system, comparative simulation analysis has been performed for severe three-line to ground (3 LG) fault between the proposed DC-link protection system and the conventional protection system. From the simulation results, it is shown that the proposed method can control well the DC-link voltage as well as other dynamic responses of PMSG such as rotor speed and active power output. Therefore it can be concluded that the dynamic performance of PMSG can be enhanced by the proposed DC-link protection system.

In Chapter 5, the wind turbines cluster system is proposed and investigated which is composed of Squirrel Cage Induction Generators (SCIGs) controlled by cluster converter with Voltage Source Converter based High Voltage Direct Current (VSC-HVDC) transmission system. The wind turbine cluster systems (multiple clusters) are installed in an offshore wind farm and

connected to onshore system through a VSC-HVDC transmission line. Doubly Fed Induction Generator (DFIG) or Permanent Magnet Synchronous Generator (PMSG) based variable speed wind turbine is also used in offshore wind farm with HVDC transmission system. These wind generator concepts require power converter for each individual wind generator. From the economical point of view, it will be desirable if the individual power converter of each wind generator can be eliminated and the wind farm can be controlled by using cluster VSC converter. The main purpose of grouping of wind turbine generators into clusters system is to reduce the number of power electronic converters that can potentially fail. In addition, higher technical availability of the wind turbines for power production can be achieved. Moreover, the provision of redundant converters can be avoided. The performance, robustness, and effectiveness of the control system for a wind farm are commonly evaluated in the transient and the steady state conditions. Currently, the grid code prosecutes that the wind generators should be remained stay online during a network disturbance, because out of synchronism of a large number of wind generators has serious impact on power system stability. In order to investigate effectiveness of the proposed wind turbine cluster system composed of Squirrel Cage Induction Generators (SCIGs) controlled by cluster converters with VSC-HVDC system, simulation analyses have been performed and the dynamic and steady state characteristics of the proposed system has been investigated. From the simulation results it can be concluded that the proposed system can enhance the performance and stability of the SCIG based offshore wind farm under both transient and steady state conditions.

In conclusion, the investigations and results presented in this thesis will be effective to enhance stable operation and effective control of grid connected wind farm in transient and steady state conditions. The operation of wind farm can be serious situation or unstable when a fault such as short circuit occurs in the connected grid system. This thesis presents analyses about dynamic characteristics of and stabilizing control for a wind farm of several structures, all of which are operated under Voltage Source Converter (VSC) system. For a wind farm with PMSGs and SCIGs installed together, the new control method is developed for VSC of PMSG to enhance the stability of the wind farm in Chapter 3. In Chapter 4, the new protection system is presented for DC-Link circuit of back to back VSC converter of PMSG, which is very effective to enhance the fault ride through capability of the wind farm. Finally the wind turbines cluster system composed of SCIGs controlled by cluster converter with VSC-HVDC system is proposed, which is suitable to enhance

stable operation of an offshore wind farm. Finally, it is hoped that this work will be of great impact in wind power application, especially for increasing and developing VSC based grid-connected wind farm.

Acknowledgement

This thesis has been carried out at Department of Electrical and Electronic Engineering of Kitami Institute of Technology, Japan for the partial fulfillment of the requirement for the degree of Ph.D. This Thesis deals with the operation and control of grid connected wind farms under VSC-HVDC system. It is my great pleasure to acknowledge the generous contribution of many individuals, experts and institutions. At first, I express my deep sense of gratitude and indebtedness to my reverend supervising professor, Prof. Junji Tamura for his advice, constant encouragement, valuable guidance and never ending enthusiasm. I shall ever remain grateful to him for his hearty cooperation, financial support and amiable demeanor in accomplishing this work. Prof. Junji Tamura has kindly reviewed this manuscript, and provided me with many helpful suggestions, and also conducted the review panel.

I am deeply grateful to co-supervisors, Associate Prof. Rion Takahashi and Assistance Prof. Atsushi Umemura of Electrical and Electronic Engineering Department, Kitami Institute of Technology, Japan, for their support and kindness I have been provided with. I am indebted to Dr. Marwan Rosyadi who inspired me to come to Japan and helps a lot in my research and during my stay in Kitami.

I wish to express my gratefulness to Kitami Institute of Technology, which has given me a unique opportunity to augment my engineering knowledge as well as has given me financial support during my study and attendance in various national and international conferences. I am so grateful to Borneo University of Tarakan, Indonesia, which has supported me to study in Japan with necessary study leave and deputation.

I would also like to thanks to all members of our laboratory, Mr. Rifat Hazari, Mrs. Effat Jahan, Mr. Takamasa Sato, Mr. Kazuhito Suzuki and Miss Kimiko Tada, for their kindness and encouragement given to me.

I am greatly indebted to my parents, Drs. HM. Alie Sindja and Hj. Norbayah. It is because of their endless pray; finally I can accomplish this work. Finally, Ya Allah, thank you very much for everything.

Linda Sartika

March 2018, Kitami Japan

References

- [1] Ellabban, Omar; Abu-Rub, Haitham; Blaabjerg, Frede, "Renewable energy resources: Current status, future prospects and their enabling technology". *Renewable and Sustainable Energy Reviews*. 39: 748–764 [749]. doi:10.1016/j.rser.2014.07.113.
- [2] REN21, Global Status Report 2016. Retrieved 8th June 2016.
- [3] “Global Wind Energy Static 2016”, GWEC Report February 2017.
- [4] REN21, Renewables 2011 Global Status Report, Version 1.1, July 2011. Online: <http://www.ren21.net>
- [5] The Global Wind Energy Council (GWEC), Global wind report 2010, April 2011. [Online]. Available: <http://www.gwec.net>
- [6] R. Doherty, E. Denny, M. O'Malley, “System operation with a significant wind power penetration”, *IEEE Power Engineering. Summer Meeting*, Vol. 1, pp. 1002–1007, Jun. 2004.
- [7] K. S. Salman, A.L.J. Teo, “Windmill modeling consideration and factors influencing the stability of a grid-connected wind power-based embedded generator”, *IEEE Trans. Power System*, Vol. 18. No. 2, pp. 793–802, May 2003.
- [8] C. Jauch, J. Matevosyan, T. Ackermann, and S. Bolik, “International comparison of requirements for connection of wind turbines to power systems”, *Wind Energy*, Vol. 8. No. 3, pp. 295–306, Jul. 2005.
- [9] Y. Shankir, “Review of wind turbines’ drive systems and why Gearless direct drive”, *RCREEE Wind Energy Building Capacity Program – Stage 2 Rabat*, Tangier 29 March – 2 April, 2010.
- [10] J. Tamura, T. Yamazaki, M. Ueno, Y. Matsumura, and S. Kimoto, “Transient stability simulation of power system including wind generator by PSCAD/EMTDC”, *IEEE Porto Power Tech*, Vol. 4, Paper no. EMT-108, 2001.
- [11] M. R. I. Sheikh, S. M. Mueen, R. Takahashi, and J. Tamura, “Transient Stability Enhancement of Power System Including Wind Farm by Using SMES”, *International Workshop on Modern Science and Technology 2010 (IWMST 2010)*, No.4, pp.253-258, Sept. 2010.

- [12] E. S. Abdin and W. Xu, Control design and dynamic performance analysis of a wind turbine-induction generator unit,” *IEEE Transaction Energy Convers.*, Vol. 15, No. 3, pp. 91–96, Mar. 2000.
- [13] C. L. Souza et al, “Power system transient stability analysis including synchronous and induction generator”, *IEEE Porto Power Tech*, Vol. 2, pp.6, 2001.
- [14] Thomas Ackermann, *Wind power in power system*, UK: John Wiley & Sons, 2005.
- [15] S. B. Papaefthimioun, S. A. Papathanassiou, “Simulation and control of variable speed wind turbine with synchronous generator”, *The XVII International Conference Electrical Machines (ICEM) 2006*, Chania, Crete Island, Greece, Ref. No. 593, Sept 2-5, 2006.
- [16] S. M. Mueen, R. Takahashi, T. Murata, J. Tamura, and M. H. Ali, “Transient stability analysis of permanent magnet variable speed synchronous wind generator,” *International Conference on Electrical Machines and Systems (ICEMS) 2007*, Soul Korea, pp.288-293, Oct 2007.
- [17] A. D. Hansen and G. Michalke: “Modeling and control of variable speed multi-pole permanent magnet synchronous generator wind turbine”, *Wind Energy*, Vol.11, no.5, 10.1002/we.278, pp.537-554, 2008.
- [18] T. sun, Z. Chen, and F. Blaabjerg: “Transient stability of DFIG wind turbines at an external short-circuit fault,” *Wind Energy*, Vol.8, No.3, pp. 354-360, 2005.
- [19] R. Takahashi, J. Tamura, M. Futami, M. Kimura, and K. Ide, “A new control method for wind energy conversion system using a double-fed synchronous generator”, *IEEJ Trans. on Power and Energy*, Vol.126, No.2, pp.225-235, Feb 2006
- [20] H. Polinder, S.W.H. de Haan, M. R. Dubois, J. Slootweg, “Basic operation principles and lectrical conversion systems of wind turbines”, *2004 Nordic Workshop on Power and Industrial Electronics*, Paper 069, Trondheim, Norway. 2004.
- [21] G. Michalke, A.D. Hansen, T. Hartkopf, “Control strategy of a variable speed wind turbine with multipole permanent magnet synchronous generator”, *2007 European Wind Energy Conference and Exhibition*, Milan, Italy, May 2007.
- [22] T. J. E. Miller, *Brushless permanent-magnet and reluctance motor drive*, New York: Oxford Univ. Press (1989)

- [23] Shuhui Li, Timothi A. Haskew, Ling Xu, "Conventional and novel control design for direct driven PMSG wind turbines," *Journal of Electric Power System research*, Vol. 80, pp. 328-338, March. 2010.
- [24] L. M. Fernandes, C. A. Garcia, F. Jurado, "Operating Capability as a PQ/PV node of a Direct-Drive Wind Turbine based on a permanent magnet synchronous generator", *Renewable Energy*, Vol. 35, pp. 1308-1318, 2010.
- [25] S. M. Mueeen, R. Takahashi, T. Murata, and J. Tamura, "Multi-Converter Operation of Variable Speed Wind Turbine Driving Permanent Magnet Synchronous Generator during Network Fault", *12th International Conference on Electrical Machines and Systems (ICEMS 2009)*, LS1C-4, Nov. 2009.
- [26] S. M. Mueeen, A. Al-Durra, J. Tamura, "Variable speed wind turbine generator system with current controlled voltage source inverter", *Electric Power Systems Research*, Vol. 80, pp. 328-338, 2010.
- [27] S. M. Mueeen, R. Takahashi, T. Murata, and J. Tamura, "A Variable Speed Wind Turbine Control Strategy to Meet Wind Farm Grid Code Requirements", *IEEE Transaction on Power Systems*, Vol. 25, No. 1, pp. 331-340, Feb. 2010.
- [28] J. F. Conroy, and R. Watson, "Low-Voltage Ride-through of a Full Converter Wind Turbine with Permanent Magnet Generator." *IET Renew. Power Generation*, Vol. 1, No. 3, pp. 182-189. 2007
- [29] S. M. Mueeen, R. Takahashi, T. Murata, J. Tamura, and M.H. Ali, "Transient Stability Analysis of Permanent Magnet Variable Speed Synchronous Wind Generator." *Proceedings of the International Conference Electrical Machines and Systems 2007 (ICEMS 2007)*, Seoul, Korea, Oct. 288-93. 2007
- [30] S. M. Mueeen, R. Takahashi, T. Murata, and J. Tamura, "A Variable Speed Wind Turbine Control Strategy to Meet Wind Farm Grid Code Requirements." *IEEE Transactions on Power Systems*, Vol. 25, No. 1, pp. 331-335, 2010
- [31] M. Rosyadi, S. M. Mueeen, R. Takahashi, and J. Tamura, "Stabilization of Fixed Speed Wind Generator by Using Variable Speed PM Wind Generator in Multi-machine Power System." *Journal of International Conference on Electrical Machines and Systems (ICEMS)*, Vol. 2 No. 1, pp 111-119. 2013
- [32] Offshore Wind Energy (Website), *Bureau of Ocean Energy Management*.

- <https://www.boem.gov/Renewable-Energy-Program/>
- [33] ABB global site, "Economic and environmental advantages" [Online]
<http://new.abb.com/systems/hvdc/why-hvdc>
- [34] M. Davies et al, "HVDC Plus-Basic and principle of operation", [Online] Available:
www.siemens.com/energy/hvdcplus
- [35] A. E. Alvarez, A. J. Ferre, J. B. Jane, F. D. Bianchi and O. G. Bellmunt, "Control of a wind turbine cluster based on squirrel cage induction generators connected to a single VSC power converter", *Electrical Power and Energy Systems*, Vol. 61, pp. 523-530. 2014
- [36] F. Wang, L Bertling, T. Le, A. Mannikoff and A. Bergman, "An overview introduction of VSC-HVDC state-of-art and potential applications in electric power systems,"
<http://www.cigre.org> , 21, rue d'Artois, F-75008 PARIS 2011.
- [37] Brendan Fox et al, "Wind Power Integration Connection and System Operational Aspects", *The Institution of Engineering and Technology, London, United Kingdom*, IET Pres, 2nd Edition, 2014.
- [38] Wind Power, Rowan University Clean Energy Program, [Available Online]:
www.rowan.edu/colleges/engineering/clinics/cleanenergy/cleanenergy_homepage.htm,
(Accessed on 2 November 2012).
- [39] Wind Energy Basics theory. [Online]: <http://windeis.anl.gov/guide/basics/index.cfm>,
(Accessed on 2 November 2012).
- [40] Wind Energy, [online]: http://leedintl.net/wind_energy. (Accessed on 2 November 2012).
- [41] V. Fthenakis, H. C. Kim, "Land use and electricity generation: A life-cycle analysis", *Renewable and Sustainable Energy Reviews*, Vol. 13. Issues 6–7, pp. 1465–1474, Aug./Sept. 2009.
- [42] R. Y. Redlinger, P. D. Andersen, P. E. Morthorst, *Wind Energy in The 21st Century*, 1st Edition, Palgrave, New York, 2002.
- [43] S. Heier, *Grid integration of wind energy conversion systems*, John Wiley & Sons Ltd, 1998.
- [44] Alejandro Rolan et al, "Modeling of a variable speed wind turbine with a permanent magnet synchronous generator", *IEEE International Symposium on Industrial Electronics (ISIE 2009)* , Seoul, Korea, July 5-8 2009.

- [45] M. Yin, G. Li, M. Zhou, and C. Zhao, "Modeling of the wind turbine with permanent magnet synchronous generator for integration", *IEEE Power Engineering Society General Meeting*, Tampa, Florida, pp. 1-6, 2007.
- [46] I. Boldea, *Synchronous Generators, United States of America*, Taylor and Francis, 2006.
- [47] S. M. Mueeen, J. Tamura, and T. Murata, *Stability Augmentation of a Grid Connected Wind Farm, Green Energy and Technology*, Springer-Verlag, 2009.
- [48] Krause, P. C. *Analysis of Electric Machinery*. New York: McGraw-Hill, 1994, p.135.
- [49] S. J. Chapman, *Electric Machinery Fundamental*, McGraw-Hill, 5 Edition , 2012.
- [50] I.G. Slootweg, "Wind Power: Modelling and Impact on Power System Dynamics", *Ph.D Thesis, Delft University Technology*, Netherlands, 2003.
- [51] D.S. Zinger, and E. Muljadi, "Annualized Wind Energy Improvement Using Variable Speeds", *IEEE Transactions on Industry Applications*, Vol.33, no.6, pp.1444-1447, 1997.
- [52] R. Hoffmann, and P. Mutschler, "The Influence of Control Strategies on the Energy Capture of Wind Turbines", *Conference Records of the 2000 IEEE Industry Applications Conference*, Vol.2, pp. 886-893, Rome, 8-12 October, 2000.
- [53] L. M. Fernandes, C. A. Garcia, F. Jurado, "Operating Capability as a PQ/PV node of a Direct-Drive Wind Turbine based on a permanent magnet synchronous generator", *Renewable Energy*, Vol. 35, pp. 1308-1318, 2010.
- [54] P. Jiuping, R. Nuqui, K. Srivastava, T. Jonsson, P. Holmberg, and Y. J. Hafner, "AC Grid with Embedded VSC-HVDC for Secure and Efficient Power Delivery", *Proc. IEEE Energy 2030 Conference*, pages. 1-6, 2008.
- [55] Kundur, P, "Power System Stability and Control", New York, McGraw-Hill, 1994.
- [56] C. L. Souza et al, "Power system transient stability analysis including synchronous and induction generator", *Proc. IEEE Porto Power Tech*, Vol. 2, pp.6, 2001.
- [57] J. Tamura, T. Yamazaki, M. Ueno, Y. Matsumura, and S. Kimoto, "Transient stability simulation of power system including wind generator by PSCAD/EMTDC," *Proc. IEEE Porto Power Tech*, 2001, vol. 4, Paper no. EMT-108.
- [58] E. S. Abdin and W. Xu, "Control design and dynamic performance analysis of a wind turbine-induction generator unit," *IEEE Trans. Energy Convers.*, vol. 15, no. 3, pp. 91–96, Mar. 2000.

- [59] L. Gyugyi: “Unified power flow control concept for flexible ac transmission system”, *Proc. Inst. Elect. Eng. C*. Vol. 139. No. 4, pp. 323-331, 1992.
- [60] S. M. Mueeen, M. A. Mannan, M. H. Ali, R. Takahashi, T. Murata, and J. Tamura, “Stabilization of wind turbine generator system by STATCOM,” *IEEJ Trans. Power Energy*, vol. 126, no. 10, pp.1073–1082, Oct. 2006.
- [61] M. Rosyadi, S. M. Mueeen, R. Takahashi, and J. Tamura, “Stabilization of Fixed Speed Wind Generator by using Variable Speed PM Wind Generator in Multi-Machine Power System,” 2012 International Conference on Electrical Machines and Systems (ICEMS2012), #DS2G5-4, Sapporo- Japan, 21-24 Oct. 2012.
- [62] PSCAD/EMTDC User’s Manual, Manitoba HVDC Research Center, Canada 1994.
- [63] Siegfried Heier, *Grid integration of wind energy conversion systems*, John Wiley & Sons Ltd 1998, pp. 34-36
- [64] MATLAB Documentation Center, Accessed November 3, 2012. [Online] <http://www.mathworks.co.jp/jp/help/>.
- [65] “Fukushima Floating Offshore Wind Farm Demonstration Project (Fukushima FORWARD).” Accessed June 22, 2015. <http://www.fukushima-forward.jp/english/>.
- [66] “The Global Wind Energy Council (GWEC), Global Wind Report 2015’, <http://www.gwec.net>, accessed April 2016.
- [67] S. B. Papaefthimiou, and Papathanassiou, S. A, “Simulation and Control of a Variable Speed Wind Turbine with Synchronous Generator.” *Proceedings of the CD Rec. XVII Int. Conf. Electrical Machines (ICEM 2006)*, Chania, Crete Island, Greece, 2006.
- [68] A. D. Hansen, and G. Michalke, “Modelling and Control of Variable Speed Multi-pole Permanent Magnet Synchronous Generator Wind Turbine.” *Wind Energy*, Vol. 11 No. 5, pp 537-54. 2008
- [69] C. Jauch, J. Matevosyan, T. Ackermann, and Bolik, S. “International Comparison of Requirements for Connection of Wind Turbines to Power Systems.” *Wind Energy*, Vol. 8, No. 3, pp. 295-306. 2005
- [70] L. M. Fernandes, C. A. Garcia, and F. Jurado, “Operating Capability as a PQ/PV Node of a Direct-Drive Wind Turbine Based on a Permanent Magnet Synchronous Generator.” *Journal of Renewable Energy*, 35, pp. 1308-1318. 2010.

- [71] S. Achilles, and M. Poller, “Direct Drive Synchronous Machine Models for Stability Assessment of Wind Farm”,
http://www.digsilent.de/Consulting/Publications/DirectDrive_Modeling.pdf.
- [72] P. M. Anderson, *Subsynchronous Resonance in Power System*. New York: IEEE Pres, 1994.
- [73] N. W. Miller, J. J. Sanchez-Gasca, W. W Price, and R. W. Delmerico, “Dynamic Modeling of GE 1.5 and 3.6 MW Wind Turbine-Generators for Stability Simulations.” Presented at *Power Engineering Society General Meeting*, Toronto, July 2003
- [74] F. M. Gonzalez-Longatt, P. Wall, and V. Terzija, “A Simplified Model for Dynamic Behavior of Permanent Magnet Synchronous Generator for Direct Drive Wind Turbines.” *Proc. IEEE Power Tech*, Trondheim, Norway. June pp. 1-7, 2011.
- [75] N. Mohan, T. M. Undeland, and W. P. Robbins, “*Power Electronics Converters, Applications and Design*”, Hoboken, NJ: John Wiley & Sons, 2003. 3rd
- [76] S. K. Chaudhary, R. Teodorescu, P. Rodriguez, and P. C. Kjaer, “Chopper Controlled Resistors in VSC-HVDC Transmission for WPP with Full-Scale Converters.” *Proc. IEEE PES/IAS Conference on Sustainable Alternative Energy (SAE)*, pp. 1-8. 2009
- [77] Offshore Wind Energy (Website), *Bureau of Ocean Energy Management*.
<https://www.boem.gov/Renewable-Energy-Program/>
- [78] The Global Wind Energy Council (GWEC), Global wind report 2015, April 2016. [Online]. Available: <http://www.gwec.net>
- [79] ABB global site, “Economic and environmental advantages” [Online]
<http://new.abb.com/systems/hvdc/why-hvdc>
- [80] M. Davies et al, “HVDC Plus-Basic and principle of operation”, [Online] Available: www.siemens.com/energy/hvdcplus
- [81] ABB global site, “AC Solutions for offshore wind connections”, [Online]
<http://new.abb.com/systems/offshore-wind-connections/ac-solutions>
- [82] D. Trudnowski, A. Gentile, J. Khan, and E. Petritz, “Fixed-speed wind generator and wind-park modeling for transient stability studies”, *IEEE Transactions on Power Systems*, Vol. 19, No. 4, pp. 1911–1917, 2004.
- [83] A. Egea-Alvarez, et al., "Sensorless control of a power converter for a cluster of small wind turbines," *IET Renew. Power Gener.*, Vol. 10, Iss. 5, pp. 721–728, 2016.

- [84] WECC Renewable Energy Modeling Task Force, WECC Wind Power Plant Dynamic Modeling Guide, August 2010.
- [85] Mohit Singh and Surya Santoso, “Dynamic Models for Wind Turbine and Wind Power Plant January 11, 2008-May 31, 2011”, *Subcontract Report NREL/SR-5500-52780 October 2011*, National Renewable Energy Laboratory, 2011.
- [86] M. Rosyadi, S. M. Mueen, R. Takahashi, J. Tamura, “Stability Augmentation of Wind Farm using Variable Speed Permanent Magnet Synchronous Generator”, *IEEEJ Transaction on Industry Applications*, Vol. 131, No. 11, pp.1276-1283, 2011.
- [87] R. Alejandro et al, “Modeling of a variable speed wind turbine with a permanent magnet synchronous generator”, *IEEE International Symposium on Industrial Electronics (ISIE 2009)*, Seoul, Korea, July 5-8 2009.
- [88] M. Yin, G. Li, M. Zhou, and C. Zhao, “Modeling of the wind turbine with permanent magnet synchronous generator for integration”, *IEEE Power Engineering Society General Meeting*, Tampa, Florida, pp. 1-6, 2007
- [89] Neil Kirby, “HVDC technology voltage source converter”, *IEEE PES T&D Expo*, Chicago, April 2014.
- [90] Yasushi Abe, Koji Maruyama, “Multi-series Connection of High-Voltage IGBTs”, *Fuji Electric Journal* Vol.75 No.8, 2002.

List of Publications

Transaction/Journal Papers:

- [1] **Linda Sartika**, Atsushi Umemura , Rion Takahashi, Junji Tamura, “Wind Turbines Cluster System Composed of Fixed Speed Wind Generators Controlled by Cluster Converter based VSC-HVDC System,” IEEJ Transaction on Power and Energy, Vol. 138, No. 3, March 2018.
(to be published)
- [2] **Linda Sartika**, Atsushi Umemura, Rion Takahashi, Junji Tamura, “Enhancement of DC-Link Protection of PMSG Based Wind Turbine under Network Disturbance by Using New Buck Controller System,” Journal of Mechanics Engineering and Automation, Volume 7, Number 4, pp.171-179, 2017

International Conference Papers:

- [1] **Linda Sartika**, Marwan Rosyadi, Atsushi Umemura, Rion Takahashi, Junji Tamura, ” Cooperated Stabilizing Control of PMSG based Grid Connected Wind Farm,” Proc. of IEEE Energy Conversion Congress and Exposition (ECCE 2015), Paper ID No.87, Montreal, Canada, September, 2015.
- [2] **Linda Sartika**, Marwan Rosyadi, Atsushi Umemura, Rion Takahashi, Junji Tamura, ”Stabilization of PMSG based Wind Turbine under Network Disturbance by using New Buck Controller System for DC-Link Protection,” Proc. of 5th IET International Conference on Renewable Power Generation (RPG 2016), Paper ID No.P2, London, September, 2016.

Other Conference Papers:

- [1] **Linda Sartika**, Marwan Rosyadi, Atsushi Umemura, Rion Takahashi, Junji Tamura,” Cooperated Stabilizing Control of Permanent Magnet Synchronous Generator Based Grid Connected Wind Farm under Network Disturbance,” 2014 Joint Convention Record, The Hokkaido chapters of IEEJ, No.32, Sapporo, Oct 2014.

- [2] **Linda Sartika**, Marwan Rosyadi, Atsushi Umemura, Rion Takahashi, Junji Tamura DC-link Protection Scheme of Permanent Magnet Wind Generator by Using Buck Converter under Network Disturbance,”2015 Joint Convention Record, The Hokkaido chapters of IEEJ, No.25, Kitami, Nov 2015.
- [3] **Linda Sartika**, Marwan Rosyadi, Atsushi Umemura, Rion Takahashi, Junji Tamura “Dynamic Performance Enhancement of PMSG based Wind Turbine by using New DC-Link Protection System with Buck Controller,” 2016 Joint Convention Record, The Hokkaido chapters of IEEJ, No.22, Sapporo, Nov 2016.